Copyright Warning & Restrictions

The copyright law of the United States (Title 17, United States Code) governs the making of photocopies or other reproductions of copyrighted material.

Under certain conditions specified in the law, libraries and archives are authorized to furnish a photocopy or other reproduction. One of these specified conditions is that the photocopy or reproduction is not to be "used for any purpose other than private study, scholarship, or research." If a, user makes a request for, or later uses, a photocopy or reproduction for purposes in excess of "fair use" that user may be liable for copyright infringement,

This institution reserves the right to refuse to accept a copying order if, in its judgment, fulfillment of the order would involve violation of copyright law.

Please Note: The author retains the copyright while the New Jersey Institute of Technology reserves the right to distribute this thesis or dissertation

Printing note: If you do not wish to print this page, then select "Pages from: first page # to: last page #" on the print dialog screen

ABSTRACT

EROSION BEHAVIOR AND SCOUR RISK OF EXTREMELY COARSE STREAMBEDS

by
Abolfazl Bayat

Bridge scour, which is the erosion of soil and rock around bridge abutments and piers, is the principal cause of bridge failure in the United States and around the world. Previous investigations of scour have focused mostly on fine sediments such as sand, silt, and small gravel, because such alluvium underlies a majority of bridges. The erosion resistance of coarser sediments has received limited attention to date, even though they dominate many small to medium-size rivers in the northern tiers of the United States, Europe, and Asia. This study focuses on the scour behavior of extremely coarse particles (ECP), namely cobbles and boulders.

A main objective of this research is to develop a relationship between critical (entrainment) velocity and grain size for sediment particles in the size range of 5 to 50 cm (2 to 20 in). This is accomplished by performing a limit analysis of sediments that exist within the stream beds of actual bridges. A basic premise is that the residual sediments reflect the maximum historic flow and velocity that has occurred over the life of the bridge.

Thirty-five bridges in Northern New Jersey are initially screened for the study, and 12 bridges are selected for final analysis. Field visits are made to characterize the grain size distribution of the ECP sediments present at each site. Due to the extreme coarseness of the sediments, nontraditional methods are employed such as optical granulometry and statistical pebble counts. To assure geologic and hydrologic diversity

for the data set, the sites span three of New Jersey's physiographic provinces: Highlands, Valley and Ridge, and Piedmont.

Hydraulic analyses are used to estimate the maximum velocity that the bridge has experienced during its lifetime. These are based on the maximum discharges measured at USGS gaging stations or computed with USGS StreamStats software. Final limit velocities range from 245 to 549 cm/sec (8 to 18 ft. /sec.).

The limit analysis is performed by regression of the particle size and velocity data. This yields a nonlinear, exponential relationship between critical velocity and median particle size. The variance fraction associated with the data set is 0.642, indicating a reasonable fit. The limit analysis results are also compared with traditional sediment transport relationships, including Newton's Law and Hjulstrøm's envelope.

Several applications of the limit analysis relationship are proposed and explored. The first is a method to assess the general scour risk for bridges underlain by ECP sediments. First, the median grain size of the bed sediments is measured. The corresponding limit velocity is then computed and compared with the desired scour design storm, e.g., Q_{100}. If the design scour velocity exceeds the limit velocity, then the bridge is considered to have a higher scour risk.

The limit analysis curve is also used to extend the useful range of the standard scour design equations, including the HEC-18 critical velocity and USACE EM 1601 riprap relations. Extrapolation of the limit results generally produces lower and more conservative critical velocities within the ECP size range than did the standard relations. Another application provides adjustment coefficients, which are useful for rapid photographic measurement of sediments (size and gradation) using WipFrag.

EROSION BEHAVIOR AND SCOUR RISK OF EXTREMELY COARSE STREAMBEDS

by
Abolfazl Bayat

A Dissertation
Submitted to the Faculty of
New Jersey Institute of Technology
in Partial Fulfillment of the Requirements for the Degree of
Doctor of Philosophy in Civil Engineering

John A. Reif, Jr. Department of Civil and Environmental Engineering

January 2017

APPROVAL PAGE

EROSION BEHAVIOR AND SCOUR RISK OF EXTREMELY COARSE STREAMBEDS

Abolfazl Bayat

Dr. John R. Schuring, Dissertation Advisor — Date
Professor of Civil and Environmental Engineering, NJIT

Dr. Robert B. Dresnack, Committee Member — Date
Professor of Civil and Environmental Engineering, NJIT

Dr. Fadi A. Karaa, Committee Member — Date
Associate Professor of Civil and Environmental Engineering, NJIT

Dr. Yuan Ding, Committee Member — Date
Associate Professor of Civil and Environmental Engineering, NJIT

Prof. Walter Konon, Committee Member — Date
Professor of Civil and Environmental Engineering, NJIT

Dr. Frank L. Golon, Committee Member — Date
Division President, Davidson-Wayne Development

BIOGRAPHICAL SKETCH

Author: Abolfazl Bayat

Degree: Doctor of Philosophy

Date: January 2017

Undergraduate and Graduate Education:

- Doctor of Philosophy in Civil Engineering,
  New Jersey Institute of Technology, Newark, NJ, 2017

- Master of Science in Civil Engineering
  New Jersey Institute of Technology, Newark, NJ, 2012

- Bachelor of Science in Mechanical Engineering
  Urmia University, Urmia, Iran, 2007

To: my loving parents, siblings, nieces, and nephews.

ACKNOWLEDGMENT

I would like to express my deepest appreciation to my research supervisor, Dr. John R. Schuring, for his guidance, encouragement, and help throughout the course of this research and dissertation. He is a true scholar and a great gentleman. It was an honor to work with him on this dissertation.

Special thanks to my friend, Dillion Collins for his help regarding my research work. Appreciation is expressed to Dr. Robert Dresnack and his hydraulic team members for their great help and support. The author is also grateful to the other members of his dissertation committee, Professor Fadi A. Karaa, Professor Walter Konon, and Professor Yuan Ding.

The graduate assistantship received from the Department of Civil and Environmental Engineering is greatly appreciated. Furthermore, the author wishes to specifically thank Dr. Taha F. Marhaba, the Chair of the Department, for his continuous support of this research.

Finally, I would like to deeply thank my parents, Monir and Allah, and express my love to my siblings for their continuous emotional and financial support.

TABLE OF CONTENTS

TABLE OF CONTENTS
(Continued)

Chapter **Page**

TABLE OF CONTENTS
(Continued)

TABLE OF CONTENTS
(Continued)

TABLE OF CONTENTS
(Continued)

LIST OF TABLES

LIST OF TABLES
(Continued)

LIST OF FIGURES

LIST OF FIGURES
(Continued)

LIST OF FIGURES
(Continued)

Figure **Page**

LIST OF FIGURES
(Continued)

CHAPTER 1

INTRODUCTION

1.1 The Problem of Bridge Scour

The devastating effects of major floods are well known, including widespread inundation and destruction of homes, businesses, and agricultural land. A less obvious threat during floods is damage to bridges over waterways due to scour. Basically, bridge scour is the erosion of soil and rock from around bridge abutments and piers caused by swiftly flowing water. An example of bridge scour is shown in **Figure 1.1**. In severe cases, scour can lead to outright collapse of a bridge.

Figure 1.1 Pier scour, Murietta Creek, Pacific Coastal, (FHWA 2006).

Not surprisingly, bridge scour is the principal cause of bridge failure in the United States and around the world (Fischer, 1993). Over one thousand bridges have collapsed in the United States over the last 50 years due to hydraulic failure resulting in large financial losses. Some of the more prominent failures due specifically to scour have included.

- 1985- During this year 73 bridges were destroyed by floods in Pennsylvania, Virginia and West Virginia (FHWA, 1988).
- 1987- During the spring floods of 1987, 18 bridges in New York and New England were destroyed by scour (Morris and Pagan-Ortiz, 1999).
- 1995- Five interstate bridges in Arroyo Pasajero, CA, built in 1967, collapsed due to stream channel degradation and scour (Parola, 1997).

One of the bridge failures in 1987 was the failure of Schoharie Creek Bridge which was built in the early 1950s with five spans and four supporting piers supported by shallow spread footings. On April 5, 1987, a 50-year flood occurred that undermined the spread foundations of one of the piers. This led to the collapse of three spans killing 10 people in vehicles. Investigators identified excessive scour under pier three as of principle cause of the collapse. This tragic event prompted national focus on the problem of bridge scour.

After the Schoharie creek Bridge failure in 1987, the FHWA established a national scour evaluation program as an integral part of the National Bridge Inspection Program. The first editions of Hydraulic Engineering Circular (HEC) No. 18, "Evaluating Scour at bridges", and HEC No. 20, "Stream Stability at Highway Structures", were also published (FHWA, 2012). Updating of these circulars has continued to the present, with HEC-18 currently in its 5th edition (April, 2012), and HEC-20 in its 4th edition (April, 2012).

The FHWA now requires that every bridge over water is inspected every two years, although longer intervals can be used when justified (FHWA, 1988). Any bridges found to be scour critical must be inspected annually until repaired or replaced. With regards to new bridges, the American Association of State Highway and Transportation Officials (AASHTO) standard specification for highway bridges (AASHTO, 1992a) requires that hydraulic studies be performed as a necessary part of the preliminary design of a bridge, including estimated scour depths at piers and abutments. Supporting foundation shall be designed such that the structural load is safely supported entirely below the probable scour depth.

1.2 Justification for the Proposed Research

As previously stated, the principal scour tool used by U.S. bridge designers for riverine flow is HEC-18 published by the FHWA (Arneson, 2012). Increasingly, practitioners recognize that some of the standard equations in HEC-18 over-predict scour depth for certain hydraulic and geologic conditions. One reason for overly conservative or erroneous calculated scour depths is poor estimation of scour variables. Misuse of methods can also be a culprit, such as applying a HEC-18 equation to a bed sediment or hydraulic condition that does not actually fall within the usable range of the relationship.

Another explanation for over-prediction of scour depth is that most of the HEC-18 relationships are based on laboratory flume studies conducted with sand-sized sediments adjusted with factors of safety. It is fair to ask whether scale modeling can effectively represent a phenomenon as complex as scour, especially in view of the wide diversity of hydrologic, hydraulic, and geotechnical conditions that exists across the nation.

The impact of over-predicting scour depth for new bridges can be significant. Designers have only two general options: (1) extend and/or stiffen the substructure; or (2) provide countermeasures. Either option increases construction costs substantially. There are additional complications when retrofitting existing bridges for scour. One is the acquisition of right-of-way easements, since installed countermeasures typically extend beyond the bridge limits. A second is the environmental impact of the countermeasure on the flora and fauna present within the stream channel. Lengthy permit approval times can occur for bridges located along environmentally sensitive watercourses.

Another reason for overly conservative scour prediction is most current scour analysis procedures focus on fine textured sediments ranging in size from sand and finer. Often, if coarser and more erosion-resistant sediments are present in the streambed, they are ignored. Mostly, this is due to difficulty in accurately sampling streambeds composed predominantly of cobble and boulder-sized particles. Both factors cause even more bias towards finer grain sizes, which, in turn, inflates predicted scour depths. **Figure 1.2** gives a close size comparison of sand and gravel with cobbles and boulders, which will be referred to as Extremely Coarse particles or ECP for the remaining of the study.

The erosion behavior and scour resistance of oversize ECP sediments have received only limited attention by past investigators. This is partly because the majority of bridges in the U.S. and abroad are underlain by fine textured alluvium composed principally of sand, silt, and gravel. In fact, fine textured alluvium dominates the central and southern regions of the U.S. (Dade & Friend, 1998) and it is also the principal sediment encountered in any large river system with wide valleys and low gradients regardless of region. As a result, numerous predictive relationships to describe the

Figure 1.2 Comparison of sand and gravel sediments with extremely coarse particle (ECP), including cobbles and boulders.

erosion of fine alluvial sediments have been proposed (e.g., Cheng, 1997; Ferguson & Church, 2004).

On the other hand, coarse particles tend to dominate the stream beds of small to medium-size streams within the northern tiers of the U.S., Europe, and Asia, especially in land areas that are either mountainous or have been subjected to continental glaciation. In the U.S., there are 15 states that contain river systems where coarse particles often dominate as summarized in **Table 1.1.** Practicing engineers in these states are often challenged to accurately characterize coarse sediments and realistically analyze bridge scour in many rivers. This is complicated by the fact that extremely coarse particles do not necessarily follow the classic relationships of sediment transport.

1.3 Research Objective

The present research is aimed at helping to fill this technological gap by providing a new approach for estimating scour in streambed with extremely coarse particles (ECP), especially for sediments in the cobble to boulder size range. The three main objectives of this study are:

1. Develop multiple, complementary approaches for measuring and analyzing the effective grain size of streambeds with ECP sediments;
2. Conduct a limit analysis of actual ECP sediments under bridges and correlate the results with classic sediment transport and scour analysis methods; and
3. Propose a relationship for the predicting entrainment velocity exclusively for use with ECP sediments.

Note that these objectives are considered original. The end goal of this research is to provide technical tools that improve the reliability of scour estimation, thereby increasing bridge safety. It will allow better or more effective use of financial resources.

Table 1.1 U.S. States with Rivers Containing Significant Amounts of Coarse Particles

New York Area	***New England States***	***Mountain States***	***Pacific Northwest***
New Jersey	Connecticut	Arizona	Oregon
New York	Maine	Colorado	Washington
Pennsylvania	Massachusetts	Idaho	
	New Hampshire	Nevada	
	Vermont	New Mexico	

CHAPTER 2

LITERATURE REVIEW

2.1 Types of Bridge Scour

Rivers are the most dynamic geomorphic system that engineers have to cope with in the design and maintenance of bridges. These geomorphic features also can change dramatically with time, especially during major floods. While a river can move its location, a bridge cannot (Richardson & Davis, 2001).

There are several ways in which channels can change and thereby jeopardize the stability and safety of a bridge. The channel bed can degrade so that bed elevations become lower, undermining the foundation of the piers and abutments. Also, deposition of sediment on the channel bed can reduce conveyance capacity through the bridge opening. Flood waters are then forced around the bridge, attacking roadway approaches, channel banks, and flood plains.

In general, bridges are designed so that the flow passes through the waterway parallel to the axes of the abutments and the piers. If the path of flow shifts laterally in either direction due to lateral movement so that the flow approaches the substructures at a significant skew angle, scour will be increased due to this misalignment.

Bridge scour is traditionally considered to have three primary components:

1. Long-term degradation of the river bed;
2. Contraction Scour due to the bridge opening; and
3. Local scour at the piers or abutments.

Many designers will add up the three scour components to obtain the total scour at a bridge foundation. This assumes that each component acts independently of the other. Recent studies have shown that in many situations this is not the case (Melville, 1992). However, summing all the components of scour does add conservatism to the design. Each of these scour components will now be briefly described.

2.1.1 Aggradation and Degradation

Aggradation and degradation are long-term changes in the stream bed elevation. These are the result of natural geomorphic trends of the river and/or modifications to the watershed (see **Figures 2.1 and 2.2**). "Aggradation" refers to the progressive buildup of sediments in the channel, and it can be identified by the presence of bars or other elevated portions of the streambed, possibly comprised of materials inconsistent with those in the rest of the channel. "Degradation" is the long-term lowering of the channel over a relatively wide area (Yang, 2003). Evidence of degradation includes stains or other marking along piers or abutment walls that indicate a previous bed elevation. It is also possible for a streambed to be in dynamic equilibrium in the vicinity of the bridge. In this situation neither aggregation nor degradation will be present.

Aggradation and degradation do not include the cutting and filling of the streambed in the vicinity of the bridge that might occur during a single runoff event; these are contraction and local scour. Rather, aggradation and degradation are long-term trends over the life of the bridge.

Figure 2.1 Streambed long term aggradation, bridge # 1809-153.

Figure 2.2 Streambed long term degradation, bridge # 2103-152.

2.1.2 Contraction Scour

Contraction scour is a lowering of the streambed across the stream or waterway at a bridge. This lowering may be uniform or non-uniform across the bed, in that the depth of scour may be deeper in some parts of the cross section (Mueller, 2002; Melville, 1992).

Contraction scour at a bridge results from the acceleration of flow due to a reduction in flow area. The most common situation is when the area of bridge opening is less than that of the upstream channel and floodplain (see **Figures 2.3 and 2.4**). Reduced area for flow will increase velocity and erodes the stream bed.

The underlying cause of most contraction scour is when the bridge length has been designed too short to reduce the initial cost of the superstructure. Some other causes include:

- Excessive number of piers in the waterway;
- Debris buildup, which often reduces the waterway opening (see **Figure 2.5**);
- Formation of sediment deposits within the waterway aggradation that constrict or reduce the available waterway opening; and
- Ice formation or ice jams that temporarily reduce the waterway opening.

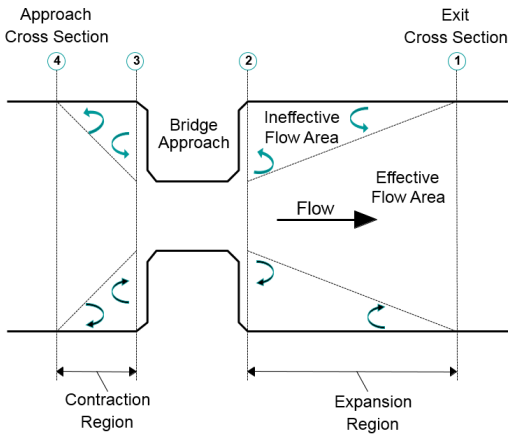

Figure 2.3 Conceptual sketch of contraction scour, (FHWA, 2006).

Figure 2.4 Contraction scour, bridge # 1404-158.

Figure 2.5 Debris build-up in the waterway, bridge # 2107-156.

2.1.3 Local Scour

Local scour occurs around an obstruction that has been placed within a stream, which causes an acceleration of the flow and results in erosion (Mueller, 1996). The mechanism

of local scour is the formation of vortices induced by obstructions. The most common obstructions that cause local scour are foundation elements, namely abutments, piers, and pile bents (see **Figures 2.6 and 2.7**).

A number of factors have been found to influence the depth of local scour around bridge foundation elements. The more significant include:

- Flow Velocity - As streamflow velocity increases, vortex action can be magnified considerably.
- Skew - Bridge abutments and piers that are skewed to the direction of streamflow can dramatically increase both local scour and contraction scour.
- Flow Depth– Deeper flow increases the vortex effect on the streambed.
- Pier Width - Scour depth for piers is proportional to width.
- Pier Shape - A square-nosed pier will produce a scour depth about 20 percent deeper than a sharp-nosed pier and 10 percent deeper than a cylinder or round-nosed pier.
- Pier Length - Long Piers can produce multiple vortices and greater scour depth if the pier is at an angle to the flow direction.

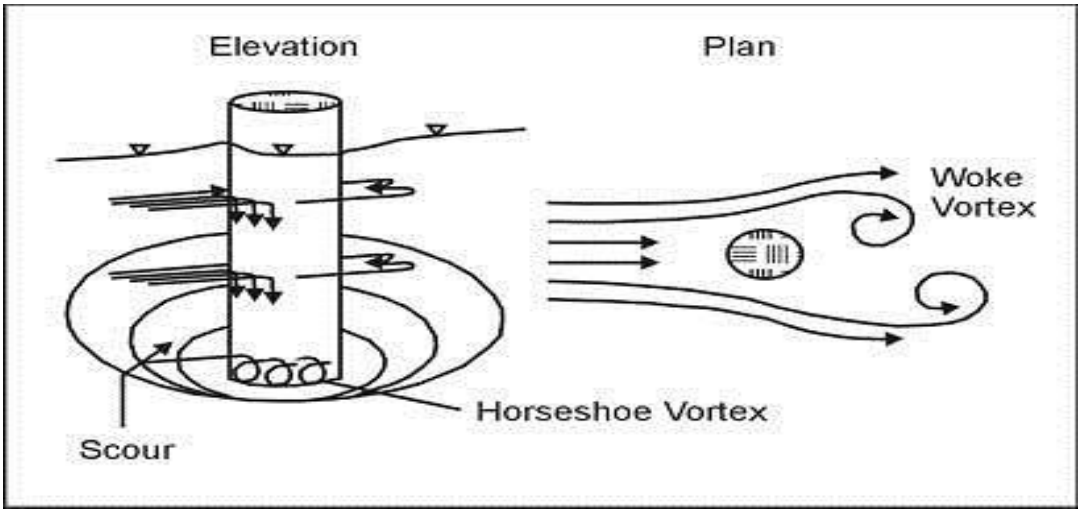

Figure 2.6 Schematic illustration of local scour at a cylindrical pier (Richardson, 2001).

Figure 2.7 Local scour at a pier, bridge # 1405-156.

Scour depths resulting from local scour are normally deeper than those from contraction scour. Bridges in tidal situations are particularly vulnerable to local scour, since a strong tidal current whose direction reverses periodically causes a complex local scour phenomenon around a bridge substructure. Surveys of local scour along the abutments and around the piers are most often done during periods of low flow when detailed measurements can be made, either by wading and probing, by probing from a boat, by the use of divers, or by sonic methods (Rantz, 1982).

2.1.4 Clear-Water versus Live-Bed Scour

Two different bed conditions can occur during contraction and local scour events: clear-water and live-bed. Clear-water scour is when there is no movement of the bed material

upstream into the bridge crossing, or when the bed material being transported stays in suspension. Thus, sediments are not deposited in any scour holes that may form. Live-bed scour occurs when there is transport of bed material from the upstream section and into the crossing (Chang & Davis, 1999). Live-bed local scour is cyclic in nature; that is, the scour hole that develops during the rising stage of a flood refills during the falling stage (FHWA, 2012).

Typical clear-water scour situations include: (1) streams with coarse-bed sediments such a ECP materials; (2) streams with flat gradients during low flow; (3) armored streambeds where the only places that tractive forces can penetrate the armor layer are at piers and/or abutments; and (4) vegetated channels or floodplain overbank areas.

2.2 Sediment Transport Relationships Applicable to ECP

Over the last century, the principles of sediment transport in river systems have been well studied. Most investigators focused on particles with small sizes that correspond to a medium sand size and smaller. The results of numerous mathematical relationships are available to describe movement of such sediments in water (e.g., Yang, 2003; Bunte, 2001)

The physics of transporting particles sizes larger than sand size is different. Geologic materials such as large gravel, cobbles, and boulders do not generally follow the classic laws of sediment transport. Relatively few investigators have examined the water transport of ECP sediments, and those that have mostly posed purely empirical relationships (Katherine & Stephen, 2004).

In this section, a brief review of available transport relationships that are potentially applicable to ECP will be presented. Note that discussion begins with Stokes' Law even though it does not be effectively describe coarse particle transport. It does serve, however, as a frame of reference for the other relations.

2.2.1 Stokes' Law

Rivers and streams are the most significant geologic agents of sediment transport on surface of Earth. When sediments are transported and deposited, they are also sorted according to particle size. For example, gravel-sized particles accumulate at one point along the channel, while sand-sized particles accumulate at another location. The underlying principle that governs how sediments are sorted within water is Stokes' Law of Settling (Van Run, 1989). Stokes' Law relates a particle's settling velocity to its diameter and density, as well to the viscosity of the fluid. In general, the settling velocity of a sediment particle is directly proportional the square of the particle diameter. Stokes' Law is based on the assumption of laminar flow conditions, i.e., Reynolds number < 2000. Stokes' Law may be stated as:

$$u_T = \frac{d^2(\rho_p - \rho_f)g}{18\mu} \tag{2.1}$$

where: u_T : settling velocity (cm/sec),
g : acceleration of gravity (m/sec^2),
d : particle diameter (cm),
ρ_p : density of particle (g/cm^3),
ρ_f : density of fluid medium (g/cm^3), and
μ: absolute viscosity of fluid medium (g/cm-s).

A plot of Stokes' Law for quartz particles settling in water is presented in **Figure 2.8**. Note that Stokes' Law is not valid above a particle size of about 0.1 mm, since the settling velocities (and thus the critical velocities needed to transport the particle) become

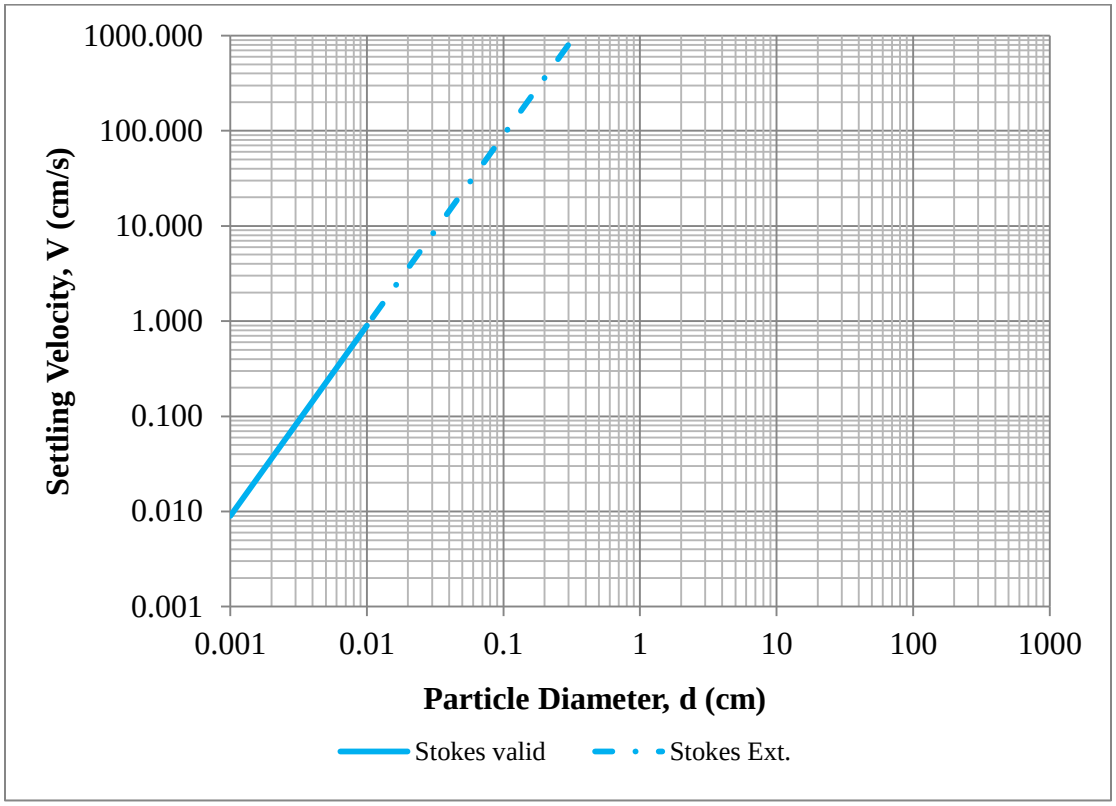

Figure 2.8 Stokes' law: settling velocity vs. particle diameter.

enormous. The explanation is larger particles are transported in turbulent flow conditions, which lowers the rate of settling (and critical) velocity. In fact, the settling velocities of coarse particles are governed by Newton's Law, which will be described in the next section.

The question arises how a settling velocity like that predicted by Stokes' Law relates to the velocity actually needed to transport a sediment particle within a flowing stream. This is called the critical velocity, and it is clearly related to the settling velocity. For cohesion-less particles such as sand and silt, the critical velocity is considered to be equal to settling velocity. But to erode sediment, a small amount of inertia is needed to

the initiate movement of a particle lying on the bed and lifts it up into the current. This is known as entrainment velocity, and for a given particle size, the erosion velocity is somewhat higher than the transportation velocity on account the inertia to be overcome.

2.2.2 Newton's Law Applied to Sediment Transport

As channel velocity increases, flow enters a turbulent state and Stokes' Law is no longer valid because inertial rather than viscous forces predominate. Newton's law is used to predict settling velocity in this flow regime. It is applicable for flows where the Reynolds number is greater than about 4000 (Antonia, 1990), which corresponds to particle diameters greater than 2 mm.

The relationship to predict settling velocity based on Newton's law is given in Equation (2.2). As indicated, the settling velocity is proportional to the particle diameter and also to a ratio of particle density to the fluid density. A plot of settling velocity versus particle diameter for Newton's Law for quartz particles settling in water is presented in **Figure 2.9**. The plot for Stokes' Law has been retained for comparison purposes. Note the significant reduction in slope due to lower velocities caused by turbulent conditions.

$$u_T = 1.74\left(\frac{d(\rho_p - \rho_f)g}{\rho_f}\right)^{1/2} \tag{2.2}$$

where: u_T : settling velocity (cm/sec),
g : acceleration of gravity (cm/sec^2),
d : particle diameter (cm),
ρ_p : density of particle (g/cm^3),
ρ_f : density of fluid medium (g/cm^3) , and
μ: absolute viscosity of fluid medium (g/cm-s).

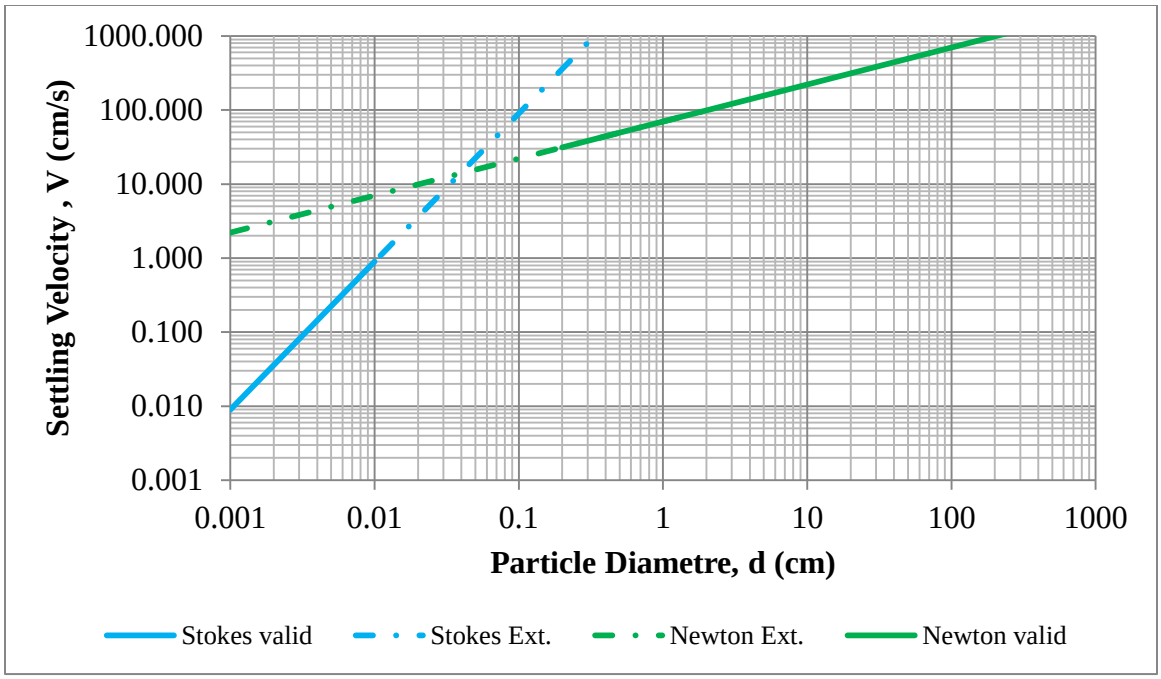

Figure 2.9 Newton's law: settling velocity vs. particle diameter.

2.2.3 Grace Method

An examination of **Figure 2.10** suggests that there is a sudden break in slope between the settling velocity functions for Stokes' Law and Newton's Law as flow enters a turbulent condition. Actually, settling velocity displays a more gradual transition as it leaves the laminar region and enters the turbulent region. Grace (1986) proposed a method to predict settling velocity in this transitional region as illustrated in **Figure 2.11**. The Grace method is considered applicable for water flow regimes where the Reynolds number ranges from 2000 to 4000 and the particle diameter ranges from 0.1 to 1 mm which is the range of very fine sand to coarse sand.

The Grace method uses two dimensionless parameters, one for particle size (Equation (2.3)) and one for settling velocity (Equation (2.4)):

$$d^* = d \times \sqrt[3]{\frac{\rho_f \left(\rho_s - \rho_f\right) \times g}{\mu_f^2}} \tag{2.3}$$

$$V_{ts}^* = V_{ts} \times \sqrt[3]{\frac{\rho_f^2}{\mu_f \left(\rho_s - \rho_f\right) \times g}} \tag{2.4}$$

The steps for finding settling velocity using the Grace Method are summarized as follows:

Step 1- For various particle diameters, calculate the dimensionless particle sizes d^* using Equation (2.3) above. For quartz particles in water, the equation simplifies to $\rightarrow \boldsymbol{d^* = 256 \times d}$

Step 2- Using the computed dimensionless particle sizes, d^*, find out the dimensionless settling velocity, V_{ts}^*, from a graph provided by Grace, which is shown in **Figure 2.10**.

Step 3- Using these values of dimensionless settling velocity, V_{ts}^*, determine the actual particle settling velocity, V_{ts}, from Equation (2.4). Substitution parameters with the actual values, the equation will be: $\boldsymbol{V_{ts} = 2.53 \times V_{ts}^*}$

Step 4- Create a plot of the actual particle size and settling velocity for the transitional flow region.

A summary plot of the Grace method applied to quartz particles settling in water are presented in **Figure 2.11**. Note the smooth transition of settling velocity from Stokes' Law to Newton's Law. Experimental evidence is generally consistent with the results of the Grace method (Cheng, 1997).

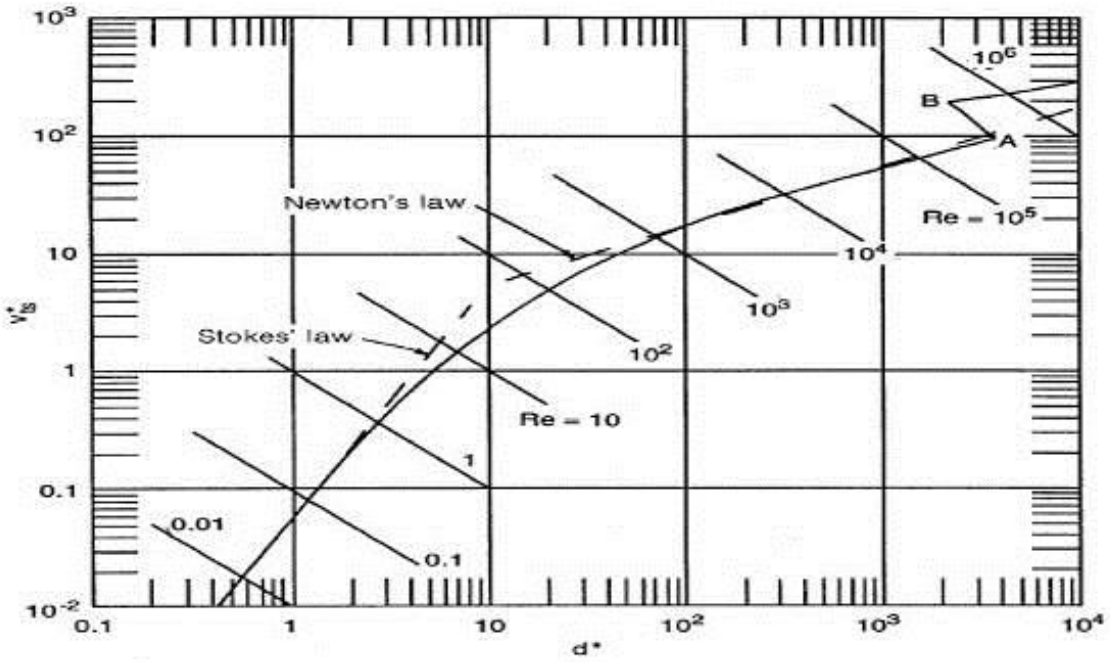

Figure 2.10 Dimensionless terminal velocity, V_{ts}^{*}, as a function of dimensionless particle diameter, d^{*}, for rigid spheres, Grace (1986).

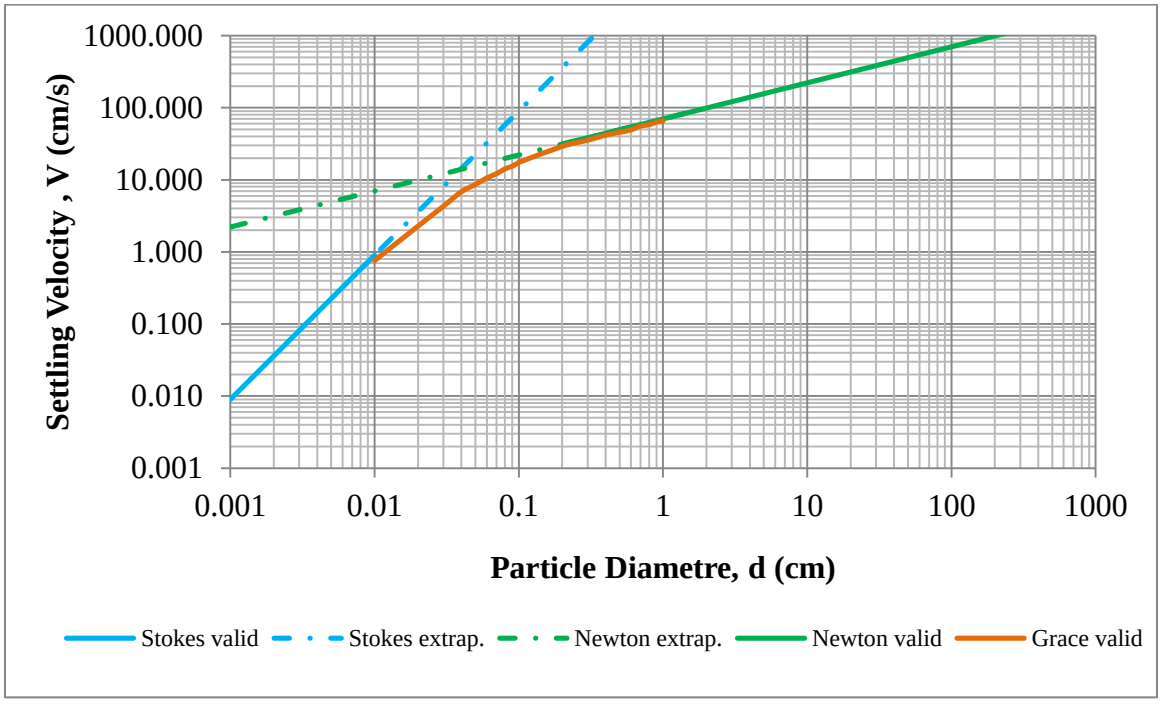

Figure 2.11 Grace method: settling velocity vs. particle diameter.

2.2.4 Hjulstrøm Envelope

Hjulstrøm (1939) performed a series a flume experiments that have direct relevance to the current ECP research. Using a one meter deep flume, he studied the entrainment velocity for a wide range of sediment sizes extending up to 100 mm in diameter (cobble-size). For the larger particles, the water velocity in combination with the rough bed assured the existence of turbulent conditions (Hjulstrøm, 1939). Thus, sediment grains move according to their mass as a direct consequence of Newton's Law. This differs from the finer textured clays, silts, and fine sands, where a laminar boundary layer and/or soil cohesion serve to protect the grain from movement.

A plot of grain size versus entrainment velocity for Hjulstrøm's results is shown in **Figure 2.12**. The curve is actually a band representing the range of data from experimental various trials. Consistent with Newton's Law, the right ascending curve has a lower slope than would be predicted by Stokes' Law. Note also the existence of a left ascending curve, which is attributed to the aforementioned effects of laminar flow and cohesion. Subsequent studies by other investigators (e.g., Sundborg, 1956) confirmed and expanded Hjulstrøm's results. Note that the Hjulstrøm curve is considered especially relevant to the current research, and it will serve as an important benchmark for field scour in ECP streambeds.

2.2.5 HEC-18

Another approach for estimating the velocity needed to erode bed sediments is to use the critical velocity equation provided in HEC-18. Critical velocity is derived by equating settling velocity with the velocity needed to keep particle suspended in the water current

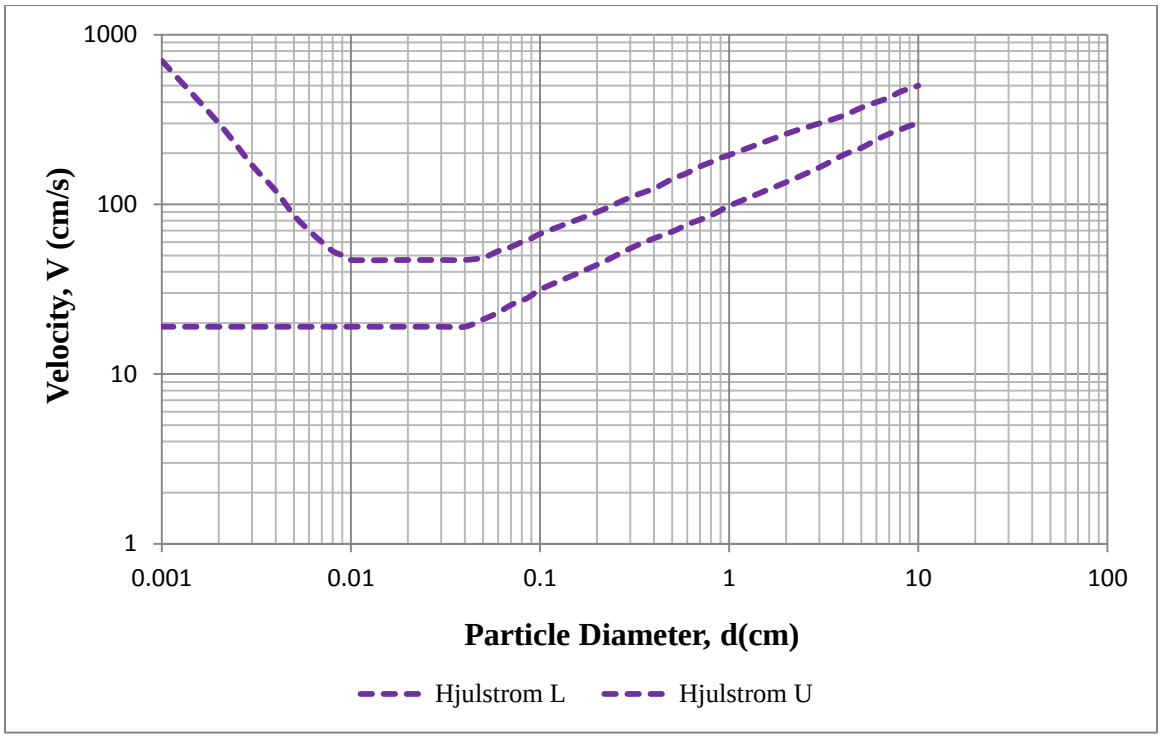

Figure 2.12 Hjulstrøm envelope: velocity vs. particle diameter.

(FHWA, 2012). The relationship, which is given below as Equation (2.5), is based on research indicating that when the approach velocity is too low to move the D_{90} size of the bed material, scour depth is reduced (Richardson & Davis, 1995).

$$V_C = K_u \times Y^{1/6} \times d^{1/3} \quad (2.5)$$

where: V_c : critical velocity (cm/sec),
Y : flow depth (cm),
d : grain size (cm), and
K_u: unit correction factor = 11.17 (ft-lb-s) = 6.19 (m-kg-s).

Based on the HEC-18 relation, critical velocity is proportional to both particle diameter and the flow depth. While velocity itself is not a force, it is often used as an index value that is related to erosive potential of the flow. Thus, for a specific particle size, the greater the depth, the higher the velocity needed to keep sediment particles in the

current. Otherwise, they will just settle to the bottom of the streambed. This is one of the reasons why clear water scour dominates in situations where there is higher flow depth.

2.2.6 U.S. Army– EM 1601

Stone riprap is the most widely used protective method to prevent scour and erosion within stream channels and around bridge structures. The most popular design method for riprap design is EM1601, which is published by the U.S. Army Corps of Engineers (USACE, 1995). Riprap is sized according to the maximum expected water velocity, and the standard also considers stone shape, size, weight, durability, gradation, and layer thickness, as well as various channel properties.

The basic design equation for selecting a representative stone size in straight or curved channels is:

$$D_{30} = S_f C_s C_V C_T\, d \times \left[\left(\frac{\gamma_w}{\gamma_s - \gamma_w}\right)^{1/2} \times \frac{V}{\sqrt{K_1 g d}}\right]^{2.5} \tag{2.6}$$

where:
S_f : safety factor,
C_s : stability coefficient for incipient failure,
C_v : vertical velocity distribution coefficient,
C_t : thickness coefficient,
d : local depth of flow (cm),
K_1 : Bank Angel Correction Factor,
Υ_w : unit weight of water, weight per volume (n/m^3),
Υ_s : unit weight of stone, weight per volume (n/m^3),
g : acceleration due to gravity (m/sec^2),
V (V_{ss}): local depth-averaged velocity, (cm/sec), and
D_{30} : riprap size of which 30 percent is finer by weight, length (cm).

In traditional riprap design, some designers prefer to specify D_{50} instead. The approximate conversion between D_{50} and D_{30} is:

$$D_{50} = D_{30} (D_{85} / D_{15})^{1/3} \tag{2.7}$$

A safety factor is normally included to compensate for small inaccuracies in these parameters. However, if conservative estimates of these parameters are used in the analysis, a safety factor is not needed, i.e., $S_f = 1.0$. In working with the Equation (2.6), it is necessary to make several "standard" assumptions with regard to the input parameters to simplify the relationship. These assumptions are summarized in **Table 2.1**.

Table 2.1 U.S. Army– EM 1601 Equation Assumptions

Variable	S_f	C_s	C_v	C_t	d (ft)	K_1	$\Upsilon_{w\ (pcf)}$	$\Upsilon_{s\ (pcf)}$
Value	1	0.3	1	1	10	1	62.4	165

Substituting the above values into Equation (2.6) yields the following two empirical equations, which are easily applied to estimate either the required riprap size given the average velocity or the "critical" average velocity corresponding to a specific particle size. Velocity and D_{30} related to each other through Equations (2.8) and (2.9).

$$D_{30} = (2.3035 \times 10^{-8}) \times V^{2.5} \tag{2.8}$$

$$V = 1135 \times D_{30}^{0.4} \tag{2.9}$$

where: V (V_{ss}) = local depth-averaged velocity (cm/sec), and
D_{30} = riprap size of which 30 percent is finer by weight (cm).

2.3 Selected Scour Equations from HEC-18

2.3.1 HEC-18 Introduction and Chronology

HEC-18 presents the state of knowledge and practice for the design, evaluation and inspection of bridges for scour. The document provides guidelines for: (1) designing new and replacement bridges to resist scour; (2) evaluating existing bridges for vulnerability to scour; (3) inspecting bridges for scour; and (4) improving the state-of-practice for estimating scour at bridges. There are two companion documents, HEC-20, entitled "Stream Stability at Highway Structures," and HEC-23, entitled "Bridge Scour and Stream Instability Countermeasures." Used in combination, these three publications summarize scour evaluation methods from studies performed by NCHRP, FHWA, State DOTs, and universities, as well as peer reviewed publications.

The 5th edition of HEC-18 (April, 2012) contains an expanded discussion on the policy and regulatory basis for the FHWA scour program, including risk-based approaches for evaluations. It also includes an updated abutment scour section, alternative procedures for estimating pier scour, and revised guidance for vertical contraction scour conditions. Those relationships that are relevant to ECP sediments will now described.

2.3.2 Contraction Scour Equation

When estimating contraction scour for ECP sediments, clear-water conditions can normally be assumed given their extreme coarseness. The presence of clear-water conditions can be double-checked using the critical velocity relation which was previously presented as Equation (2.5). If critical velocity is greater than channel

velocity, then the clear-water conditions prevail and Laursen relationship may be used to estimate contraction scour, y_s:

$$y_2 = \left[\frac{K_u Q^2}{{D_m}^{2/3} W^2}\right]^{3/7} \tag{2.10}$$

$$y_s = y_2 - y_o \tag{2.11}$$

where: y_s : average contraction scour depth,(cm),
y_2: average equilibrium depth in the contracted section after contraction scour, (cm),
y_0 : average existing depth in the contracted section, (cm),
Q : discharge through the bridge or on the set-back overbank area at the bridge associated with the width W, (cm^3/sec),
D_m : diameter of the smallest non-transportable particle in the bed material ($1.25 \times D_{50}$) in the contracted section, (cm),
D_{50} : median diameter of bed material, (cm),
W : bottom width of the contracted section less pier widths, (cm), and
K_u : 0.0077 for English units (0.025 for SI units).

2.3.3 Pier Scour Equation

Local scour around piers for coarse particle beds may be estimated using the FHWA pier scour equation, which is based upon USGS field data (FHWA, 2012). The pier scour equation is for clear-water conditions only, and it may be stated as:

$$y_s = 1.1 K_1 K_2 a^{0.62} {y_1}^{0.38} tanh\left(\frac{H^2}{1.97\sigma^{1.5}}\right) \tag{2.12}$$

where: y_s : scour depth, (cm),
K_1 : correction factor for pier nose shape (refer to Figure 7.3 and Table 7.1 in HEC-18,
K_2 : correction factor for angle of attack of flow (refer to Equation (7.4) and Table 7.2 in HEC-18,

$$K_2 = \left(Cos\theta + \frac{L}{a} Sin\theta\right)^{0.65} \tag{2.13}$$

Θ : angle of attack of the flow, degree,
A : pier width, (cm),
y_1 : flow depth directly upstream of the pier, (cm),
H = densimetric particle Froude Number,

$$H = \frac{V_1}{\sqrt{g(S_g - 1)D_{50}}} \tag{2.14}$$

V_1 : mean velocity of flow directly upstream of pier, cm/sec,
g : acceleration due to gravity (m/sec^2),
D_{50}: median bed material size, (cm),
S_g : specific gravity of bed material, and
σ : sediment gradation coefficient, (D_{84}/D_{50}).

This equation is only applicable for sediments with D_{50} > 20 mm and a gradation coefficient of σ ≥ 1.5, which ranges from 1.48 to 4.14, (USGS, 2011). Note that HEC-18 does not suggest an upper bound of particle size for which the relation is valid.

2.3.3 Abutment Scour Equation

HEC-18 does not currently contain an equation specifically for local abutment scour in coarse particle beds. The NCHRP 24-20 method, which estimates total scour at abutments, may be used (Arneson, 2012). For ECP sediments, only the clear-water version of the relationship is recommended, especially for New Jersey bridges due to their typically low contraction ratios. The relations for computing scour depth, y_s, for clear-water are provided below:

$$y_s = y_{max} - y_0 \tag{2.15}$$

$$y_{max} = \alpha_B y_c \tag{2.16}$$

$$y_c = \left[\frac{q_{2f}}{K_u D_{50}{}^{1/3}}\right]^{6/7} \tag{2.17}$$

where: y_s : abutment scour depth, (cm),
y_{max} : maximum flow depth resulting from abutment scour, (cm),

y_0 : Flow depth prior to scour, (cm),
α_B : amplification factor for clear-water conditions (refer to HEC-18 Figs. 8.11 & 8.12),
y_c : flow depth including clear-water contraction scour, (cm),
q_f : unit discharge upstream, Q/w, (cm^2/sec),
q_{2f} : unit discharge in the constricted opening, Q/w, (cm^2/sec),
K_u : 11.17 for English units (6.19 for SI), and
D_{50} : particle size with 50 percent finer, (cm).

2.4 Scour Evaluation Method (SEM)

NJIT is currently engaged in a research study funded by the New Jersey Department of Transportation (NJDOT) and the Federal Highway Administration (FHWA) focusing on bridge scour. It is the third in a series of scour grants. During the first and second grants, NJIT developed a new method for analyzing the scour risk of existing bridges known as the Scour Evaluation Model (SEM). The current research study, which is known as the Implementation Phase, is aimed at disseminating SEM into statewide practice.

In general, the New Jersey SEM is a tiered, parametric, risk-based decision tool (Schuring, 2010). In applying the model, a variety of geotechnical, hydrologic, and hydraulic data are inputted for a particular bridge (see **Figure 2.13**). Bridge importance, as reflected in the average daily traffic (ADT) and detour length, is also evaluated and factored into the final priority rating. In a final step, the priority ratings are linked to specific recommended actions, which may range from prompt repair of high risk bridges to removal of the bridge from the critical list if the bridge is deemed to be of low risk.

These data are analyzed to determine two risk levels, one geotechnical and the other hydrologic/hydraulic. The risk levels can be either “low,” “medium.” or “high.” The user then enters the risk results into a two-dimensional Risk Decision Matrix to generate a priority rating (see **Figure 2.14**). Bridge importance, as reflected in the

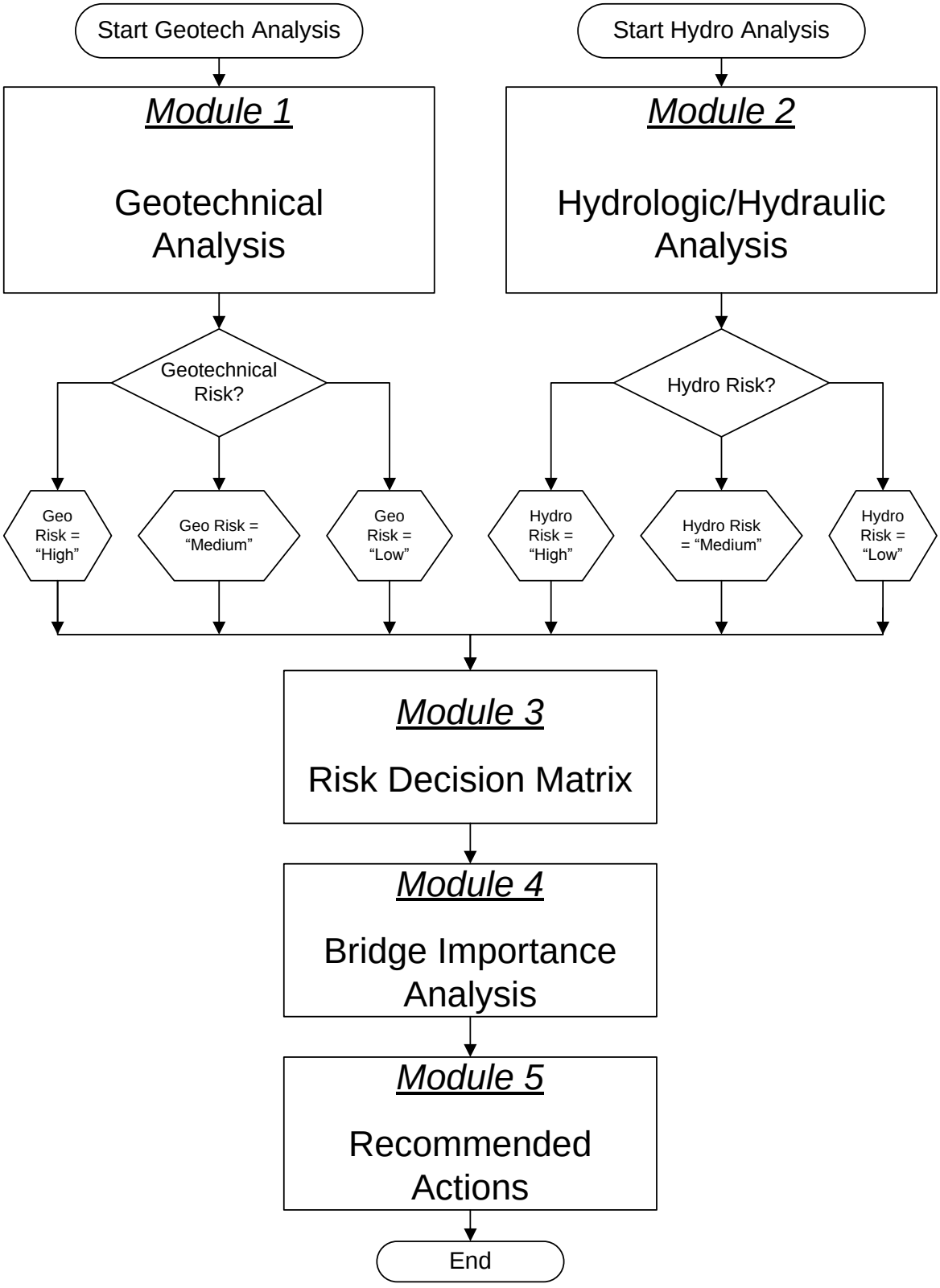

Figure 2.13 Overview flow chart of SEM modules.

average daily traffic (ADT) and detour length, is also evaluated. This leads to a final priority rating that is linked to specific recommended actions, which may include priority installation of countermeasures, real time scour monitoring, or removal from the scour critical list.

Note that some of the data analyzed for this study was extracted from field data collected during course of the three NJIT / FHWA grants.

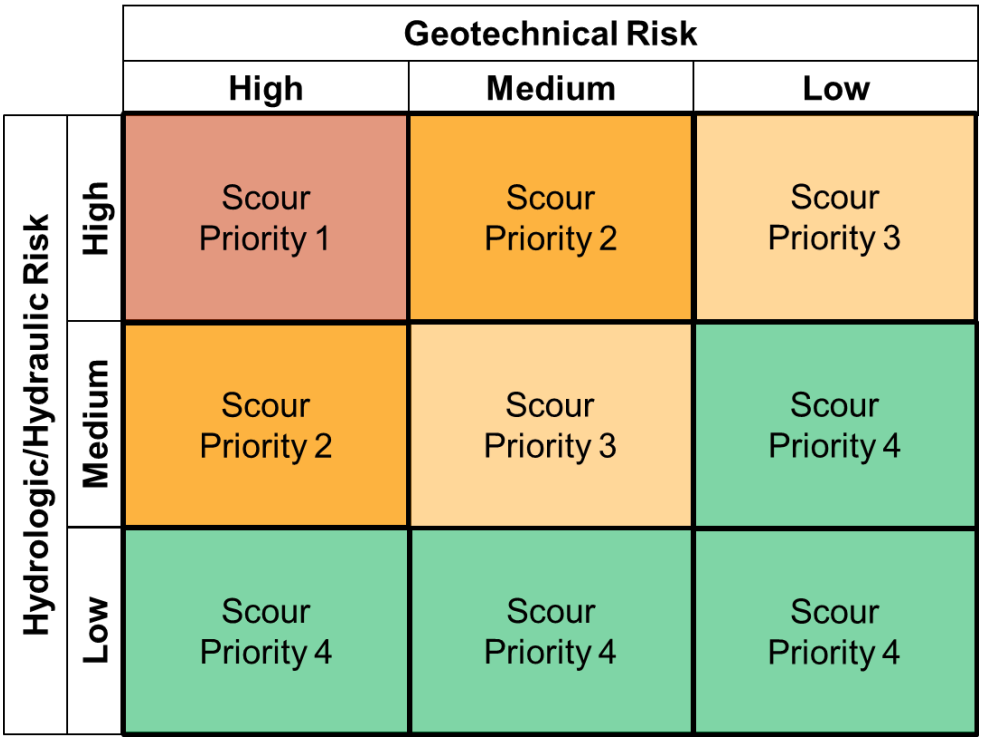

Figure 2.14 SEM two-dimensional Risk Decision Matrix.

CHAPTER 3

RESEARCH METHODOLOGY

3.1 Research Objectives and Plan

3.1.1 Overview

This research encompassed both model analyses and field studies. The work commenced by analyzing extremely coarse particles (ECP) using a blend of classical sediment transport equations and other empirical methods. Extrapolations of the relationship between critical velocity and particle diameter were made as needed since oversize particles do not necessarily conform to standard relationships.

Next, a large number of actual bridge sites were screened and a limited number selected for detailed analysis. A flow rate/velocity history of each channel was recreated, and the actual particle size distribution for each stream bed was estimated as accurately as possible. A limit analysis was then performed to reconcile the maximum historical velocity with the existing particle gradation of the stream bed.

In the final phase, a comparative analysis was conducted of the selected bridges using data regression methods and existing scour models with the objective of developing a best-fit predictive model for ECP. In addition, potential applications for the predictive model were identified and will be presented.

In summary, this research involved in four major tasks:

1. Summarize fundamental sediment transport relationships for ECP.
2. Select candidate bridge sites in Northern New Jersey and characterize sediment sizes and flow velocity histories.
3. Perform limit analysis of field erosion data.

4. Develop of a best fit predictive model and identify potential applications.

The methods for each of these research tasks are described in the following sections.

3.1.2 Summary of Fundamental Sediment Transport Relationships for ECP

This section summarizes the fundamental sediment transport relationships applicable to extremely coarse particles. The goal is to compare and contrast each method in preparation for analyzing our actual bridge data.

A composite plot of grain size versus velocity for all the transport relationship previously described in Section 2.2, Literature Search, is presented in **Figure 3.1**. The supporting data are contained in **Appendix B**.

Stokes' law shown as 'curve 1', is specifically for quartz particles in water. The limitation to the current study that is the law is valid only for sediments finer than 0.1 mm, so it is not suited for analyzing ECP. But Stokes' law is the classic approach for analyzing settling velocity, and it serves as context for the other methods.

The next relationship, Newton's law, is shown as 'curve 2' in **Figure 3.1**. Newton's law is applicable to particles with diameters greater than approximately 2 mm (very fine gravel), and so is useful for analyzing the transport velocity of ECP.

There is clearly a data gap between Stokes' law and Newton's law, which neither of the methods addresses. It occurs in the particle size range of fine sand (0.1 mm) to fine gravel (2 mm). This is the region in which Grace's method provides a smooth transition between settling velocity and particle size, which is shown as the 'curve 3' in **Figure 3.1**.

Hjulstrøm's method is the next fundamental relationship and is considered especially relevant for analyzing ECP. In **Figure 3.1**, it is appears as an envelope curve

(curve 4). Note that the Hjulstrøm envelope plots above both the Stokes' and Newton's curves because it is an entrainment velocity instead of a settling velocity. More velocity is needed to "pluck" a particle from the streambed than just to transport it.

The results for the HEC-18 method are plotted on **Figure 3.1** as 'curve 5'. Since this is an empirical design relationship, certain standard assumptions were necessary with regard to flow depth and correction factor as previously described in Section 2.2. It is apparent that HEC-18 curve is not that consistent with either Newton's method or Hjulstrøm's envelope. A main difficulty in applying the HEC-18 method to ECP is the difficulty of sampling such particles, which is being addressed in this research study.

The final sediment transport method presented on **Figure 3.1** is U.S. Army EM 1601. Again, because this is an empirical design relationship, certain standard assumptions were necessary with regard to flow depth, safety factor, etc. (see Section 2.2). It is interesting that the EM 1601 line (curve 6) nearly parallels the HEC-18 method.

In summary, the "region of interest" for this study is the area circled in blue in **Figure 3.2**. This corresponds to an approximate particle size range of 2 to 50 centimeters. Discussion will now move onto Task 2 and the selection and characterization of bridge sites.

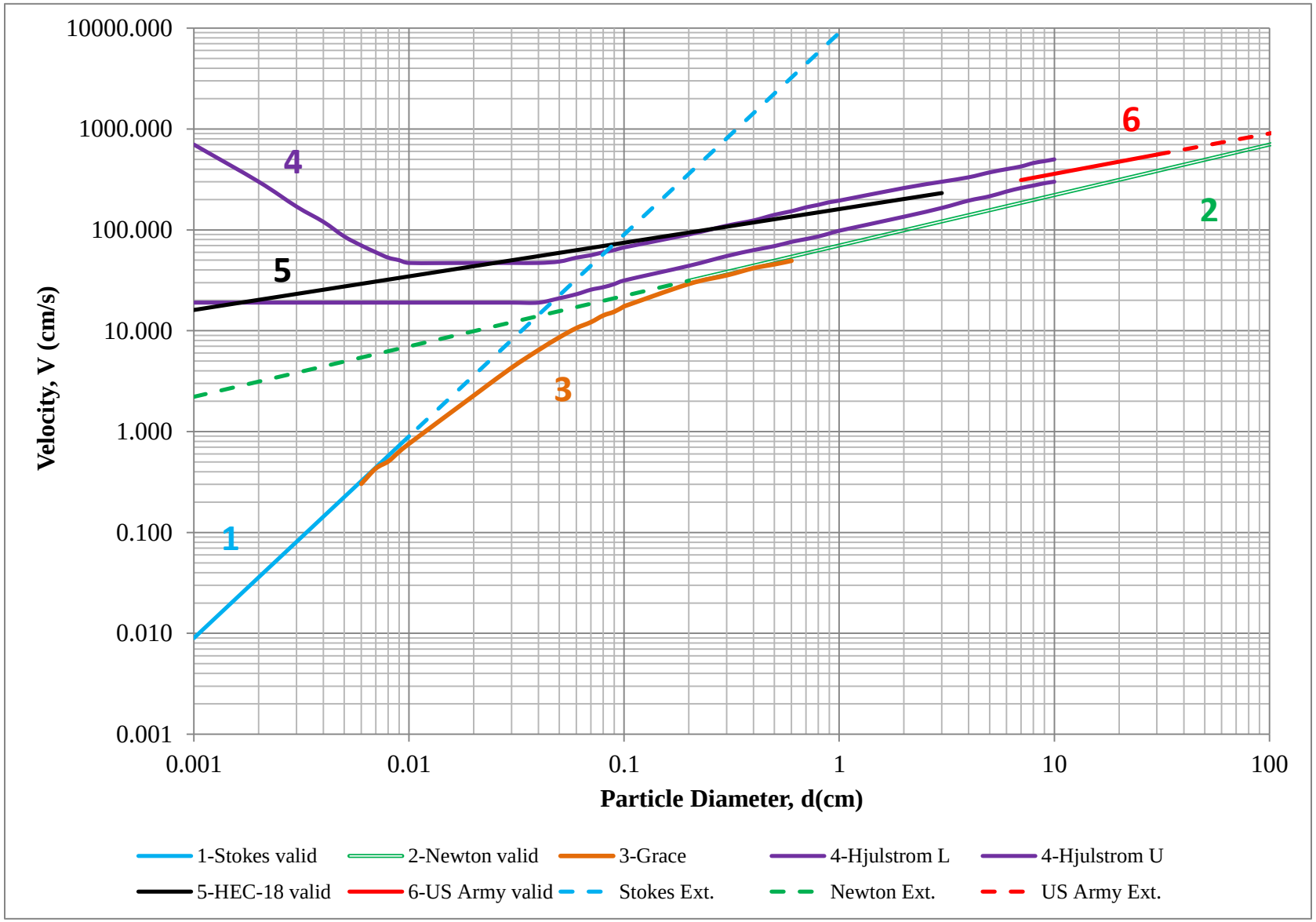

Figure 3.1 Summary of all fundamental and empirical sediment transport relationships.

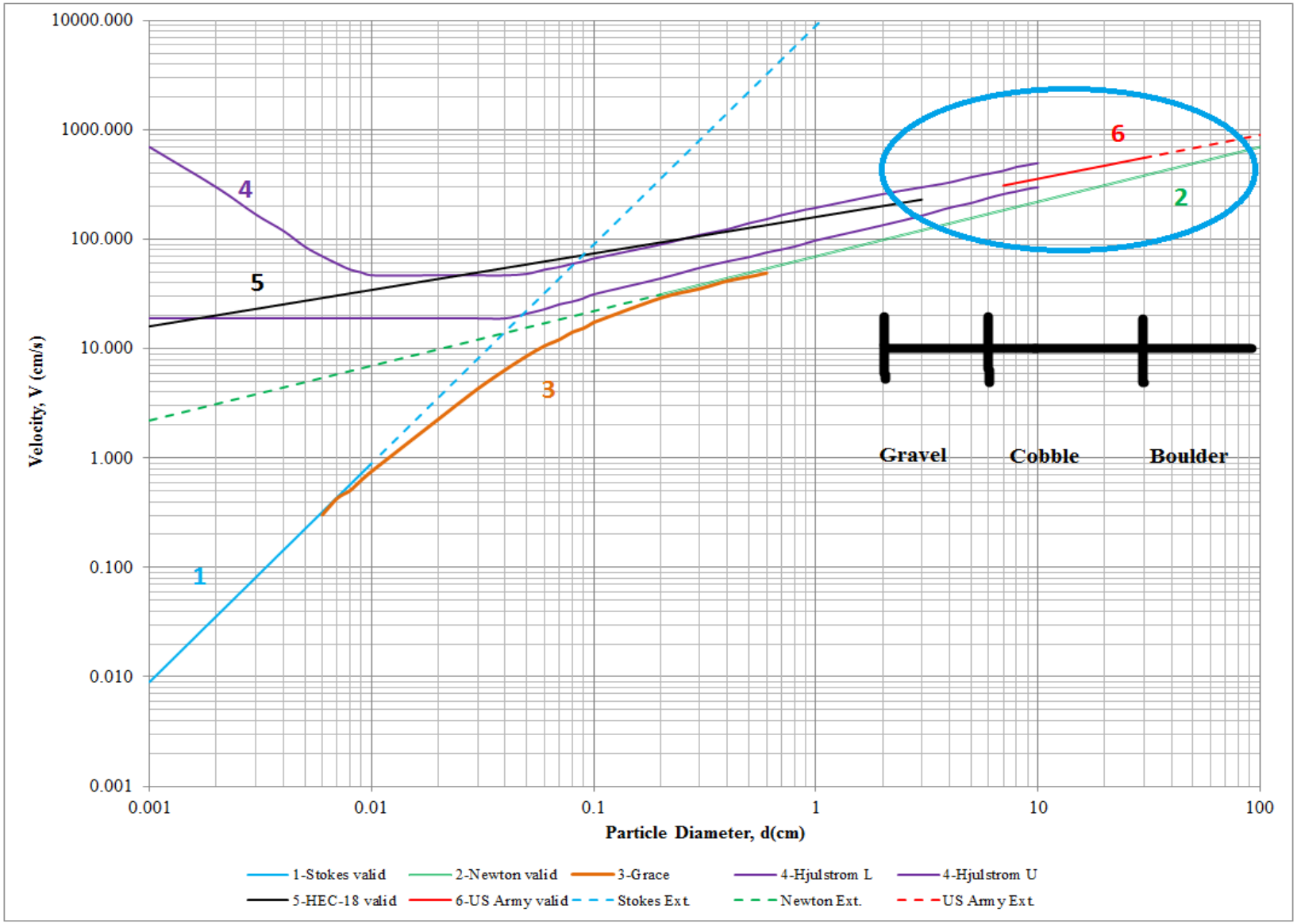

Figure 3.2 Region of interest for the current study: velocity vs. particle diameter.

3.2 Candidate Bridges

3.2.1 Bridge Selection Criteria

The Highlands and the Ridge and Valley physiographic provinces of New Jersey each contain dozens of bridges underlain by sediments that classify as ECP. Additional cases are also present in the glaciated section of the Piedmont province. During this research task, numerous bridge sites were screened for favorable characteristics, and then some selected for further study. The end goal was to identify at least ten bridges with ECP sediments for analysis.

Over the last several years, NJIT has been engaged in a research study funded by NJDOT and FHWA aimed at applying a new risk-based scour evaluation model known as SEM (see Section 2.4). During this period, both reconnaissance and field data have been collected on more than 100 scour critical bridges. It is from this database that the study bridges have been selected.

The following criteria were used during the selection process:

- The stream bed must contain ≥ 60% of particles classified as either cobbles or boulders (see **Appendix A** for definitions of particle size systems).
- The stream bed must be visible during low-water conditions, so that it can be sampled and photographed to reasonably estimate the grain size distribution.
- The stream must a have a USGS gage installed, preferably at the bridge site or in close proximity, so that accurate stream flow measurements are available.
- The USGS gage must have a sufficient flow history, preferably one that captured recent super storms Irene and Sandy.

A preliminary screening of the field reconnaissance reports was conducted to develop a list of potential bridge sites for future study. This initial screening yielded 35 bridges that appeared to satisfy some or all of the selection criteria. The result of the initial screening are listed in **Table 3.1**.

Table 3.1 Candidate Bridge Sites for Evaluation

	Bridge #	Bridge Location			Estimated Grain Size			USGS Gage	
			Township	County	Boulder %	Cobble %	Fines %	Number	Estimated Distance
1	1605-175	NJ Route 23 North over Pequannock River	W. Millford	Passaic	50	35	15	1382170	Located at the Bridge
2	2107-156	Route 46 over paulins kill	Knowlton	Warren	40	50	10	1443500	8 Miles Upstream
3	1417-157	Route 206 Over Tributary to Drakes Brook	Mt. Olive	Morris	25	60	15	01396152	0.3 Miles Downstream
4	1405-156	Route 23 over Pequannock River/ Hamburg Turnpike	W. Millford	Passaic	70	20	10	01382500	1.7 Miles Downstream
5	1605-156	NJ Route 23 South over Pequannock River	W. Millford	Passaic	65	20	15	1382500	Located at the Bridge
6	1605-162	NJ Route 23 over Pequannock River	W. Millford	Passaic	50	30	20	01382500	3.51 Miles Upstream
7	1605-167	NJ Route 23 over Pequannock River	W. Millford	Passaic	60	20	20	01382500	Regulated River
8	1605-153	NJ Route 23S over Pequannock River	W. Millford	Passaic	50	30	20	1382500	0.5 Miles Downstream
9	2111-155	Route 31 over Pequest River	White	Warren	50	30	20	1445500	1.1 Miles Upstream
10	1402-150	NJ Route 10 over Malapardis Brook	Hanover	Morris	10	50	40	1381500	2 Miles Downstream
11	1903-153	NJ Route 23 over Branch of Franklin Lake	Hardyston	Sussex	40	45	15	01367690	0.5 Miles Upstream
12	2106-164	Route 57 over Hances Brook	Mansfield	Warren	15	45	40	01399510	8.4 Miles SE
13	1912-160	Route 206 over Big Flat Brook	Sandyston	Sussex	20	50	30	1439800	Located at the Bridge
14	1605-158	NJ Route 23 North over macopin River	W. Millford	Passaic	50	20	30	01382500	0.66 Miles Upstream
15	1407-153	Route 46E over Branch of Mine Brook	Washington	Morris	35	50	15	1396152	6 Miles off Stream
16	1809-153	Route 202 over Branch of Mine Brook	Bernardsville	Somerset	5	45	50	1399100	0.6 Miles off Stream
17	1417-156	Route 206 over South Branch of Raritan River	Mt. Olive	Morris	60	25	15	1396500	0.4 Miles Downstream
18	1407-152	Route US 46 WB over Mine Brook	Washington	Morris	0	50	50	01396152	5.81 Miles West
19	1922-150	Route 15 over Beaver Run	lafayette	Sussex	10	60	30	01443280	1.66 Miles Downstream
20	1402-150	Rt. 10 over Malapardis Brook	Hanover	Morris	5	55	30	01381500	3.2 Miles Upstream

Table 3.1- (Continued) Candidate Bridge Sites for Evaluation

	Bridge #	Bridge Location			Estimated Grain Size			USGS Gage	
			Township	County	Boulder %	Cobble %	Fines %	Number	Estimated Distance
21	2108-162	Rt. 46 over Musconetcong River	Hackettstown	Warren	20	50	30	01456000	3 Miles Downstream
22	0711-150	Route 10 over Canoe Brook	Livigston	Essex	0	65	35	01379519	2.44 Miles NW
23	0709-150	Rt. 10 over Willow Meadow Brook	Livigston	Essex	0	60	40	01379519	1.5 Miles NW
24	1612-154	Route 208 Ramp A over Goffle Brook	Hawthorne	Passaic	10	60	30	01390810	4 Miles South
25	1013-152	Route 31 over Willboughby River	Clinton	Hunterdon	10	35	55	01396582	2 Miles South East
26	1810-155	Rt. 206 over Cruisers Brook	Montgomery	Somerset	5	30	65	01401650	1.11 Miles North
27	0225-166	I-80 / Market St. Main St. & Saddle River	Saddle Brook	Bergen	5	10	85	01391500	0.33 Miles Upstream
28	1912-158	Route 206 over BR Big Flat Brook	Sandyston	Sussex	10	40	50	01439800	0.1 Miles South
29	1801-153	Route 22 EB over N BR Raritan River	Bridgewater	Somerset	0	40	60	01399830	0.1 Miles Downstream
30	1304-151	Route 33 over Millstone River	Millstone	Monmouth	0	20	80	01400630	8.6 Miles Upstream
31	1304-156	Route 33 over BR Manalapan Brook	Manalapan	Monmouth	0	35	65	01405400	12.2 Miles Downstream
32	1303-155	US Route 9 over Milford Brook	Manalapan	Monmouth	5	40	55	01407290	4.82 Miles West
33	0319-152	US Route 130 over Crosswicks Creek	Bordentown	Burlington	0	15	85	01464500	4.8 Miles Downstream
34	0206-181	Route 4 over Flat Rock Brook	Englewood	Bergen	45	25	30		
35	1801-161	US Route 22 over Peters brook	Bridgewater	Somerset	5	45	50		

3.2.2 Preliminary Bridge Site Visits and Data Collection

Having a list of 35 initially selected bridges, the first phase of site visits commenced over a 14 months period from May 2015 through July 2016. During these initial bridge visits, the research team assessed general channel geometry, footing exposure, average water depth, and existing scour zones. Among all bridge and steam characteristics, particular attention was given to the bed sediments under the bridge. Field assessment was aided with the use of a six page field inspection form developed by the NJIT Scour Team that covers all aspects of scour evaluation.

A main focus of the initial visits was to establish the grain size distribution of the bed sediments. This included a careful visual estimation of the percentage of boulders, cobbles, gravel, and fines conducted. Notations were also made of any special variations in grain size. The estimated percentage of each sediment category for each of the initial 35 bridges is presented in **Table 3.1**.

3.2.3 Final Selection of Study Bridges

All data from the initial 35 bridge visits was carefully reviewed and evaluated to select the final study bridges. A principal criterion was the dominance of ECP sediments. It was also important that they be natural and not be infiltrated with displaced riprap. Another factor was geographical diversity since it was desired that all three geographic provinces present in northern New Jersey be represented. There also an attempt to include streams and watersheds of varying size.

Considering all of the above criteria, 12 bridges were finally selected for complete evaluation. These bridges are listed in **Table 3.2**.

Table 3.2 Final 12 Study Bridges

	Bridge #	Location	Province	County	Estimated Grain Size				Coordinates
					Boulder %	Cobble %	Gravel %	Fines %	
1	0709-150	NJ Route 10 over Willow Meadow Brook	Piedmont	Essex	0	30	60	10	+40° 47' 46.66", -74° 20' 35.86"
2	1809-153	NJ Route 202 over Branch of Mine Brook	Piedmont	Somerset	5	25	40	30	+40° 42' 23.52", -74° 35' 48.16"
3	0711-150	NJ Route 10 over Canoe Brook	Piedmont	Essex	0	40	40	20	40° 47' 49.56", -74° 18' 29.52"
4	1612-154	NJ Route 208 Ramp A over Goffle Brook	Piedmont	Passaic	10	60	20	10	+40° 58' 4.05", -74° 9' 12.52"
5	2108-162	NJ Route 46 over Musconetcong River	Highlands	Warren	20	50	20	10	+40° 50' 40.27", -74° 48' 38.69"
6	1605-158	NJ Route 23 NB over Macopin River	Highlands	Passaic	50	10	10	30	+41° 1' 33.69", -74° 24' 29.87"
7	1417-156	NJ Route 206 over SB Raritan River	Highlands	Morris	25	50	20	5	+40° 51' 3.81", -74° 42' 3.65"
8	1605-153	NJ Route 23 SB over Pequannock River	Highlands	Passaic	50	25	10	15	+41° 0' 48.90", -74° 23' 22.23"
9	1405-156	NJ Route 23 over Pequannock River	Highlands	Morris	70	20	5	5	+41° 0' 41.43", -74° 22' 13.85"
10	1912-160	NJ Route 206 over Big Flat Brook	Valley & Ridge	Sussex	20	50	20	10	+41° 12' 22.29", -74° 48' 12.72"
11	2107-156	NJ Route 46 over Paulins Kill	Valley & Ridge	Warren	40	50	10	0	+40° 55' 14.67", -75° 5' 17.11"
12	2111-155	NJ Route 31 over Pequest River & RR	Valley & Ridge	Warren	50	30	10	10	+40° 49' 54.02", -75° 0' 3.04"

3.3 Grain Size Distribution Approach

3.3.1 Introduction

The grain composition of the streambeds and banks is an important facet of stream character, influencing channel form hydraulics, sediment supply, and other parameters. In particular, grain size has a significant effect on the erosion behavior of stream sediments. Thus, the size distribution of the grains is also very important to how bed sediments will develop scour.

This research required an accurate assessment of the grain size distribution of the stream beds for the 12 study bridges. Four grain size analysis methods were used for each bridge to increase confidence level. As discussed previously, traditional mechanical analysis with soil sieves cannot be applied to ECP sediments due to their extreme coarseness. So, blends of traditional and innovative methods were used, including:

1. Wolman Pebble Count
2. Rosin- Rammler
3. Optical Granulometry
4. Visual Estimation

Each of these methods will now be described.

3.3.2 Wolman Pebble Count

One reasonable approach to measure the grain size of a coarse stream bed is to randomly select a significant number of particles from a streambed and analyze their sizes. This procedure is known as the "Wolman Pebble Count," which was introduced by M.G. Wolman in 1954.

A variation of the Wolman Pebble Count method was adopted for this research. The procedure was essentially as follows:

1. A tapeline is laid across a stream cross-section.
2. Samples are taken at predetermined at regular intervals along the cross-section so that 100 unique samples are taken.
3. In a two-person team, one person takes the sample and measures it, while the other records the data.
4. It is essential that the individual doing the sampling reaches down and grabs each sample without bias.
5. The particle is measured along its "intermediate" axis. If the sample is smaller than 4 millimeters, it is called out as "fines."

The Wolman Pebble Count is labor intensive. Typically, at least three different sections are analyzed owing to variations in particle size. The procedure requires picking up and measuring clasts from the streambed, with some weighting more than 20 pounds. Larger clasts that cannot be moved are examined in situ and their size estimated by extrapolation of shape. Conducting a full count takes up to a whole day depending on bridge size. It should be noted that the method has a bias towards larger particle sizes because larger particles occupy a more volume, and are therefore more likely to be encountered than smaller particles. The photos in **Figures 3.3 and 3.4** illustrate a Wolman Pebble Count in progress.

3.3.3 Rosin- Rammler

The Rosin- Rammler relationship (Rinne, 2008) originated in the field of material science to analyze the grinding and pulverization of solid materials such as powdered coal. But it has since been applied to many other types of materials, including sediments (Brezani, 2010).

Figure 3.3 Wolman Pebble Count particle selection and measurement.

The basic Rosin- Rammler distribution is given by the following equation:

$$Y(x) = e^{-(\frac{x}{x_c})^n} \tag{3.1}$$

where Y(x) is the cumulative percent retained of the particle sizes, x is the mesh size or particle size, x_c is the characteristic size of the distribution or the mean particle size (36.8% retained), and n is a measure of the spread of the particle sizes. Thus, the cumulative percent passing is given by:

$$Y(x) = 1 - e^{-(\frac{x}{x_c})^n} \tag{3.2}$$

When using the Rosin Rammler equation, the n parameter can be estimated with fitting software or by linear regression of sample data.

Figure 3.4 Wolman Pebble Count section installation, bridge # 1405-156.

3.3.4 Optical Granulometry

Optical granulometry is a technique for analyzing grain size from photographic or video-graphic images (Maerz et al. 1996). Every image must contain a known scale of reference. Recent advances in digital photography and associated software have greatly improved the capability of optical granulometry. The most common applications include material manufacturing, mining, and construction aggregates.

A proprietary software known as WipFrag was employed for this study. WipFrag is an automated, image based, granulometry system that uses digital images and automatic algorithms to identify individual blocks and create a grain image "net." It uses state of the art edge detection and also allows manual intervention (editing of the image net) to improve fidelity. WipFrag then measures the 2-D image and reconstructs a 3-D distribution using principles of stereology and geometric probability (Maerz et al. 1996).

Inherent weaknesses of WipFrag include the accumulation of errors due to block mis-identification, which can result from poor images, poor lighting, and perspective errors. Over the last few years, the NJIT Research Scour Team has been working to improve the reliability of WipFrag by: (1) taking high quality close shut pictures; (2) using a more fitted scale; (3) performing manual edge detection to avoid software edge errors; and (4) analyzing multiple pictures for each bridge and averaging the final results. To our knowledge, this is the first application of the method to analysis of stream sediments. Additional details of the method are described in **Appendix C**.

3.3.5 Visual Estimation

An experienced inspector can make a reasonable visual estimation of the percentages of boulders, cobbles, gravel, and fines present in a streambed. The count is supplemented with probing by steel rods and also shallow sampling. The results are then independently verified by a second inspector. While this is a semi-quantitative procedure, it has proven helpful in assessing stream bed texture and density, when applied consistently.

Once the percentage of each sediment category has been estimated, a grain size distribution curve is created using the following size boundaries: 300 millimeter (mm) for boulders, 160 mm for cobbles, 33 mm for gravels, and 0.5 mm for sand and silt (see USCS definitions of particle size in **Appendix A**. The visual estimation method has shown remarkably good agreement with the Wolman Pebble Count at streams where both have been applied.

3.4 Hydrologic Discharge Calculation

The maximum flow discharge and flow velocity that a bridge has experienced during its lifetime is key parameter for the limit analysis. This requires a hydrologic analysis of the river and drainage basin. The analysis method used for this research was developed by the NJIT Hydraulic Team of Dr. Robert Dresnack and research assistants James Falcetano and Thomas Bandeira. The comprehensive yet straight forward procedure is outlined in **Figure 3.5**.

The analysis begins with a reconnaissance study of available data about the bridge and its physiography. The USGS software, “StreamStats,” is next consulted to locate all the gages installed on the stream or nearby streams. Flow records of the gages are then

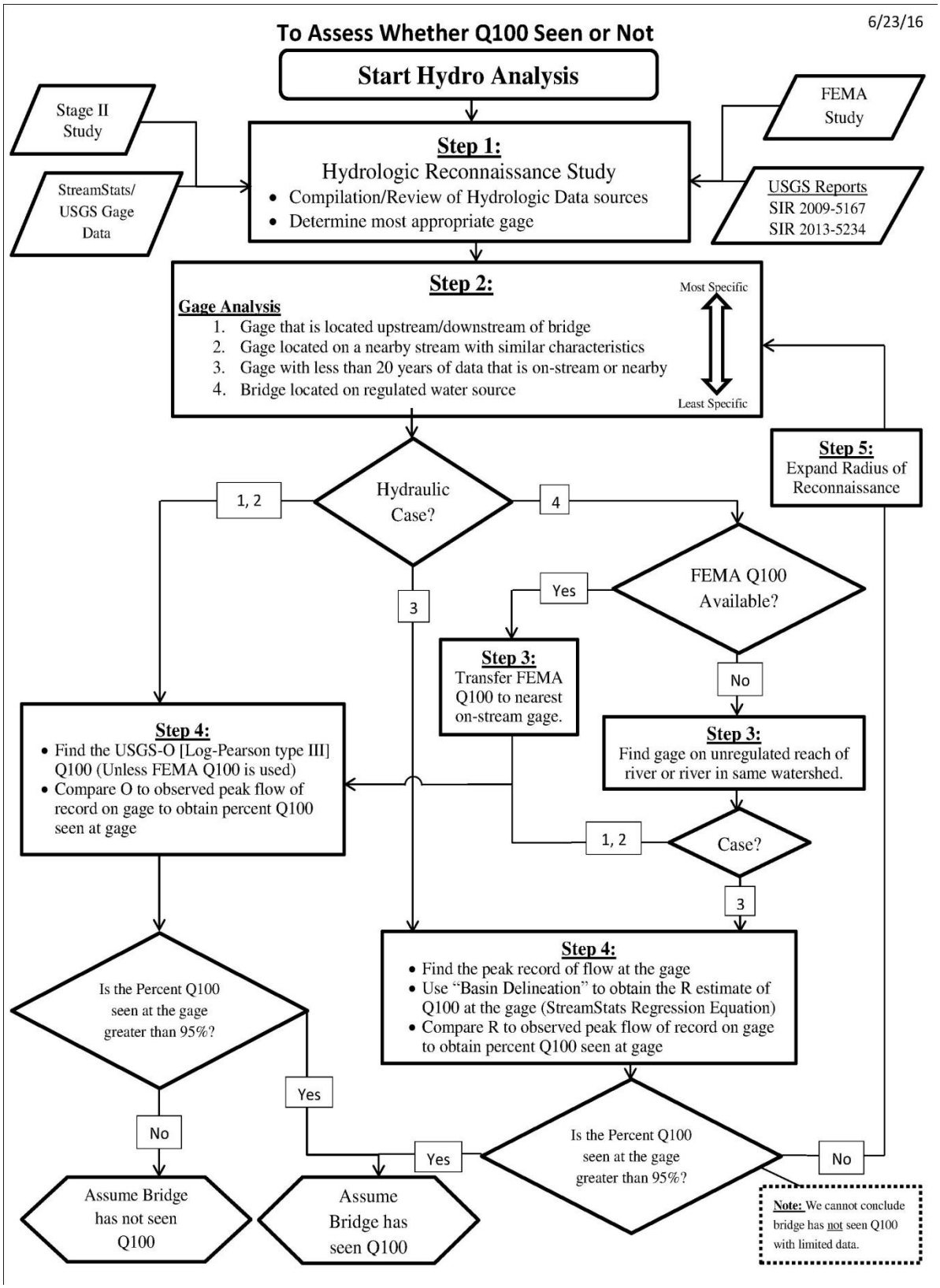

Figure 3.5 Hydrologic analysis flow chart.

checked to identify those with the longest record and highest flows. The proximity of the gage to the bridge is also considered. Three general analysis cases have been defined. The best is “case 1,” where the gage located upstream or downstream of the bridge, is fairly close, and has more than 30 years of recorded flow. “Case 2” is a situation where the gage is not installed on the same stream as the bridge, but is instead on nearby stream with similar characteristics. If a bridge is less than 30 years old or has less than 30 years of gage record on stream or on a nearby stream, the StreamStats software is used to make the estimate. This situation considered to be “case 3.” The final scenario is “case 4” where stream is regulated in some fashion or has another human improvement such as a dam, reservoir, or waste water inflow into the stream. In such situations, FEMA studies are used since they are based on regional modeling.

Over the last 12 months, the NJIT Hydraulic team has been gathering data for all the scour critical bridges in New Jersey. The hydrologic information for the 12 bridges in this study is presented in **Table 4.7** (see next chapter).

3.5 Velocity Calculation

3.5.1 Interpolation / Extrapolation from HEC-RAS Sections

The limit analysis requires that the average flow velocity through the bridge be determined as accurately as possible. In general concept, this may be determined by applying the equation of continuity. The challenge though, is knowing the flow depth and flow area, which varies because of the constriction caused by the approach embankment and bridge opening.

The most common computation tool for correlating flow depth, flow area, and velocity is HEC-RAS. This software generates 2-D, hydraulic cross sections along a river channel. Fortunately HEC-RAS analyses were available for the study bridges in the Stage II scour evaluation reports. The reports also contain extensive information about bridge location, geometry, channel sediments, and scour conditions. Hydraulic cross sections for the 50-year, 100-year, and 500-year design storms were available.

To determine the highest flow velocity ever recorded for bridge, it was first necessary to generate a plot flow rate versus velocity using the HEC-RAS results. Next, the maximum discharge (see Section 3.4) was entered into the plot. Finally, the corresponding velocity was determined by interpolation or extrapolation.

This approach to estimate velocity is considered quite reliable and was used for 10 out of 12 of the study bridges. The remaining two bridges have some flow and channel irregularities, so alternative methods were needed to estimate maximum velocity. These alternative methods were also used as double check for the interpolation/extrapolation approach, and they are described in the next section.

3.5.2 Alternative Velocity Calculations

Another approach for estimating velocity is to use the water surface elevation and channel geometry presented in the Stage II reports. This provides a base value for the bridge opening flow area. Then, dividing the maximum discharge value for each bridge by the 100-year flow area provides an alternative estimate of the maximum velocity during the history of the bridge.

A third approach to estimate velocity was to apply the Manning equation, which is the most common relationship for analyzing open channel flow. First presented in 1889

by Robert Manning, the semi-empirical equation is useful for channels and culverts where the water is open to the atmosphere and not flowing under pressure.

The Manning equation is most often expressed in the form:

$$V = K/n * R^{2/3} * S^{1/2} \quad (3.3)$$

where:

Q : flow rate, ($ft.^3/s$),
V : velocity, (ft./s),
A : flow area, ($ft.^2$),
n : Manning's roughness coefficient,
R : hydraulic radius, (A/P), (ft.), and
S : slope of water surface, (ft./ft.).
k is a unit conversion factor: k=1.49 for English units (feet and seconds). k=1.0 for SI units (meters and seconds).

For uniform flow, the slope of the water surface (or energy grade line) may be equated to the slope of the bottom of the channel. Manning's, n, varies with the roughness of the pipe, culvert, or channel. The rougher the streambed, the higher is the n value. Based on USGS study, channel roughness may be presented as:

$$n = (n_b + n_1 + n_2 + n_3 + n_4) * m \quad (3.4)$$

where

n_b : base value of n for a straight, uniform, smooth channel in natural materials,
n_1 : correction factor for the effect of surface irregularities,
n_2 : value for variations in shape and size of the channel cross section,
n_3 : value for obstructions,
n_4 : value for vegetation and flow conditions, and
m : correction factor for meandering of the channel.

In order to obtain reliable results from the Manning equation, accurate estimates of roughness, n, and slope, s, are essential. Channel roughness factors were based on field observations during the numerous visits to each bridge. Channel slope estimates using both Stage II data and direct measurement from contours on USGS quadrangle maps.

CHAPTER 4

RESEARCH ANALYSIS AND RESULTS

4.1 Grain Size Distribution Analyses

4.1.1 Wolman Pebble Count Analysis and Results

The Wolman Pebble Count is the most reliable method for measuring the grain size distribution of ECP sediments. A full Wolman Pebble Count was performed for all 12 study bridges to characterize the grain size and distribution as accurately as possible. Three cross sections were analyzed for most bridges: upstream, under the bridge, and downstream. A typical data set generated from a count presented in **Table 4.1**. For this particular bridge, the lengths of the three sections were 68 feet, 53 feet, and 23 feet and the median grain size was 13.99 cm, 14.62 cm, and 11.60 cm, respectively. Overall, the median grain size for this bridge was 13.83 cm, which falls in the range of boulder size. The final Wolman Pebble Count results for the study bridges summarized in **Table 4.2**.

4.1.2 WipFrag Analysis and Results

Although the Wolman Pebble Count is the most accurate method for grain size analysis of ECP sediments, it takes enormous amount of time to conduct the field measurement. This was the motivation for NJIT Scour Team to pursue automated image-based granulometry system. The system chosen was WipFrag, proprietary software that is faster and yet produces reliable grain size results.

Table 4.1 Wolman Pebble Count Sediment Size Measurements for Bridge # 2108-162

Up-Stream				Under Bridge - Right Span				Under Bridge - Left Span	
Section length = 68 ft				Section length = 53 ft				Section length = 23 ft	
Distance (ft)	Diameter (cm)	Distance (ft)	Diameter (cm)	Distance (ft)	Diameter (cm)	Distance (ft)	Diameter (cm)	Distance (ft)	Diameter (cm)
0	13	36	30	0	6.5	36	8	0	53
1	13.5	37	6	1	32	37	18	1	53
2	21	38	11	2	23	38	7	2	6.5
3	22	39	3	3	20	39	7.5	3	4.5
4	21	40	19	4	8	40	45	4	4
5	8.5	41	14.5	5	3	41	8	5	5.5
6	7.5	42	16.5	6	6	42	6.5	6	18
7	7.5	43	18	7	25	43	10	7	18
8	16	44	0.7	8	9	44	6.2	8	4
9	25.5	45	18	9	6	45	3	9	7
10	21	46	9	10	1.2	46	14	10	13.5
11	8	47	11	11	19	47	13	11	3.7
12	3	48	4.3	12	4.7	48	9	12	3
13	35	49	7.2	13	5.6	49	2.5	13	6
14	16.5	50	10.5	14	20	50	5	14	5.3
15	6	51	5.5	15	16	51	4.5	15	5
16	10	52	6.8	16	15	52	10.5	16	8
17	23	53	0.2	17	12	53	12.5	17	6.3
18	24	54	0.2	18	6.6			18	10
19	24	55	9.5	19	18			19	8.5
20	16	56	11.5	20	22			20	14
21	20	57	7.3	21	14			21	8
22	13	58	19	22	24			22	9
23	1	59	8	23	46			23	4.7
24	2.5	60	10.6	24	46				
25	13	61	7.3	25	35				
26	12	62	33	26	35				
27	1.3	63	33	27	6				
28	13.7	64	63	28	6.5				
29	15.5	65	63	29	39				
30	7.5	66	2.2	30	2				
31	6.3	67	2.6	31	2				
32	2.8	68	5.5	32	32				
33	23			33	17				
34	15			34	7				
35	9.5			35	9				
Section median grain size			13.99 cm			14.62 cm			11.60 cm
Overall median grain size				**13.83 cm**					

Table 4.2 Wolman Pebble Count Median Grain Size for 12 Study Bridges

	Bridge #	Location	Province	County	Wolman Sections Median Grain Size						**Median Grain Size**	Category
					Section 1	# Particles	Section 2	# Particles	Section 3	# Particles	cm	
1	0709-150	NJ Route 10 over Willow Meadow Brook	Piedmont	Essex	6.09	38	5.21	38			**5.65**	Cobble
2	1809-153	NJ Route 202 over Branch of Mine Brook	Piedmont	Somerset	6.41	23	5.2	24			**5.79**	Cobble
3	0711-150	NJ Route 10 over Canoe Brook	Piedmont	Essex	6.09	60	5.41	46			**5.80**	Cobble
4	1612-154	NJ Route 208 Ramp A over Goffle Brook	Piedmont	Passaic	14.19	30	16.02	30	8.3	31	**12.79**	Cobble
5	2108-162	NJ Route 46 over Musconetcong River	Highlands	Warren	14	69	14.62	54	11.6	24	**13.83**	Cobble
6	1605-158	NJ Route 23 NB over Macopin River	Highlands	Passaic	16.96	44	19.31	30			**17.92**	Boulder
7	1417-156	NJ Route 206 over SB Raritan River	Highlands	Morris	33.06	17	8.49	31	26.55	22	**20.13**	Boulder
8	1605-153	NJ Route 23 SB over Pequannock River	Highlands	Passaic	25.12	59	18.82	45			**22.39**	Boulder
9	1405-156	NJ Route 23 over Pequannock River	Highlands	Morris	30.58	65					**30.58**	Boulder
10	1912-160	NJ Route 206 over Big Flat Brook	Valley & Ridge	Sussex	11.56	46	12.24	45			**11.90**	Cobble
11	2107-156	NJ Route 46 over Paulins Kill	Valley & Ridge	Warren	21.02	125	13.58	76			**18.21**	Boulder
12	2111-155	NJ Route 31 over Pequest River & RR	Valley & Ridge	Warren	22.68	52	27.88	48			**25.17**	Boulder

The first step in a WipFrag analysis is to take a number of close, high quality pictures of stream bed sediments with a known scale of reference (**Figure 4.1a**). The next step is to upload the photos into the software and set the measuring scale and edge detection parameters (Blur, Threshold, and Valley threshold). The software then creates a raw net. Next, manual adjustments are made to the edge detections which produce a final net (see **Figure 4.1b**). Finally, the software generates a table and plot of the grain size distribution of the sediment (see **Figure 4.2**). Final processing of a photo takes about ten minutes. WipFrag also computes the maximum and minimum size of the particles in a given sediment photo, median grain size, X_c, as well as n value, which indicates how well or poorly graded is the sediment.

The WipFrag method also has some limitations. First, the software considers particles around the edge to be part of the picture frame. The analyzer needs to draw edges for those particles manually to avoid an error. Second, WipFrag tends to break down big particles into smaller particles during the net creation process. These are also corrected manually with a side by side comparison with the original picture. Third, small particles like gravel sometimes hide under the shadow of larger boulders and cobbles, which skews the final grain size analysis result to be coarser than it actually is. This source of error cannot be eliminated manually, but instead is handled by edge detection parameters. Fourth, it is very difficult to take clear pictures of streambeds covered by more than one foot flowing water due to reflection and refraction of light. Thus, for scour applications, WipFrag is best applied to dry streambeds.

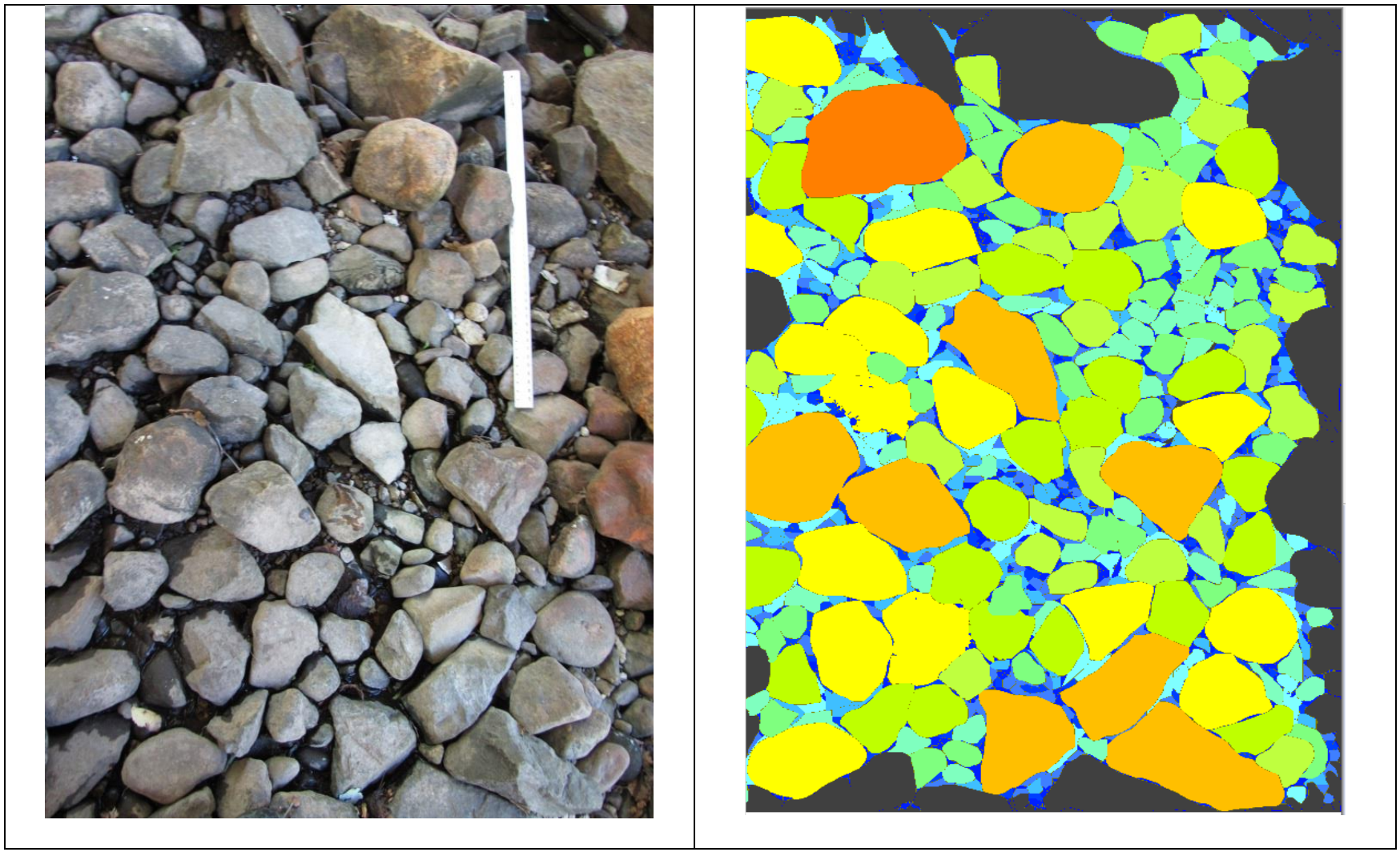

Figure 4.1 Streambed sediments photo and its WipFrag edge detection and net creation, Bridge # 1405-156.

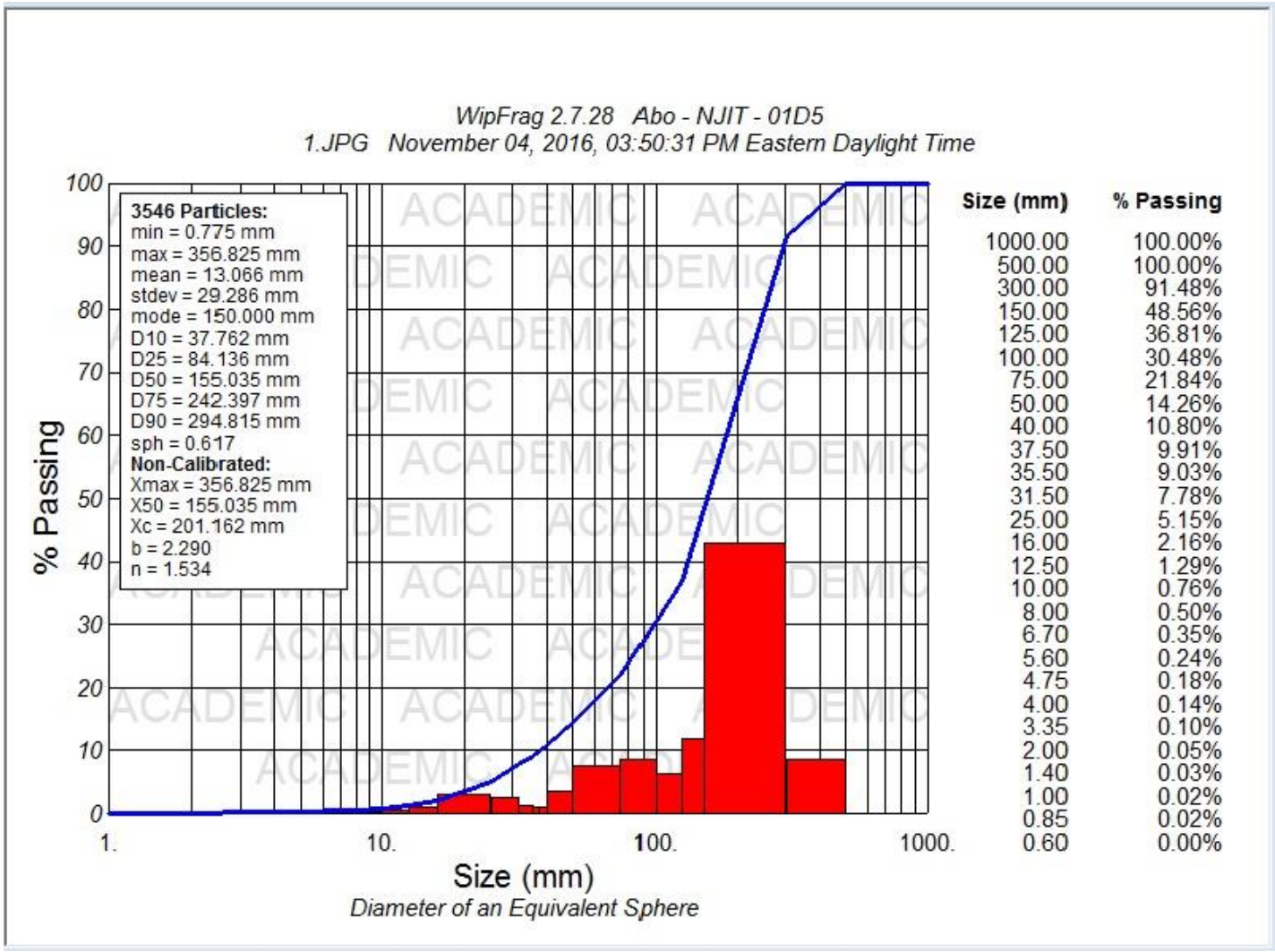

Figure 4.2 Result of WipFrag analysis for picture presented in Figure 4.1.

4.1.3 Correlating the Wolman and WipFrag Methods

In the previous sections, both the Wolman and WipFrag methods were shown to be effective in analyzing the grain size of ECP sediments. It is also desirable to know if there is consistency between the two methods. A comparative plot of grain size distributions for both is shown in **Figure 4.3** for one of the study bridges. A surprisingly close match between the Wolman Pebble Count results and the results of the manually adjusted WipFrag is indicated. One may conclude that there is good agreement and either can be used effectively.

The problem is both the Wolman Pebble Count and the manually adjusted WipFrag are labor intensive, which will discourage their use in field scour evaluations. Thus, The NJIT Geotechnical Team came up with the idea to calibrate the 'raw' WipFrag photo analysis based upon the Wolman Pebble Count and manually adjusted WipFrag. The goal was to determine an 'adjustment coefficient' based on the results for the 12 studied bridges. Having such a coefficient would allow one to find the grain size distribution in a fast and easy manner by multiplying the results of a raw, unadjusted WipFrag with adjustment coefficient, K_1.

The coefficient was derived using the 'n' parameter from Rosin-Rammler equation. Recall that the n value represents the spread or grading of the particle sizes. In general, 'n' value in the range of 0.5 to 1.5 is considered to be well graded, while range of 1.5 to 3 represents poorly graded sediment. Since the Wolman Pebble Count considered is the most accurate method, the average n value for this method was computed using the Rosin-Rammler equation for each of the study bridges. These results are shown in **Table 4.2**.

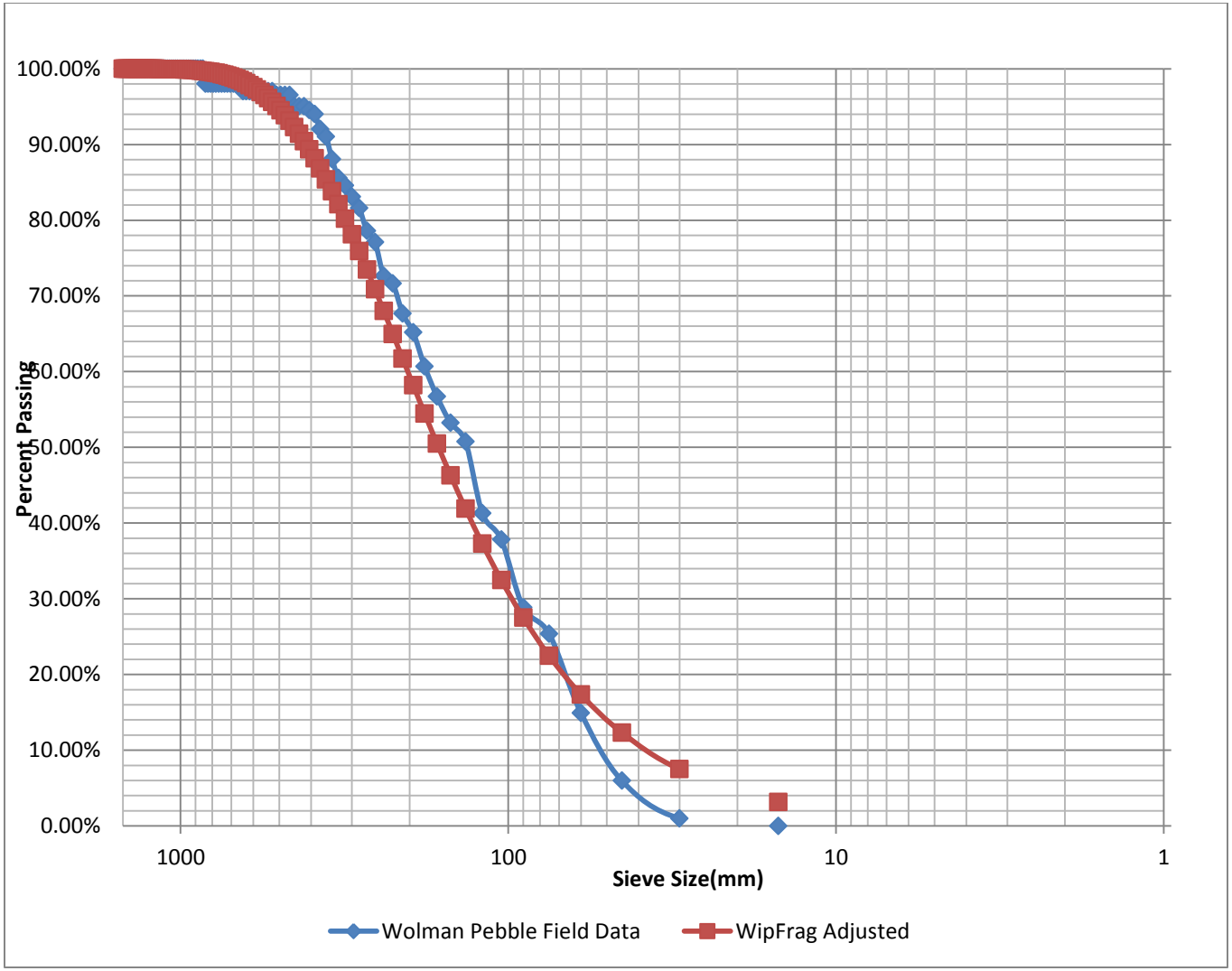

Figure 4.3 WipFrag Adjusted grain size distribution analyses, bridge # 2107-156.

In the next step, the following three parameters were defined: $K_1 = n_2/n_1$, ratio of sediment grading; $K_2 = X_{c2}/ X_{c1}$, ratio of average grain size; and $K_3 = D_{50\text{-}2} / D_{50\text{-}1}$ ratio of the 50 percent finer by size. The reliable computation of these parameters can only be done for bridges with sediments that were mostly exposed. Four study bridges met this criterion, and those results are summarized in **Table 4.3**.

An examination of **Table 4.3** indicates that for most cases, K_1, K_2, and K_3 are always larger than one. First, this means sediments are less well graded than what the raw WipFrag analysis shows. It also indicates that average sediment size is larger, since both the grain size ration (K_2) and the D_{50} ratios (K_3) are greater than one. The main reason is that the software tends to break down big particles like boulders during net creation. Similarly, D_{50} is larger than what WipFrag gives.

In conclusion, if photos are available of sediments from all around the bridge, these should be first processed by the WipFrag software. This will generate the characteristic Rosin-Rammler parameters, 'n' and 'X_c'. Finally, these should be adjusted using coefficients 'K_1' and 'K_2' to give the best possible grain size distribution as if the Wolman Pebble Count method was used.

Table 4.3 Median Grain Size 'Xc', and Grading Coefficient 'n', for the 12 Study Bridges

	1	2	3	4	5	6	7	8	9	10	11	12
Bridge #	0709-150	1809-153	0711-150	1612-154	2108-162	1605-158	1417-156	1605-153	1405-156	1912-160	2107-156	2111-155
Xc (mm)	56.49	57.92	57.98	127.86	138.29	179.16	201.30	223.91	305.80	118.99	182.05	251.73
n	1.49	1.13	1.68	1	1.22	1.52	0.78	0.98	1.38	1.35	1.38	1.06

Table 4.4 WipFrag Adjusted Coefficient Factor

	Bridge #	# Pictures	# Sections	Sediment grading factor			Median Grain Size (mm)		
				n2	n1	K1	Xc2	Xc1	K2
1	1417-156	4	1	1.12	1.08	1.03	148	59	2.62
2	1605-158	11	3	1.28	0.86	1.51	191	151	1.37
3	2107-156	18	4	1.41	1.15	1.24	199	157	1.61
4	1405-156	8	2	1.45	1.04	1.40	270	180	1.96
	Average					**1.30**			**1.89**

4.1.4 Visual Estimation Method

Before any bridge visit, NJIT Geotechnical Research Team performed a geotechnical reconnaissance of each bridge to become familiar with texture of sediments under and around the bridge. Then, during the visit, the sediments were carefully inspected. To develop a visual estimate the percentages of boulders, cobbles, gravel, and fines. An example grain size calculation for study bridge number 2111-155 is presented in **Table 4.5**.

While the visual estimation method is fast and easy to apply, the only concern is how accurate are the results compared with a more rigorous method such as the Wolman Pebble Count. A comparison of the two methods for the study bridges is shown in **Table 4.6**. On average, the visual method tends to predict median grain size by approximately 25 percent error compared with the more accurate Wolman Pebble Count method. It appears that the visual method is suitable for a quick preliminary estimate, pending a more detailed evaluation. Visual estimation results for the study bridges are presented in **Table 4.6**, and detailed calculations are presented in **Appendix C.3**.

Table 4.5 Visual Estimation Method, G.S.D. Analysis, Bridge # 2111-155

Category	Estimat	Category Median Size (mm)	Calculation	Category Average
Boulders	50%	300	300*0.5	150
Cobbles	30%	160	160*0.3	48
Gravel	10%	33	33*0.1	3.3
Sand/Silt	10%	0.5	0.5*0.1	0.05
Overall Sediment Median Grain Size				**201.35**

4.1.5 Summary of Geotechnical Results for 12 Study Bridges

As the grain size distribution of the streambed was a core part of this research, a maximum effort was directed toward its determination. The preceding sections have detailed the various grain size distribution methods, data analyses, and results for this study. **Table 4.7** presents a final summary of the median grain size 'D_{50}' that will be used in the limit analysis.

Table 4.6 Comparison of Wolman and Visual Methods

	Bridge #	Median Grain Size		Error
		Wolman	Visual	
1	0709-150	56.49	84.81	-50%
2	1809-153	57.91	81.00	-40%
3	0711-150	57.99	96.63	-67%
4	1612-154	127.86	156.94	-23%
5	2108-162	138.29	165.56	-20%
6	1605-158	179.16	163.31	9%
7	1417-156	202.99	179.84	11%
8	1605-153	223.91	197.34	12%
9	1405-156	305.8	242.47	21%
10	1912-160	118.99	165.56	-39%
11	2107-156	182.04	218.63	-20%
12	2111-155	251.73	207.31	18%
Average Error				**26.33%**

Table 4.7 Final Grain Size Distribution Results for 12 Study Bridges

	Bridge #	Location	Province	County	**Median Grain Size (cm)**
1	0709-150	NJ Route 10 over Willow Meadow Brook	Piedmont	Essex	**5.65**
2	1809-153	NJ Route 202 over Branch of Mine Brook	Piedmont	Somerset	**5.79**
3	0711-150	NJ Route 10 over Canoe Brook	Piedmont	Essex	**5.80**
4	1612-154	NJ Route 208 Ramp A over Goffle Brook	Piedmont	Passaic	**12.79**
5	2108-162	NJ Route 46 over Musconetcong River	Highlands	Warren	**13.83**
6	1605-158	NJ Route 23 NB over Macopin River	Highlands	Passaic	**17.92**
7	1417-156	NJ Route 206 over SB Raritan River	Highlands	Morris	**20.13**
8	1605-153	NJ Route 23 SB over Pequannock River	Highlands	Passaic	**22.39**
9	1405-156	NJ Route 23 over Pequannock River	Highlands	Morris	**30.58**
10	1912-160	NJ Route 206 over Big Flat Brook	Valley & Ridge	Sussex	**11.90**
11	2107-156	NJ Route 46 over Paulins Kill	Valley & Ridge	Warren	**18.21**
12	2111-155	NJ Route 31 over Pequest River & RR	Valley & Ridge	Warren	**25.17**

4.2 Velocity Analysis

4.2.1 Hydrology Calculation

The first step in determining the velocity for the limit analysis was to find the highest flow discharge ever recorded at the bridge. Following the procedures described in section 3.4, the NJIT Scour Team estimated these flows which are summarized in **Table 4.8**.

4.2.2 Estimation of Flow Velocities

As discussed in Chapter 3, the preferred method for computing maximum velocity was interpolation or extrapolation from the Stage II data. This approach uses hydraulic cross-sections generated by HEC-RAS of the channel upstream, underneath, and downstream of the bridge.

Table 4.8 Hydrologic Data, All 12 Study Bridges

	Bridge #	Location	Gage #	Bridge Location Relative to Gage	DA Bridge (mi^2)	Record Date	**Q100 at Bridge Transference (CFS)**	% Q100 Seen at Gage
1	0709-150	Rt. 10 over Willow Meadow Brook	01379520	2.44 mi NW	N/A	9/16/1999	**398**	153.3%
2	1809-153	Rt 202 Over Branch of Mine Brook	01378690	3.45 mi SW	1.38	8/28/1971	1569	82.1%
			01399525	6.43 mi W	1.38	9/16/1999	**1473**	70.1%
3	0711-150	Rt. 10 over Canoe Brook	01379519	2.44 mi NW		7/23/1954	**797**	110.1%
4	1612-154	Rt. 208 Ramp A over Goffle Brook	01390810	4 mi S	4.85	9/16/1999	**1520**	141.3%
			01389765	2 mi NW	4.85	5/16/1990	1764	83.9%
5	2108-162	Rt. 46 over Musconetcong River	01456000	3 mi Downstream	75.7	8/19/1955	**5290**	96.0%
			01457000	17.47 mi Upstream	75.7	1/25/1979	5286	94.4%
6	1605-158	Rt. 23 NB over Macopin River	01382500	0.66 mi Upstream	5.33	8/28/2011	**1248**	80.8%
7	1417-156	Rt. 206 over SB Raritan River	01396152	0.3 mi Downstream	2.21	8/28/2011	**1360**	204.8
8	1605-153	Rt. 23 SB over Pequannock River	01382500	01382500	63.7	4/5/1984	**5384**	90.5%
9	1405-156	Rt. 23 over Pequannock R./Hamburg Turnpike	01382500	1.7 mi Downstream	67.3	4/5/1984	**5572**	90.5%
10	1912-160	Rt. 206 over Big Flat Brook	0144000	11 mi Upstream	23.8	8/28/2011	4339	131.1%
			01439800	At bridge	23.8	8/19/1955	**4490**	145.3%
11	2107-156	Rt. 46 Over Paulins Kill	01443500	9.15 mi Downstream	177	9/8/2011	**7837**	101.7%
			01443500	9.15 mi Downstream	177	8/19/1955	7837	136.4%
12	2111-155	Rt. 31 over Pequest River	01445500	1.1 mi Downstream	114	9/8/2011	**2461**	100.5%

A summary of HEC-RAS flow discharges and velocities for the 50, 100, and 500 year storms is given in **Table 4.9**. These data were plotted to establish the trends of discharges, 'Q', versus velocity, 'V'. The resulting trend lines for each of the study bridges are presented in **Figure 4.4**. Next, the maximum recorded flow discharge (see **Table 4.7**) was plotted on the corresponding trend line for each bridge. In a final step, the maximum velocity, V_{Limit}, was estimated by interpolation or extrapolation.

Because of certain flow and channel irregularities, alternative methods were applied for two of the study bridges. Note that these methods were also used for a reasonableness check of the interpolation/extrapolation approach described above. The first alternative method involved scaling the flow areas from the Stage II reports to NJIT's maximum discharges. The second method involved Manning's equation as detailed in Section 3.5.3. This required estimation of two key parameters, namely the channel roughness coefficient, 'n', and the slope of the channel,'s'. The roughness coefficient depends on the size and gradation of the streambed sediments, as well as other channel characteristics including degree of irregularity, variation in cross section, effect of obstructions, amount of vegetation, depth of the flow, and degree of meandering. A thorough study of channel characteristics was undertaken for each of the 12 study bridges, and these are summarized in **Table 4.10**. The table also contains the final values of 'n' used for the study.

The other sensitive Manning parameter is slope of the channel. In most cases, the HEC-RAS sections provided values of slope. But given the importance of this parameter it was decided to also compute slope from a USGS quadrangle map. The advantage is this provides the slope over a longer reach of the stream than the HEC-RAS data. Thus, it is

Table 4.9 Interpolation and Extrapolation of Discharge and Velocity Values

	Bridge #	Q50	V50	Q100	V100	Q500	V500	Q limit	V limit	V limit
		cfs	ft/s	cfs	ft/s	cfs	ft/s	cfs	ft/s	cm/s
1	0709-150	600	9.91	720	9.96	1200	12.77	610	**9.92**	**302**
2	1809-153	430	8	545	8.2	920	8.5	1033	**9**	**274**
3	0711-150	1150	11.47	1405	12.26	2200	14.15	877	**8.04**	**245**
4	1612-154	1525	8.24	1920	9.29	2945	12.01	2148	**9.9**	**302**
5	2108-162	2450	4.58	2926	6.03	4264	8.61	5078	**10.17**	**310**
6	1605-158	1446	11.38	2059	12.75	3500	15.21	1008	**9.9**	**302**
7	1417-156	984	30.92	1215	31.92	2065	33.83	2785	**43.1**	**1314**
8	1605-153	2602	13.77	3440	14.86	5200	17.15	4873	**16.8**	**512**
9	1405-156	3515	10.03	4265	10.84	6285	13.77	5043	**12**	**366**
10	1912-160	1969	6.12	2398	7.2	3395	7.84	6524	**10**	**305**
11	2107-156	6783	11.76	8117	11.77	11939	11.8	10690	**11.77**	**359**
12	2111-155	2010	5.1	2372	5.5	3025	6	2473	**5.7**	**174**

likely more representative of actual slope. The procedure requires two consecutive contour lines of elevation that span the bridge to establish ‘rise’. Next, the distance between these contours is measured along the curvature of the channel to establish the ‘run’.

Finally, dividing the rise in elevation over the run of the channel results in the channel slope. A sample quadrangle map calculation for bridge number 1605-153 is presented in **Figure 4.5**. The slope calculation results for all 12 study bridges are presented in **Table 4.11**.

4.2.3 Summary of Velocity Analysis

Determination of maximum velocity was another core part of this research. Utilizing the historic maximum discharges provided by the NJIT Hydraulic Team, the limit velocities for all 12 of the study bridges were computed. The final results of the velocity calculation are presented in **Table 4.12**.

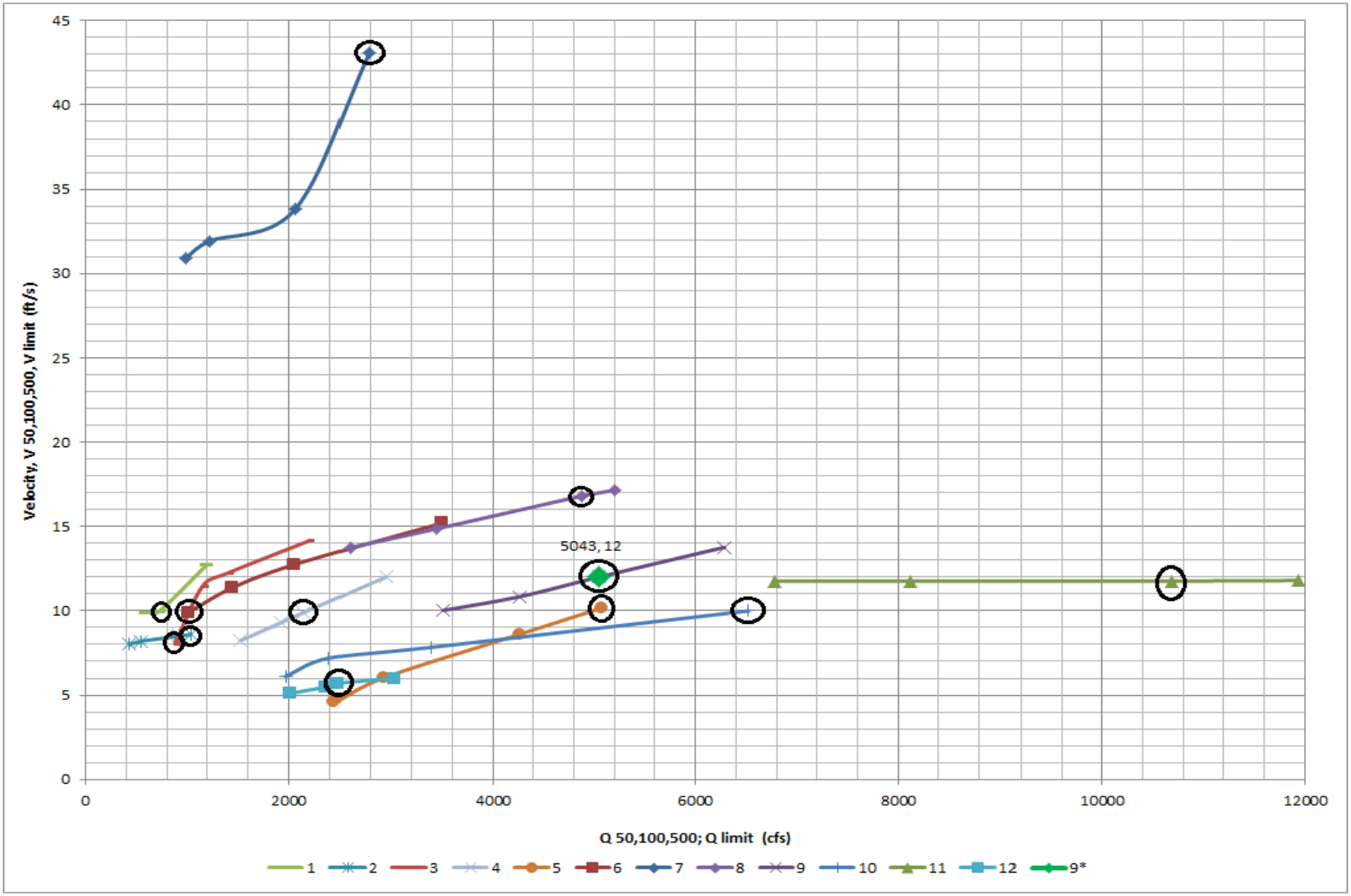

Figure 4.4 Trend line, flow discharge vs. velocity.

Table 4.10 Manning's Roughness Coefficient

	Bridge #	"n" Base Range	Base Value	Degree of Irregularity			Variation in Ch. Cross-section		Effect of Obstruction		Amount of Vegetation		Deg. of Meandering		Add up	Initial "n"	Final "n"
			Nb	n1			n2		n3		n4		m				
				Range	Value	Reason	Range	Value	Range	Value	Range	Value	Range	Value			
1	0709-150	0.028 - 0.035	0.03	0.001-0.005	0.001	L. migration	0	0	0.000-0.004	0.001	0.002-0.01	0.002	Minor	1	0.004	0.034	**0.034**
2	1809-153	0.028 - 0.035	0.03	0.001-0.005	0.001	L. migration	0	0	0.000-0.004	0	0.002-0.01	0.005	Minor	1	0.006	0.036	**0.036**
3	0711-150	0.028 - 0.035	0.03	0.001-0.005	0.001	L. migration	0	0	0.000-0.004	0	0.002-0.01	0.003	Minor	1	0.004	0.034	**0.034**
4	1612-154	0.03 - 0.05	0.035	0.001-0.005	0.001	L. migration	0	0	0.000-0.004	0.001	0.002-0.01	0.002	Minor	1	0.004	0.039	**0.039**
5	2108-162	0.03 - 0.05	0.035	0.001-0.005	0.003	Slope	0.001 - 0.005	0.002	0.000-0.004	0.004	0.002-0.01	0.005	Minor	1	0.014	0.049	**0.049**
6	1605-158	0.03 - 0.05	0.04	0.001-0.005	0.002	Flow depth low	0	0	0.000-0.004	0.002	0.002-0.01	0.002	Minor	1	0.006	0.046	**0.046**
7	1417-156	0.03 - 0.05	0.045	0.001-0.005	0.001	L. migration	0	0	0.000-0.004	0.002	0.002-0.01	0.002	Appreciable	1.15	0.005	0.05	**0.058**
8	1605-153	0.03 - 0.05	0.045	0.001-0.005	0.005	L. migration; Slope	0	0	0.000-0.004	0.002	0.002-0.01	0.002	Minor	1	0.009	0.054	**0.054**
9	1405-156	0.04 - 0.07	0.055	0.006-0.01	0.006	L. migration; Slope	0.001 - 0.005	0.005	0.000-0.004	0.004	0.002-0.01	0.002	Minor	1	0.017	0.072	**0.072**
10	1912-160	0.03 - 0.05	0.035	0.001-0.005	0.001	L. migration	0.001 - 0.005	0.001	0.000-0.004	0.002	0.002-0.01	0.003	Minor	1	0.007	0.042	**0.042**
11	2107-156	0.03 - 0.05	0.04	0.001-0.005	0.001	Slope	0	0	0.000-0.004	0.004	0.002-0.01	0.002	Minor	1	0.007	0.047	**0.047**
12	2111-155	0.04 - 0.07	0.05	0.001-0.005	0.005	Slope	0	0	0.000-0.004	0.002	0.002-0.01	0.003	Minor	1	0.01	0.06	**0.060**

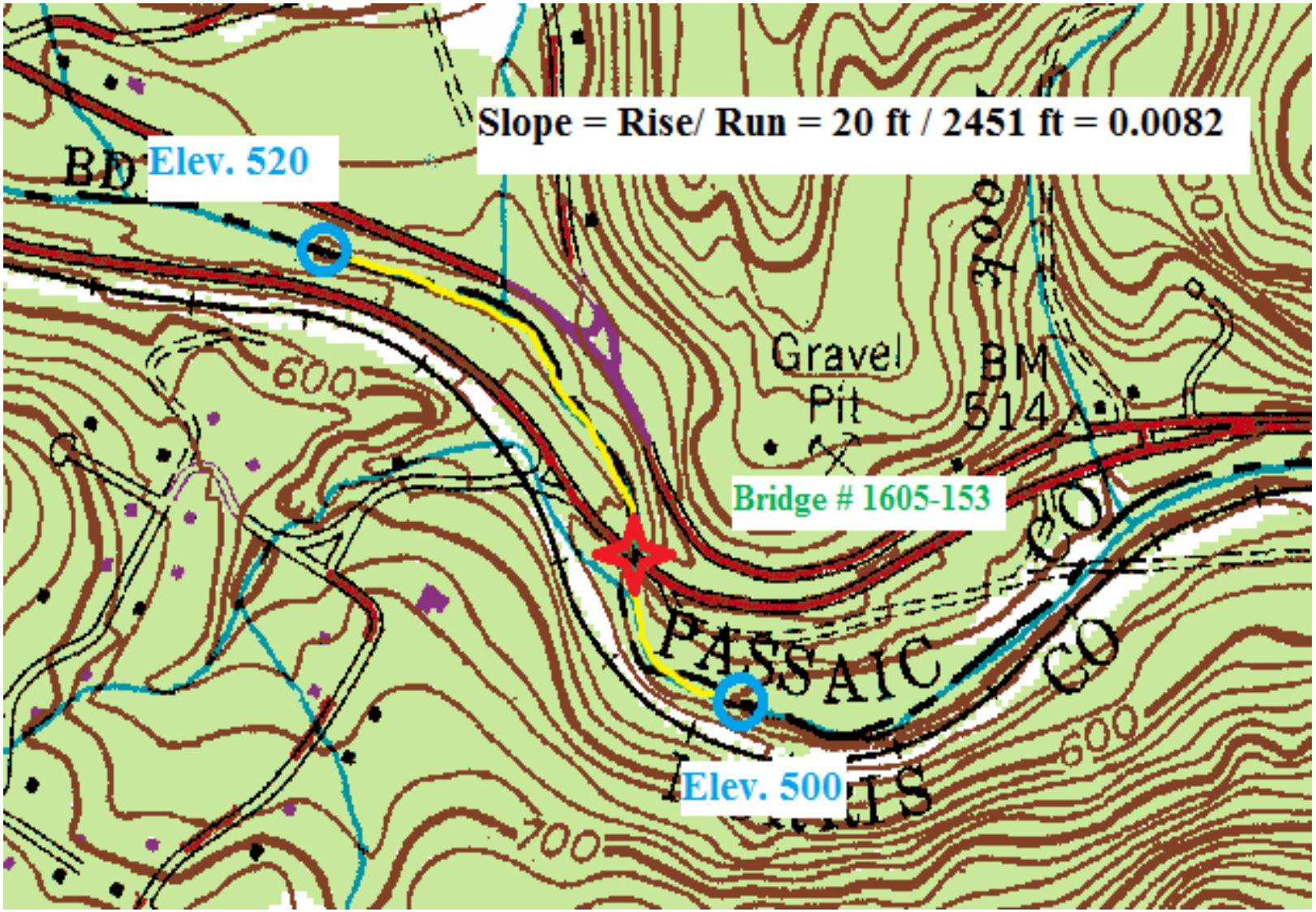

Figure 4.5 Geotechnical quadrangle map, bridge # 1605-153.

Table 4.11 Stream Slope through Geotechnical Quadrangle Maps

	Bridge #	Contour			Distance				**Slope**
		Upstream	Downstream	Value	Scale			Length (ft)	ft/ft
		a	b	c = a-b	d	e = 5280/d	f- Scale	g = e*f	s = c / g
1	0709-150	190	180	10	149 S = 1 M	35.44	42	1488	**0.0067**
2	1809-153	280	260	20	256 S = 1 M	20.63	46	949	**0.0211**
3	0711-150	320	300	20	124 S = 1 M	42.58	68	2895	**0.0069**
4	1612-154	120	110	10	208 S = 1 M	25.38	56	1422	**0.0070**
5	2108-162	520	500	20	204 S = 1 M	25.88	144	3727	**0.0054**
6	1605-158	620	600	20	210 S = 1 M	25.14	46	1157	**0.0173**
7	1417-156	800	780	20	304 S = 1 M	17.37	40	695	**0.0288**
8	1605-153	520	500	20	252 S = 1 M	20.95	117	2451	**0.0082**
9	1405-156	460	440	20	252 S = 1 M	20.95	64	1341	**0.0149**
10	1912-160	540	520	20	176 S = 1 M	30.00	80	2400	**0.0083**
11	2107-156	300	280	20	60 S = 1 M	88.00	344	30272	**0.0007**
12	2111-155	380	360	20	147 S = 1 M	35.92	136	4885	**0.0041**

Table 4.12 Summary of Velocity Analysis for 12 Study Bridges

	Bridge #	Location	Province	Q limit (cfs)	V limit (cm/s)
1	0709-150	NJ Route 10 over Willow Meadow Brook	Piedmont	610	**273**
2	1809-153	NJ Route 202 over Branch of Mine Brook	Piedmont	1033	**262**
3	0711-150	NJ Route 10 over Canoe Brook	Piedmont	877	**245**
4	1612-154	NJ Route 208 Ramp A over Goffle Brook	Piedmont	2148	**302**
5	2108-162	NJ Route 46 over Musconetcong River	Highlands	5078	**310**
6	1605-158	NJ Route 23 NB over Macopin River	Highlands	1008	**302**
7	1417-156	NJ Route 206 over SB Raritan River	Highlands	2785	**399**
8	1605-153	NJ Route 23 SB over Pequannock River	Highlands	4873	**512**
9	1405-156	NJ Route 23 over Pequannock River	Highlands	5043	**366**
10	1912-160	NJ Route 206 over Big Flat Brook	Valley & Ridge	6524	**305**
11	2107-156	NJ Route 46 over Paulins Kill	Valley & Ridge	10690	**359**
12	2111-155	NJ Route 31 over Pequest River & RR	Valley & Ridge	2473	**549**

CHAPTER 5

LIMIT ANALYSIS AND APPLICATIONS

5.1 Limit Analysis and Summary of Results

The most unique aspect of this research is it converts a real stream channel into an experimental flume. This eliminates the need to use scaling factors or other corrections as is done with laboratory flume studies. The other singular aspect of this research is that it is believed to be the first erosion study that has focused solely on extremely coarse particles. Mostly, this is because of the difficulty in measuring the grain size of such large sediments reliably. Fortunately, access to a significant database of flow and particle size data from the ongoing NJDOT / FHWA scour research project has made this study possible.

This section begins with a summary of experiments results, which are then used to perform a limit analysis. The basic premise is the sediments found in and around the bridge at present reflect the maximum historic flow and velocity in the stream channel. The end goal is to define a limit relationship between maximum velocity and median grain size for ECP sediments.

The geotechnical characteristics and grain size distribution of the sediments were previously investigated and analyzed using three different methods. The median grain size finally selected for each of the 12 study bridges is presented in **Table 5.1**. It varies over a wide range from 5 centimeters, which correspond to medium gravel, up to 31 centimeters, representing large cobbles and medium-size boulders. A grain size distribution curve for each bridge streambed sediments is presented in **Figure 5.1,** and the supporting tabular data are contained in **Appendix C**.

Table 5.1 Summary of Data for Limit Analysis

	Bridge #	Median Grain Size	Q limit	V limit
		cm	cfs	cm/s
1	0709-150	5.65	610	273
2	1809-153	5.79	1033	262
3	0711-150	5.80	877	245
4	1612-154	12.79	2148	302
5	2108-162	13.83	5078	310
6	1605-158	17.92	1008	302
7	1417-156	20.13	2785	399
8	1605-153	22.39	4873	512
9	1405-156	30.58	5043	366
10	1912-160	11.90	6524	305
11	2107-156	18.21	10690	359
12	2111-155	25.17	2473	549

The stream gage records for each bridge site were analyzed to determine the flow rate history as accurately as possible. Interestingly, Hurricane Irene caused the maximum flow discharge for a number of the study bridges. The maximum recorded discharge for each of the studied bridges presented in **Table 4.7**. Using these discharges, maximum stream velocities were determined using three different methods as described in Chapter 4. In general, the interpolation/extrapolation of HEC-RAS data appeared to give the most accurate value of velocity. The final maximum flow velocities calculated for the study bridges are also presented in **Table 5.1**.

Equipped with the median particle size and maximum velocity for each bridge, a limit analysis was performed by plotting them on a log-log scale. For reference purposes, the limit analysis data have been superimposed over the classic sediment transport

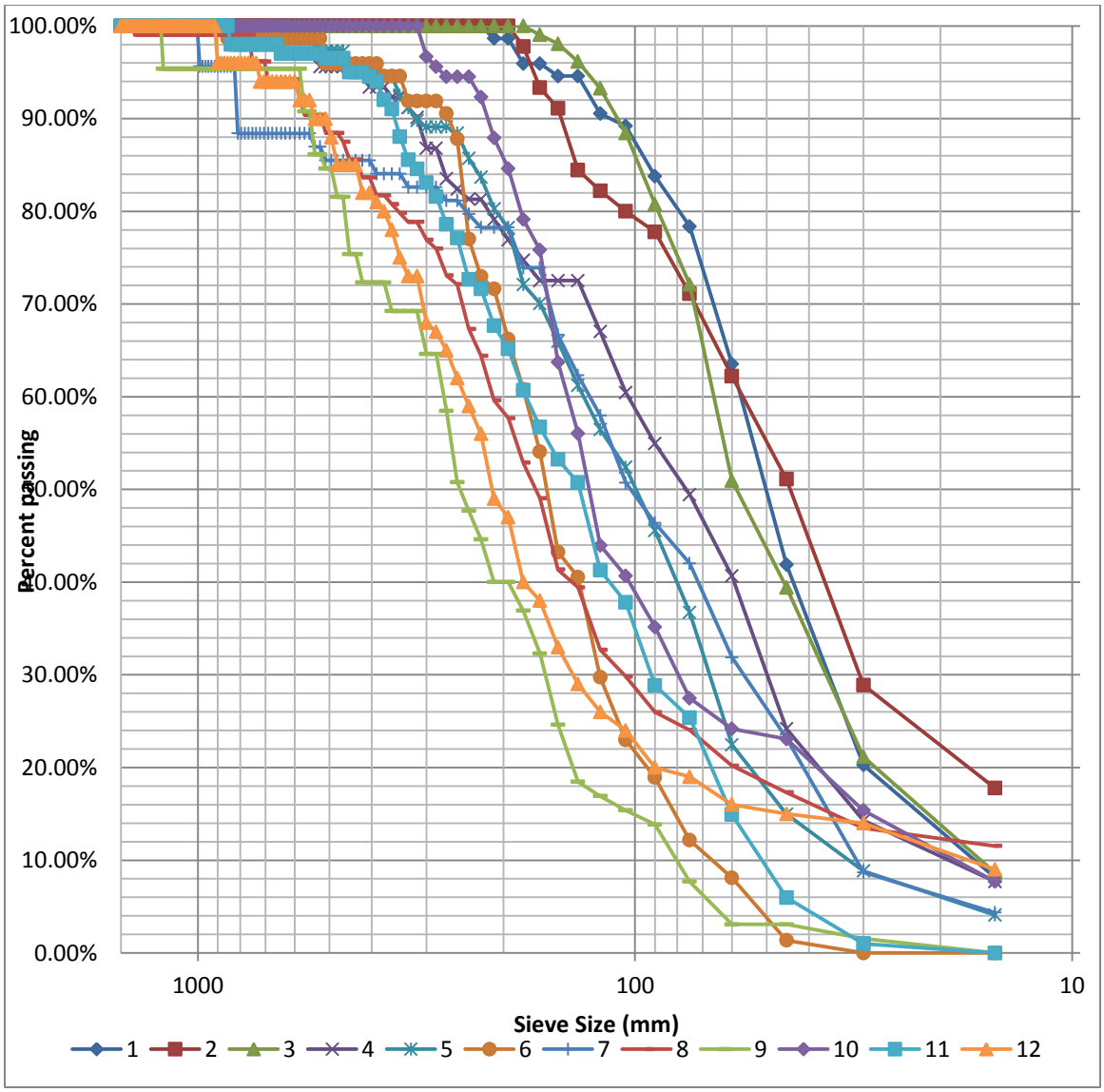

Figure 5.1 Grain size distribution for 12 study bridges.

relationships previously discussed in Chapter 3. The results are shown in **Figure 5.2**. At first glance, the results of the limit analysis appear to be generally consistent with the other transport methods.

Figure 5.3 provides an enlarged detail of the region of interest for ECP sediments. This allows a better comparison of the limit data with the reference data. The

first thing to notice is there are very few classic transport relationships within the range of the limit analysis. It is also observed that all except one of the study bridges fall above Newton's Law. The likely explanation is Newton's Law describes the theoretical behavior of a single particle within a fluid, while the data from this research represents particles that are packed together in a bed. The fact that the bridge data are higher suggests that more velocity is required to disconnect a particle from its neighbors. In addition, examination of **Figure 5.2** shows that the limit data mostly plot lower than the U.S. Army practical design equation. This suggests that the two relationships are less conservative for the ECP sediments than the limit analysis. That is, for a given grain size, this research indicates entrainment occurs at lower stream velocity than U.S. Army. The impact of this will be further discussed in the application discussion (Section 5.3).

In summary, the limit analysis provides a realistic relationship between limit (entrainment) velocity and particle size for ECP sediments. It is expected that over the history of the bridge, all the finer particles have been winnowed out and transported downstream. The grain size of the particles remaining behind provides a good measure of the actual resistance of sediments to future flow velocities.

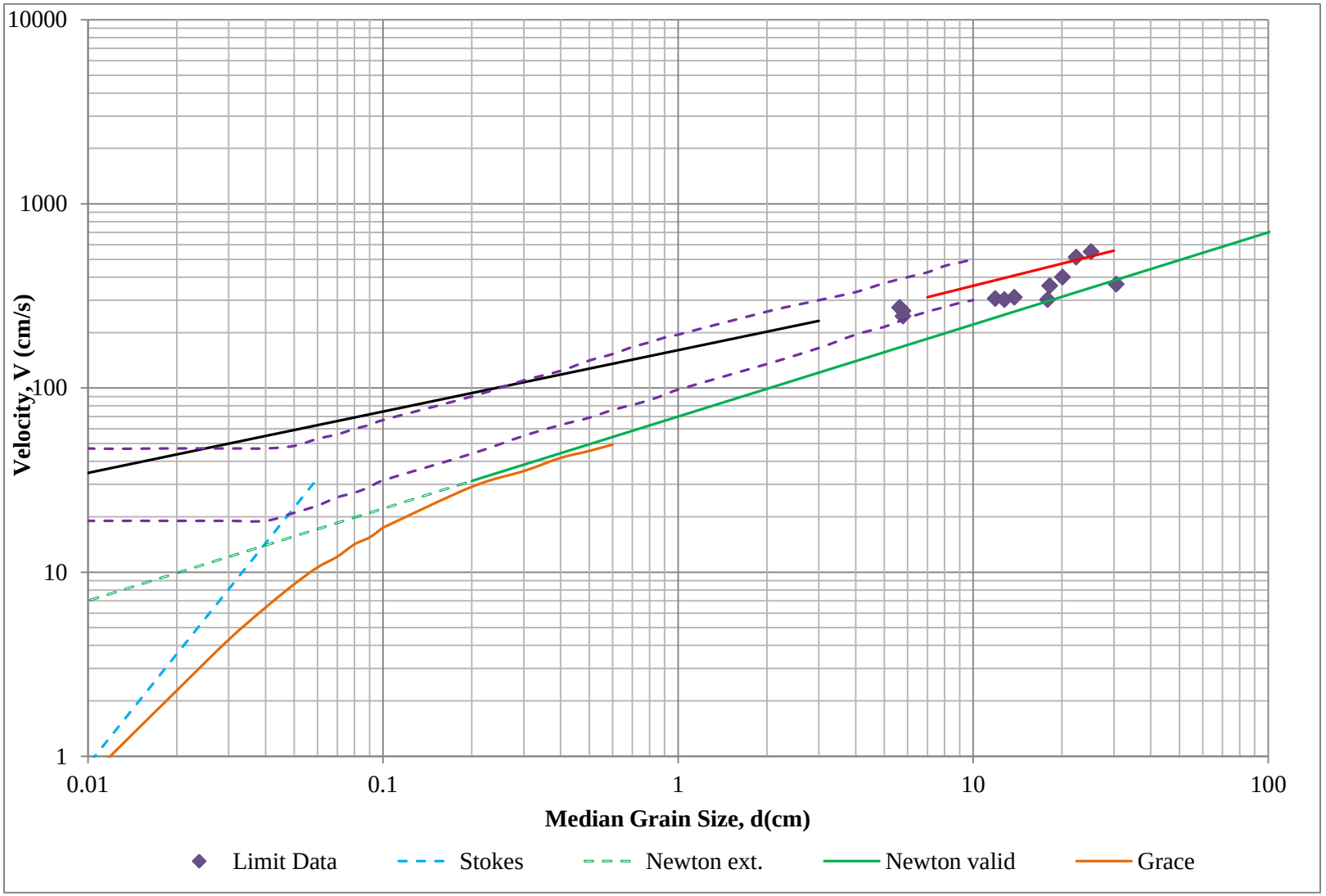

Figure 5.2 Limit data velocity vs. median grain size.

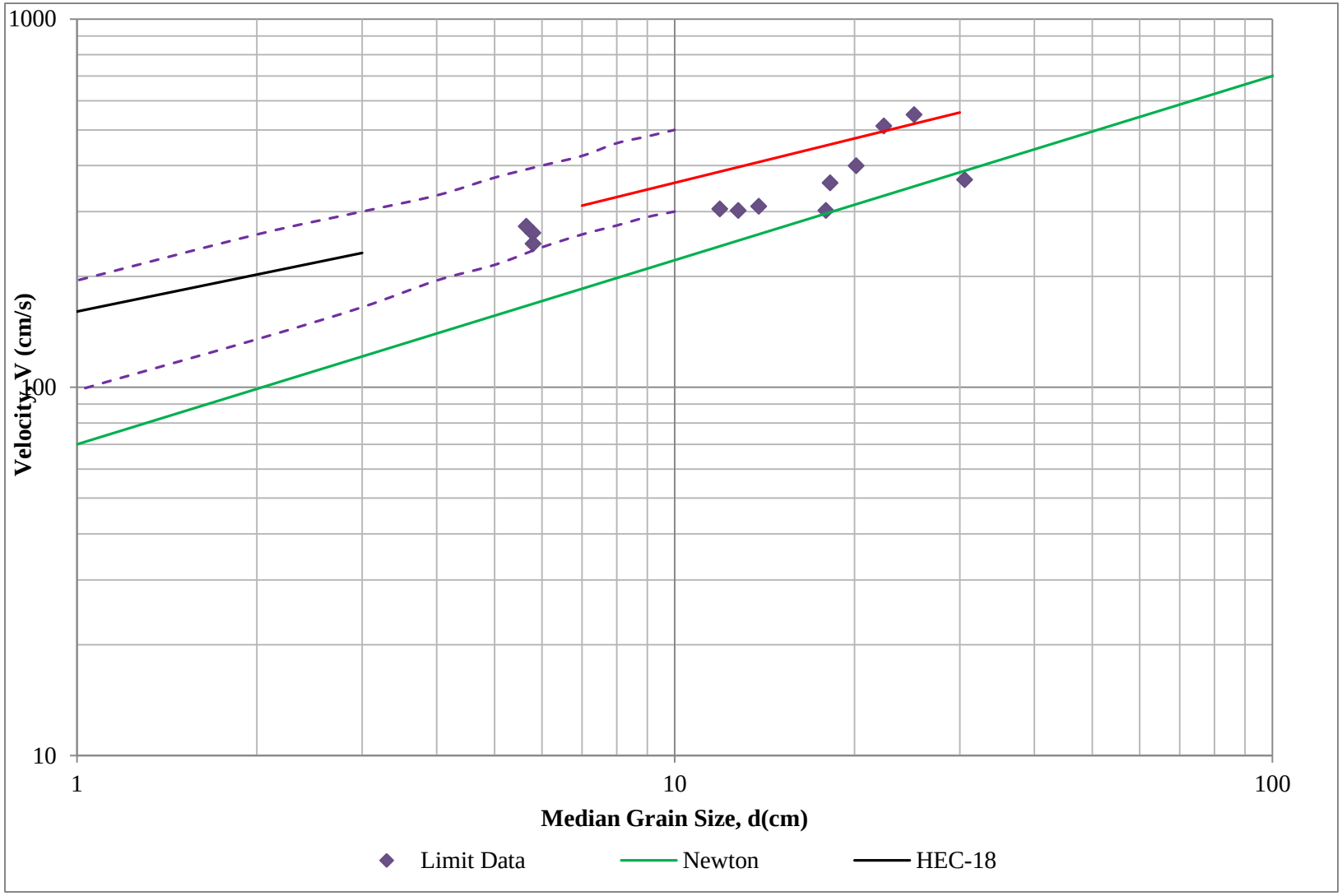

Figure 5.3 Enlarged plot, limit data velocity vs. median grain size.

5.2 Develop a Best-Fit Predictive Model

In order to use the limit analysis results as a predictive model, a best fit curve was developed. Rather, two best fit curves were regressed. The first curve shown in **Figure 5.4** is based on a nonlinear power regression of all 12 study bridges. The relationship is:

$$V_{Limit} = 137.8 \times d^{0.34} \quad (5.1)$$

Where: V_{Limit} : maximum entrainment velocity, (cm/s); and
d : median grain size of streambed, (cm)

Note that the correlation coefficient, R^2, is the fraction of the total variance of V_{Limit}. It is equal to 0.643, which indicates that the trend line represents 64 percent of the limit data, which is promising.

A second best fit curve was drawn through the limit data utilizing an exponential regression, which is shown in **Figure 5.5**. This yields the expression:

$$V_{Limit} = 226.7 \times e^{0.025 \times d} \quad (5.2)$$

The first thing to notice is the correlation coefficient is identical. Secondly, the curve displays a gradual upward trend that converges with the HEC-18 and U.S. Army relationships for the largest grain sizes. However, the total number of limit data points is not believed sufficient to justify higher order relation. Thus, the proposed working form of the limit analysis will be Equation (5.1).

In summary, the limit analysis defines the erosion behavior of particle grains from 2 to 50 centimeters in diameter, a size range that has not been previously well studied. In addition, the results are for natural sediments in a river channel as opposed to an artificial flume. Such data are potentially very useful for sediment transport analyses in river basin studies. There are also several practical engineering applications of the limit analysis, which will now be discussed.

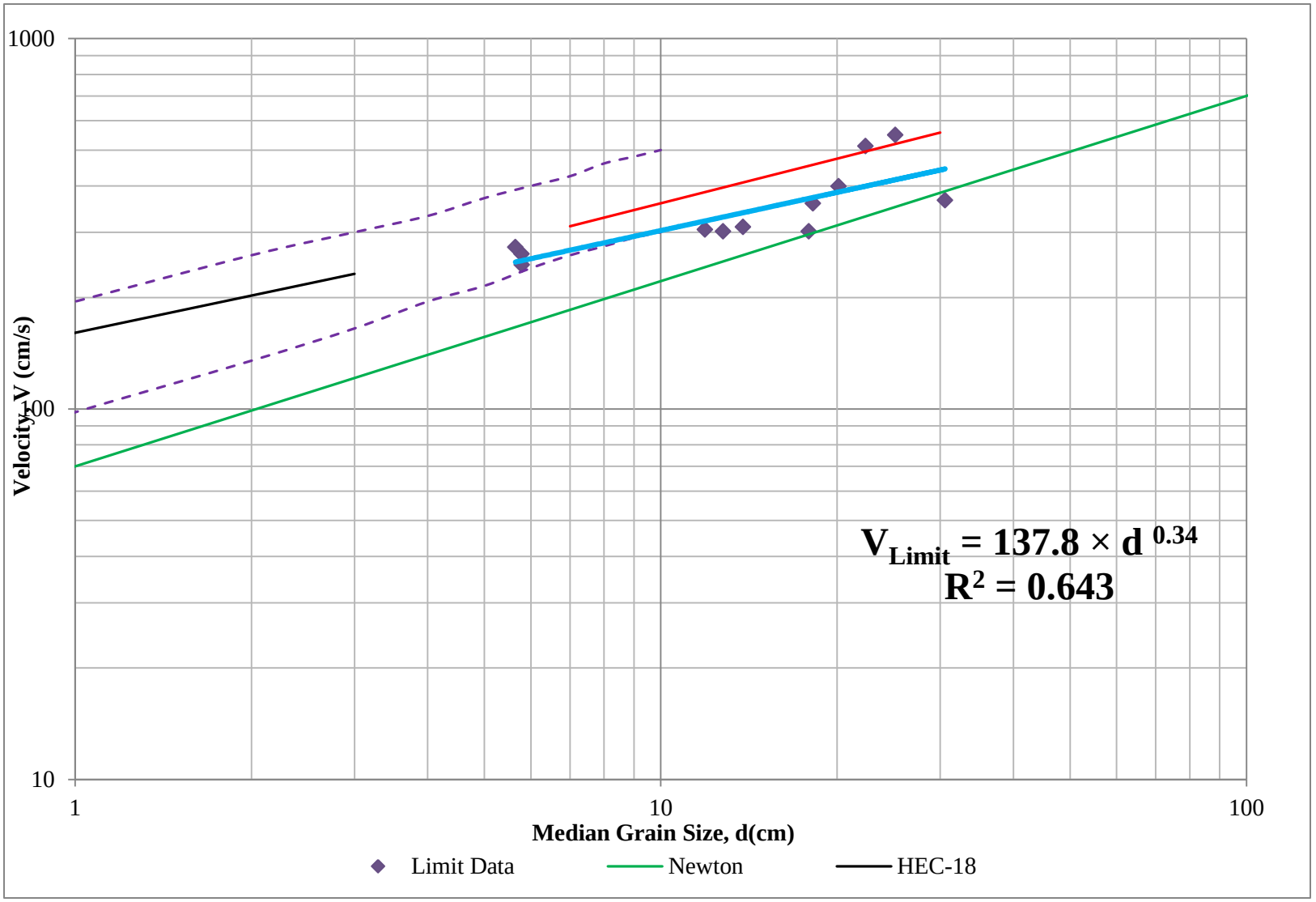

Figure 5.4 Best fit predictive model- power line, new analytical erosion relationship for ECP sediments.

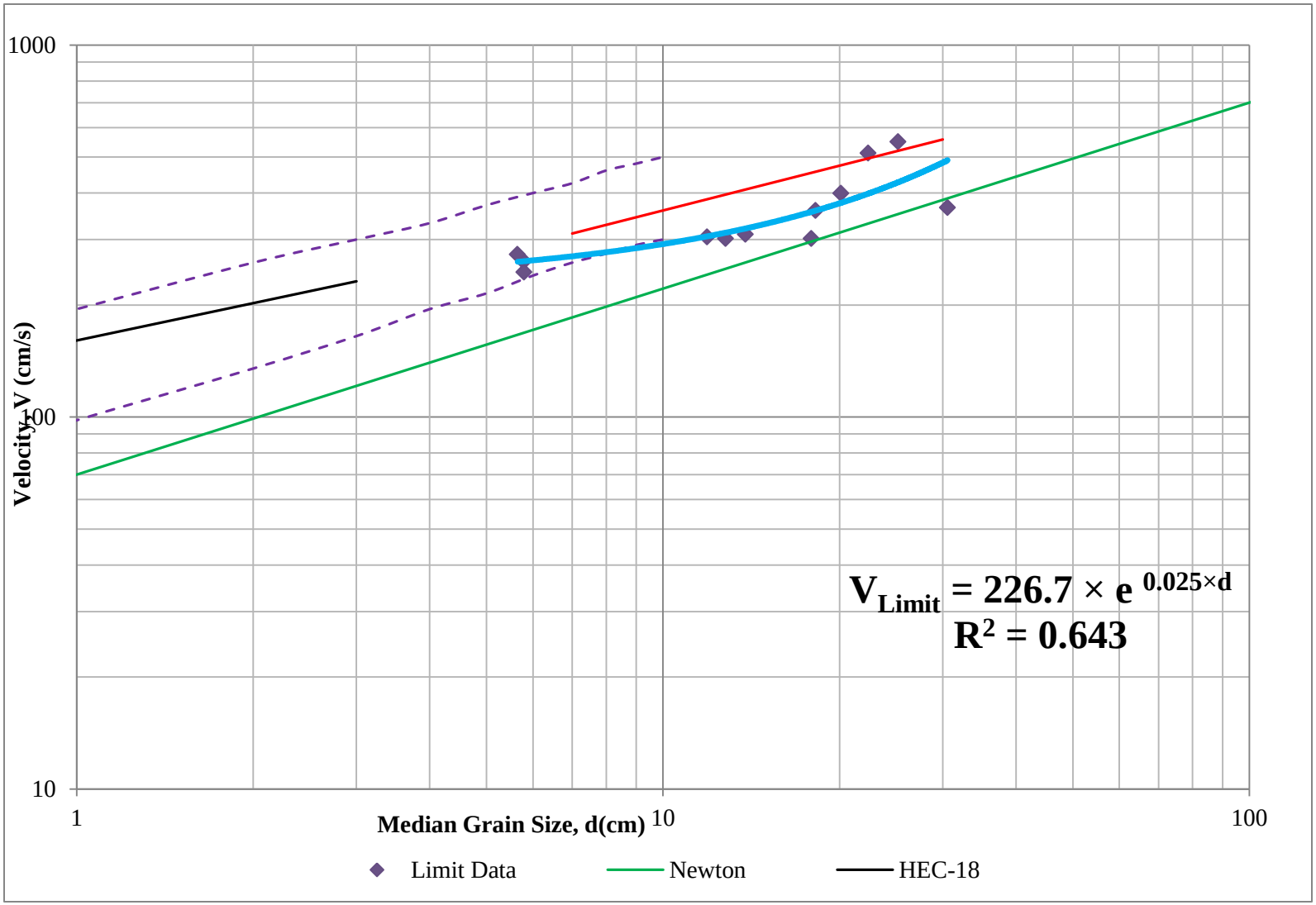

Figure 5.5 Best fit predictive model- exponential line, new analytical erosion relationship for ECP sediments.

5.3 Research Applications

5.3.1 General Scour Risk Assessment

The proposed first application of this research is to use the limit analysis results as a rapid and direct assessment of scour risk for bridges underlain by ECP sediments. The procedure for performing the assessment is:

Step 1. Estimate the grain size distribution of the bed using one of the methods discussed in Section 4.1, e.g., WipFrag, Wolman Pebble Count. This establishes the median grain size, D_{50}.

Step 2. Next calculate the limit velocity using Equation (5.1) or **Figure 5.4**.

Step 3. The third step is to choose a scour design storm and compute the corresponding flow velocity. For existing bridges, Q_{100} is commonly used. Alternatively, the maximum historic discharge according to USGS data might be used.

Step 4. Finally, the scour design velocity is compared with the limit velocity for the chosen median grain size (see **Figure 5.4**). If the scour design velocity is less than limit velocity, then the bridge is likely to have a low scour risk. But if the scour design velocity exceeds the limit velocity, then the bridge may not be safe and countermeasures or monitoring should be contemplated.

Note that it is important to supplement this general assessment procedure with field inspection and other scour assessment methods. But the limit analysis does provide a useful tool for evaluating scour risk of sediments where traditional scour relationships are not applicable. An example illustrating use of the general scour risk assessment is presented in **Appendix F**.

5.3.2 Extension of Design Methods into ECP Range

Another application of this research is it extends the particle size range of current scour design methods. For example, the HEC-18 relationship for critical velocity (Equation (2.5)) is considered valid for granular sediments up to and including gravel size (3 cm). The limit analysis extends beyond this range and into the ECP sizes as shown in **Figure 5.6**. Note that the limit curve plots slightly lower than the extrapolated HEC-18 relation. This means that the limit results are more "conservative". That is, for a given grain particle size, the limit velocity to entrain a particle is lower than predicted by the HEC-18 equation. Thus, the limit analysis defines erosion behavior in a size range where no reliable data was previously available.

In a similar way, this research also supplements U.S Army EM 1601, which is the most widely used riprap design procedure (see Equation (2.6) in Section 2.2.6). Referring again to Figure 5.6, the limit curve approximately parallels the EM 1601 relation, which adds validity to both methods. But again, the limit analysis curve is lower, which means it is more conservative. Note that this could be due to in part to riprap angularity, which increases the entrainment velocity. This research is not meant to invalidate the widely applied riprap design procedure. But it does suggest that a higher factor of safety may be appropriate for this popular design equation.

Based on the limit analysis, a new safety factor can be derived by comparing velocity ratios for a given grain size. For sediments in the size range of cobbles to boulders, a safety factor of 1.5 to 2.0 is recommended. This result is consistent with the observation that riprap installations designed according to EM 1601 sometimes fail. Use of a new higher safety factor from the limit analysis will help reduce such failures.

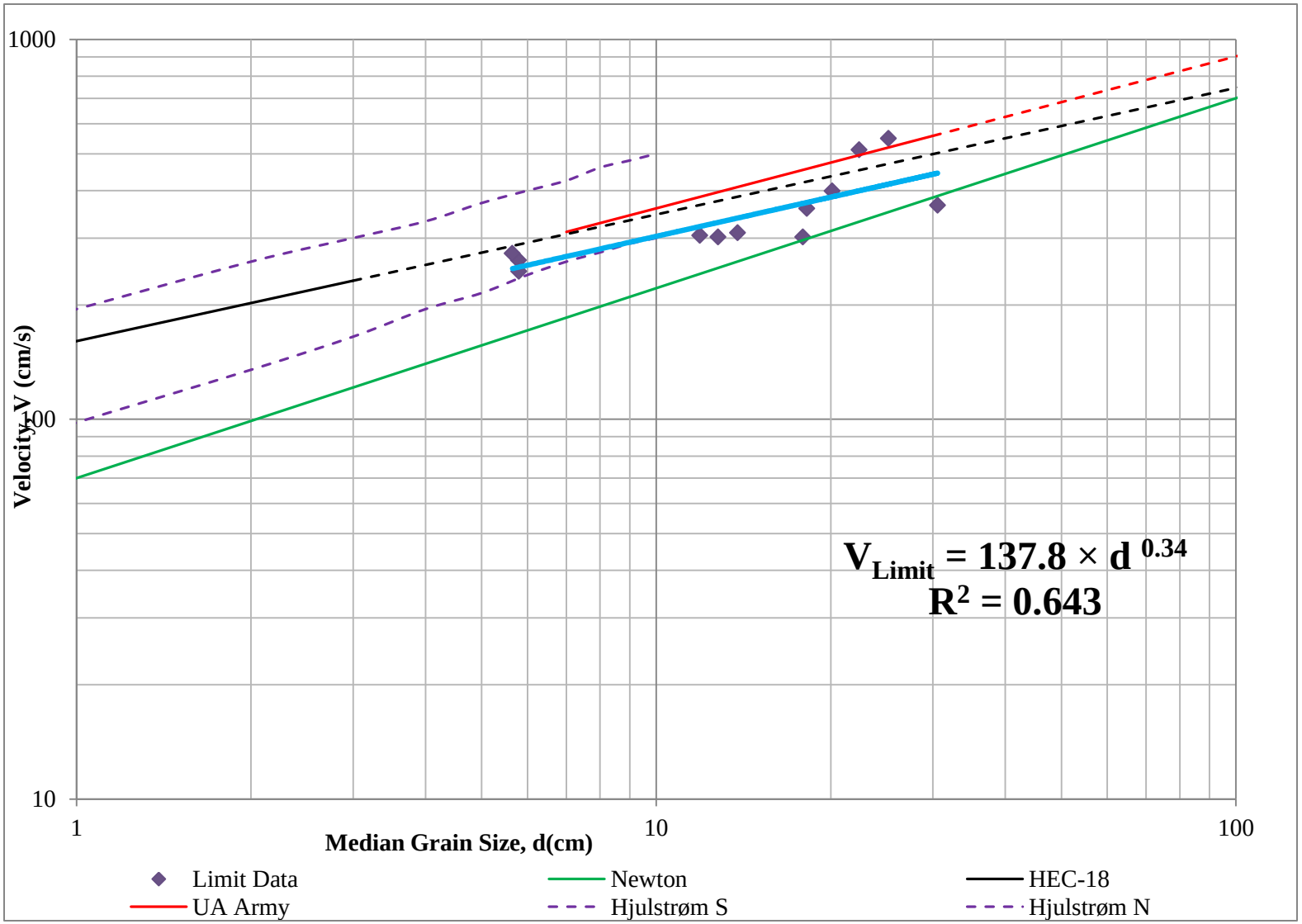

Figure 5.6 Extended relationship for ECP sediments, velocity vs. median grain size.

5.3.3 Rapid Field Determination of ECP Grain Sizes

During the course of this research study, the NJIT Geotechnical Team developed a new and more rapid field method for determining the grain size distribution of ECP sediments. It was recognized that the Wolman Pebble Count and manually adjusted WipFrag methods are very labor intensive, so they are not likely to be used for standard scour evaluations.

The approach was to determine 'adjustment coefficients' based on the vast database of grain size results from the study bridges. This would allow an unadjusted WipFrag photo to be converted simply and quickly by multiplying the raw grain size results by the adjustment factors.

The approach for deriving the adjustment coefficients was to utilize the 'n' parameter from Rosin-Rammler equation (see Section 4.1.3). Recall that the n value represents the spread or grading of the particle sizes. In general, if the n value is in the range of 0.5 to 1.5 the sediment is well graded. For n values greater than 1.5, the sample is poorly graded. Since the Wolman Pebble Count is considered to be the most accurate grain size method for ECP sediments, the n from this method was computed for all the study bridges. These results are shown in **Table 5.2.**

For the next step, two new grain size parameters were defined: $K_1 = n_2/n_1$, ratio of sediment grading, and $K_2 = X_{c2}/ X_{c1}$, ratio of median grain size. Reliable computation of these parameters requires a large number of WipFrag photos and can only be done if the bridge streambed is mostly dry. Four study bridges met this criterion, and the results are summarized in **Table 5.3**. Detailed calculations are presented in **Appendix C.2**.

Table 5.2 Median Grain Size 'Xc', and Grading Coefficient 'n', for the 12 Study Bridges

	1	2	3	4	5	6	7	8	9	10	11	12
Bridge #	0709-150	1809-153	0711-150	1612-154	2108-162	1605-158	1417-156	1605-153	1405-156	1912-160	2107-156	2111-155
Xc (mm)	56.49	57.92	57.98	127.86	138.29	179.16	201.30	223.91	305.80	118.99	182.05	251.73
n	1.49	1.13	1.68	1	1.22	1.52	0.78	0.98	1.38	1.35	1.38	1.06

Table 5.3 WipFrag Adjusted Coefficient Factor

	Bridge #	# Pictures	# Sections	Sediment grading factor			Median Grain Size (mm)		
				n2	n1	K1	Xc2	Xc1	K2
1	1417-156	4	1	1.12	1.08	1.03	148	59	2.62
2	1605-158	11	3	1.28	0.86	1.51	191	151	1.37
3	2107-156	18	4	1.41	1.15	1.24	199	157	1.61
4	1405-156	8	2	1.45	1.04	1.40	270	180	1.96
	Average					**1.30**			**1.89**

An examination of **Table 5.3** indicates that for most cases, K_1 and K_2 are always larger than one. This means sediments are typically less well graded than what the raw WipFrag analysis shows us. The table further shows that average sediment size is also larger. The main reason for these trends is that the software tends to break down large particles like boulders into smaller particles during net creation.

To apply this new method, the sediments are first photographed and then processed with the WipFrag software. This determines the 'raw' Rosin-Rammler parameters, n and X_c. Next, these values are multiplied by coefficients K_1 and K_2 to generate a more realistic grain size distribution for ECP channel sediments.

5.3.4 Particle Size Trends for New Jersey's Geologic Provinces

New Jersey has a diverse geology considering its relatively small size. This diversity is reflected in the state's four physiographic provinces, which are shown in **Figure 5.7**. The current research has focused on the three most northern provinces (Piedmont, Highlands, Valley and Ridge), since this is where ECP sediments are encountered. The actual locations of the 12 study bridges are also shown in **Figure 5.7**.

A couple of useful data trends may also be observed in Table 5.4 and Figure 5.7. First, the median grain size appears to be a function of the geology of each Province. The average median grain size of the sediments in the Highlands was the largest (20.97 cm). This is consistent with the province's bedrock geology which consists of resistant crystalline igneous and metamorphic rocks. In contrast, the sediments of Piedmont were the smallest (7.50 cm), reflecting the weaker sedimentary rocks that underlie the province. The bridge sites in the Valley and Ridge had sediments of intermediate size (18.43 cm), which corresponds to the mid-range strengths of the dolomites, slates, and conglomerates throughout the region.

There also appears to be a trend of decreasing coarseness to the south within each individual province. This is attributed to the effect of the Wisconsin glacier, which advanced from north to south over northern New Jersey. Overall, the observed geologic trends might suggest that higher scour design storms are appropriate in the northern part of the state.

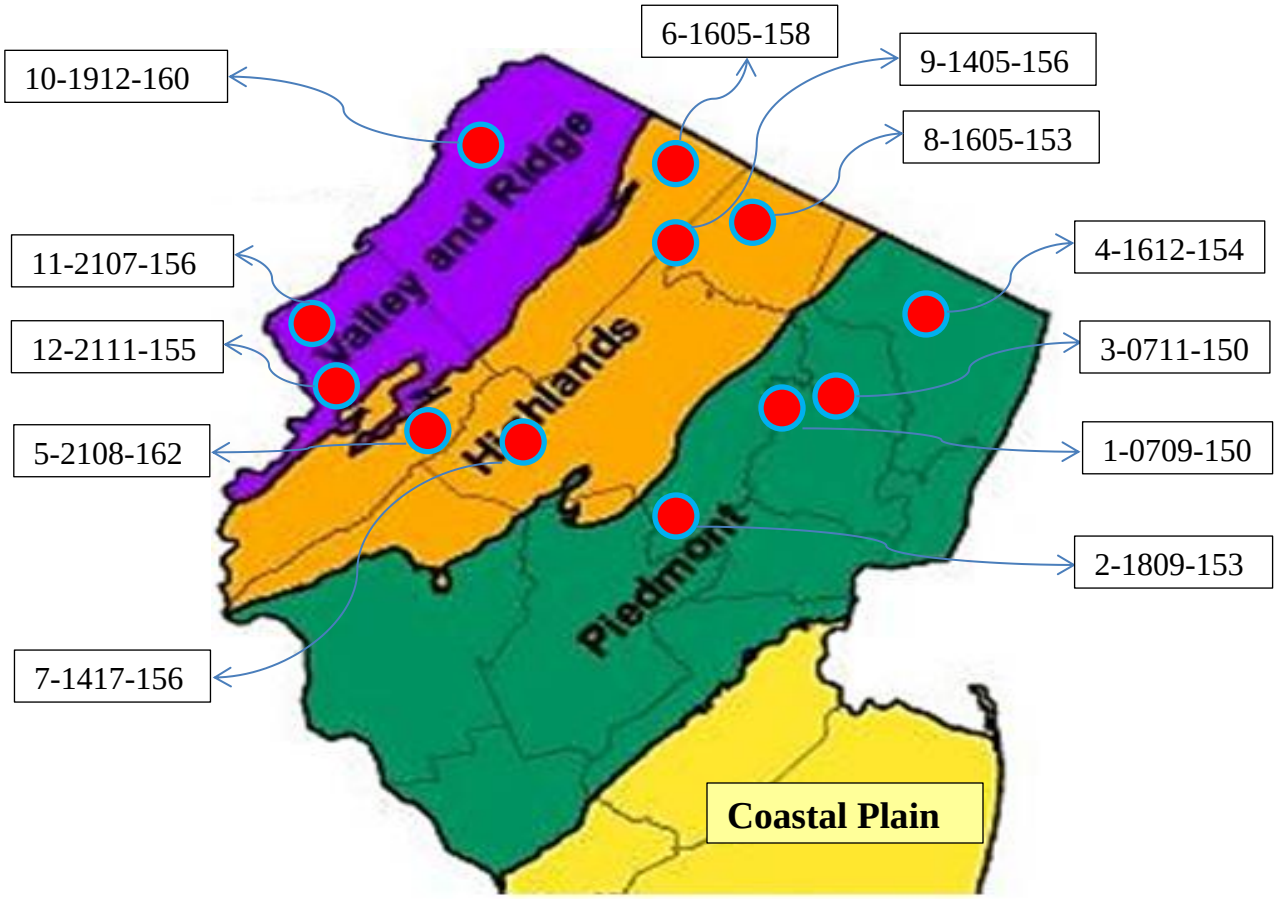

Figure 5.7 New Jersey geologic province map.

Table 5.4 Grain Size Distribution Trend based on New Jersey Geological Provinces

	Bridge #	Province	Median Grain Size	Estimated Grain Size			
			cm	Boulder %	Cobble %	Gravel %	Fines %
1	0709-150	Piedmont	5.65	0	30	60	10
2	1809-153	Piedmont	5.79	5	25	40	30
3	0711-150	Piedmont	5.80	0	40	40	20
4	1612-154	Piedmont	12.79	10	60	20	10
5	2108-162	Highlands	13.83	20	50	20	10
6	1605-158	Highlands	17.92	50	10	10	30
7	1417-156	Highlands	20.13	25	50	20	5
8	1605-153	Highlands	22.39	50	25	10	15
9	1405-156	Highlands	30.58	70	20	5	5
10	1912-160	Valley & Ridge	11.90	20	50	20	10
11	2107-156	Valley & Ridge	18.21	40	50	10	0
12	2111-155	Valley & Ridge	25.17	50	30	10	10

CHAPTER 6

CONCLUSIONS AND RECOMMENDATIONS

6.1 Conclusions

Failure of Schoharie Creek Bridge due to excessive scour in 1987 prompted a national focus on the problem of bridge scour. Bridge scour is the erosion of soil and rock from around bridge abutments and piers, and it remains a principal cause of bridge failure in the United States and around the world. This is because bridge scour involves complex hydraulic and geologic phenomena, and attempts to reliably predict scour depth have met with limited success.

Previous investigations of scour have focused mostly on fine sediments such as sand, silt, and small gravel, because a majority of bridges are underlain by such alluvium. The erosion behavior and scour resistance of coarser sediments has received limited attention, even though they dominate many small to medium-size rivers in the northern tiers of the United States, Europe, and Asia. As a result, the present research is aimed at helping to fill this technological gap by providing a new approach for estimating scour risk in streambed with extremely coarse particles (ECP), especially for sediments in the cobble to boulder size range.

A main objective of this research was to develop a relationship between critical (entrainment) velocity and grain size for sediment particles in the size range of 5 to 50 cm (2 to 20 in). This was accomplished by precisely investigating the geologic characteristics and hydrologic history of actual bridges, and then performing a limit analysis of sediments that occur within the stream beds of the bridges. Converting a real

stream channel into an experimental flume is a unique aspect of this research, because it eliminates the need to use scaling factors or other corrections as is done with laboratory flume studies. A basic premise is the residual sediments reflect the maximum historic flow and velocity that has occurred over the life of the bridge. The end goal of this research is to provide technical tools that improve the reliability of scour estimation, thereby increasing bridge safety and reducing long term infrastructure costs.

An overview of the study and the general conclusions will now presented:

1. This research encompasses both model analyses and field studies. The work commenced by summarizing and comparing the classical sediment transport relationships potentially applicable to ECP. These included Stokes' Law, Newton's law, Hjulstrøm envelop curve, and the HEC-18 critical velocity equation. A composite plot of grain size versus critical velocity for all the transport relationships was developed to establish a "region of interest" for the particle size range of 5 to 50 centimeters.

2. Thirty-five bridges in Northern New Jersey were initially screened for the study. The principal selection criteria for the bridges included: (1) the streambed must be composed of more than 60% cobbles and boulders; (2) the stream bed must be visible during low-water conditions; and (3) the stream must have a USGS gage installed with sufficient flow history. Twelve bridges were finally selected for detailed analysis.

3. Field visits were made to characterize the grain size distribution of the ECP sediments present at each site. Different grain size distribution methods were employed such as optical granulometry, statistical pebble counts, and visual estimation. These nontraditional methods were necessary on account of the large grain size of the study streambeds. To assure geologic and hydrologic diversity for the data set, the sites span

three of New Jersey's physiographic provinces: Highlands, Valley and Ridge, and Piedmont.

4. Hydraulic analyses were used to estimate the maximum velocity that the bridge experienced during its lifetime, which was a key parameter for the limit analysis. These were based on the maximum recorded discharges at the closest USGS gage stations to the bridge. The USGS software "StreamStats" was also consulted to compute drainage areas and to help locate additional nearby gages. Three different methods were employed for estimating maximum velocity depending on flow history and channel characteristics. The preferred method was interpolation or extrapolation of HEC-RAS computations for the bridges. Final limit velocities ranged from 245 to 549 cm/sec (8 to 18 ft./sec).

5. A limit analysis was performed to reconcile the maximum historical velocity with the existing particle gradation of the stream bed. A regression of the data yielded a nonlinear, exponential relationship between critical velocity and median particle size. The variance fraction associated with the data set was 0.642, indicating a reasonable fit. In summary, the limit analysis provides a realistic relationship between limit (entrainment) velocity and particle size for ECP sediments.

6. A number of applications for the limit analysis relationship were proposed and explored. One is to use the limit analysis results as a rapid and direct assessment of scour risk for bridges underlain by ECP sediments. This may be accomplished by first measuring the median grain size of the sediments. Next, a scour design storm is chosen, e.g., Q_{100}, and the corresponding flow velocity is computed. Finally, the limit velocity is determined from the best fit limit relationship, which is then compared with scour design

storm. If the design scour velocity exceeds the limit velocity, then the bridge is considered to have high scour risk.

7. The HEC-18 critical velocity relations is valid for scour evaluation of granular streambeds with a grain size up to approximately 3 centimeters. The limit analysis curve therefore extends the useful range of this design equation up to a median grain size of approximately 50 centimeters. Note that the limit analysis extrapolation trends lower and produces more conservative critical velocities in the ECP size range than does HEC-18.

8. This research also supplements U.S. Army EM 1601, which is the most widely used riprap design procedure. But, again, the limit analysis results trend lower, which means they are more conservative. A comparative analysis between the two methods for sediments in the size range of cobbles to boulders suggests that a safety factor of 1.5 to 2.0 should be applied when designing for riprap in the size range of cobbles to boulders with the U.S. Army equation.

9. Another new application is a rapid field method for analyzing the grain size of ECP sediments through the use of optical granulometry. With the help of vast database of grain size results, ‘adjustment coefficients’ were determined that can be used to correct ‘raw’ photographs processed with WipFrag software. The method generates a realistic grain size distribution for channel sediments, which can then be used for various purposes.

6.2 Future Work Recommendations

The following are recommendations for future research into the erosion behavior and scour risk of extremely coarse particles (ECP):

1. The database of ECP bridges should be expanded to increase the confidence level of the limit analysis, including:

    a. Sites having a particle size within the range of the current research; and

    b. Sites having a particle size outside the current research:

        i. $2 \text{ cm} < D < 5 \text{ cm}$

        ii. $D > 30 \text{ cm}$

2. It is recommended to investigate the influence of natural armoring on the behavior of ECP streambeds in the vicinity of bridges, including:

    a. Trends of particle gradation with depth (graded bed vs. reverse graded bed);

    b. Effect of provenance, e.g., soft sedimentary vs. hard igneous/metamorphic; and

    c. Effect of original landform, e.g., valley train vs. colluvium

3. The current research focused mainly on the effects degradation and contraction scour on the streambed beneath a bridge. The influence of piers should also be investigated, including and how the limit analysis compares with the new HEC-18 coarse particle equation.

4. The effect of angularity of ECP sediments, which leads to greater erosion resistance and a higher value of entrainment velocity, was not addressed in this study. It is recommended to investigate the influence of particle shape on the limit analysis.

5. Residual sediments reflect the maximum historic flow and velocity that has occurred over the life of the bridge. In order to document changes of the bed sediments over time, it is recommended to create a photographic record for ECP bridges at specified intervals, say every 5 years. This would permit study of sediment movements, which could be correlated with USGS gage data.

6. In this study, optical granulometry and WipFrag were only used to analyze bed sediments that were exposed "in the dry" during low water conditions. It is recommended to explore the possibility of using underwater photography of ECP streambeds 9.1 meters (30 feet) below water and greater to extend the applicability of these methods, along with comparing the scour behavior of extremely coarse particles (ECP) under a sustained water from with the intermittent surge flows from Q_{100} design storms.

APPENDIX A

PARTICLE SIZE CLASSIFICATION AND SYSTEMS

The grain-size information from the Field Reconnaissance Studies where used to find an approximate median size (D_{50}) for the streams in question. In these estimations, the Unified Soil Classification System (USCS) was followed, which is shown in **Table A.1.** That is, boulders were classified as particles larger than 300 millimeter (mm), and cobbles were categorized as particles larger than 75 mm but smaller than 300 mm. Gravel was considered to be smaller than 75 mm, but larger than 4.75 mm, while sand, silt, and clay were lumped together as those particles smaller than 4.75 mm.

Table A.1 USCS Definitions of Particle Size

Soil Fraction	Size Range (mm)
Boulders	Greater than 300
Cobbles	75 - 300
Coarse Gravel	75 - 19
Fine Gravel	19 - 4.75
Coarse Sand	4.75 - 2.0
Medium Sand	2.0 - 0.425
Fine Sand	0.425 - 0.075
Silt	Less than 0.075
Clay	Less than 0.075

There are two other grain-size systems in the geologic sciences that are also used for characterizing sediments. The first is the Wentworth System, which is summarized in **Table A.2.** The other is the AGU System, which is given in **Table A.3**. These are provided for reference. As indicated, the soil fraction definitions vary slightly compared with the Unified System.

Table A.2 Wentworth (1922) Grain Size Classification

	Soil Fraction	Size Range (mm)
Gravel	Boulder	256 - 4096
	Cobble	64 - 256
	Pebble	4.0 - 64
	Granule	2.0 - 4.0
Sand	Very Coarse Sand	1.0 - 2.0
	Coarse Sand	0.5 - 1.0
	Medium Sand	0.25 - 0.5
	Fine Sand	0.125 - 0.25
	Very Fine Sand	0.0625 - 0.125
Silt	Coarse Silt	0.031 - 0.0625
	Medium Silt	0.0156 - 0.031
	Fine Silt	0.0078 - 0.0156
	Very Fine Silt	0.0039 - 0.0078
Mud	Clay	0.00006 - 0.0039

Table A.3 AGU's Soil Technology Classification of Particles

Name	Soil Fraction	Size Range (mm)
Gravel	Very coarse	64-32
	Coarse	32-16
	Medium	16-8
	Fine	8-4.0
	Very fine	4-2.0
Sand	Very coarse	2-1.0
	Coarse	1-0.5
	Medium	0.5-0.25
	Fine	0.25-0.125
	Very fine	0.125-0.062
Silt	Coarse	0.062-0.031
	Medium	0.031-0.016
	Fine	0.016-0.008
	Very fine	0.008-0.004
Clay	Coarse	0.004-0.002
	Medium	0.002-0.001
	Fine	0.001-0.0005
	Very fine	0.0005-0.0002

APPENDIX B

CALCULATION OF ALL FUNDAMENTAL AND APPLICATION RELATIONSHIPS OF SEDIMENT TRANSPORT

Table B Calculation of All Fundamental Relationships of Sediment Transport

	Stocks	Newton	Grace Law				HEC-18			US Army- EM 1601	Hiulstrom	
d (cm)	Vt(cm/s)	Vt(cm/s)	d(cm)	d*	Vts*	Vts	d(m)	Vc (m/s)	Vc(cm/s)	V (cm/s)	Vs (cm/s)	Vn (cm/s)
0.001	0.009	2.214	0.001	0.253	0.0035	0.008855	0.00001	0.16	**16.06**	9.02	19	700
0.002	0.036	3.130	0.002	0.506	0.013	0.03289	0.00002	0.20	**20.23**	11.90	19	300
0.003	0.081	3.834	0.003	0.759	0.031	0.07843	0.00003	0.23	**23.16**	14.00	19	170
0.004	0.144	4.427	0.004	1.012	0.06	0.1518	0.00004	0.25	**25.49**	15.71	19	120
0.005	0.225	4.950	0.005	1.265	0.09	0.2277	0.00005	0.27	**27.46**	17.17	19	86
0.006	0.323	5.422	0.006	1.518	0.12	0.3036	0.00006	0.29	**29.18**	18.47	19	70
0.007	0.440	5.857	0.007	1.771	0.17	0.4301	0.00007	0.31	**30.72**	19.65	19	60
0.008	0.575	6.261	0.008	2.024	0.2	0.506	0.00008	0.32	**32.12**	20.73	19	53
0.009	0.728	6.641	0.009	2.277	0.25	0.6325	0.00009	0.33	**33.41**	21.73	19	50
0.01	0.898	7.000	0.01	2.53	0.3	0.759	0.0001	0.35	**34.60**	22.66	19	47
0.02	3.593	9.899	0.02	5.06	0.9	2.277	0.0002	0.44	**43.59**	29.90	19	47
0.03	8.085	12.124	0.03	7.59	1.7	4.301	0.0003	0.50	**49.90**	35.17	19	47
0.04	14.373	14.000	0.04	10.12	2.7	6.831	0.0004	0.55	**54.92**	39.45	19	47
0.05	22.458	15.652	0.05	12.65	3.4	8.602	0.0005	0.59	**59.16**	43.14	21	48.5
0.06	32.339	17.146	0.06	15.18	4.2	10.626	0.0006	0.63	**62.87**	46.40	23	53
0.07	44.017	18.520	0.07	17.71	4.8	12.144	0.0007	0.66	**66.19**	49.35	25.5	58
0.08	57.491	19.799	0.08	20.24	5.6	14.168	0.0008	0.69	**69.20**	52.06	28	61
0.09	72.762	21.000	0.09	22.77	6.1	15.433	0.0009	0.72	**71.97**	54.57	30	63
0.1	89.830	22.136	0.1	25.3	6.9	17.457	0.001	0.75	**74.54**	56.92	31.5	67
0.2	359.320	31.305	0.2	50.6	11.5	29.095	0.002	0.94	**93.92**	75.11	44	90
0.3	808.470	38.341	0.3	75.9	14	35.42	0.003	1.08	**107.51**	88.33	55	110
0.4	1437.280	44.272	0.4	101.2	16.5	41.745	0.004	1.18	**118.33**	99.10	63	124
0.5	2245.750	49.497	0.5	126.5	18	45.54	0.005	1.27	**127.47**	108.36	69	145
0.6	3233.880	54.222	0.6	151.8	19.5	49.335	0.006	1.35	**135.45**	116.55	76	153
0.7	4401.670	58.566	0.7	177.1	22	55.66	0.007	1.43	**142.60**	123.97	81	170
0.8	5749.120	62.610	0.8	202.4	23	58.19	0.008	1.49	**149.09**	130.77	86	180
0.9	7276.230	66.408	0.9	227.7	25	63.25	0.009	1.55	**155.06**	137.08	92	190
1	8983.0	70.000	1	253	26	65.78	0.01	1.61	**160.60**	142.98	100	195
2	35932.0	98.995	2	506	36	91.08	0.02	2.02	**202.34**	188.66	135	260
3	80847.0	121.244	3	759	44	111.32	0.03	2.32	**231.62**	221.88	165	300
4	143728.0	140.000	4	1012	53	134.09	0.04	2.55	**254.93**	248.94	195	330
5	224575.0	156.525	5	1265	60	151.8	0.05	2.75	**274.62**	272.18	215	375
6	323388.0	171.464	6	1518	67	169.51	0.06	2.92	**291.83**	292.77	240	400
7	440167.0	185.203	7	1771	71	179.63	0.07	3.07	**307.21**	311.39	260	425
8	574912.0	197.990	8	2024	75	189.75	0.08	3.21	**321.20**	328.48	275	460
9	727623.0	210.000	9	2277	80	202.4	0.09	3.34	**334.06**	344.32	290	480
10	898300.0	221.359	10	2530	84	212.52	0.1	3.46	**346.00**	359.14	300	500
20	3593200.0	313.050	20	5060	120	303.6	0.2	4.36	**435.93**	473.89	420	670
30	8084700.0	383.406	30	7590	140	354.2	0.3	4.99	**499.02**	557.34	510	800
40	14372800.0	442.719	40	10120	170	430.1	0.4	5.49	**549.24**	625.31	600	900
50	22457500.0	494.975					0.5	5.92	**591.65**	683.69	675	1000
60	32338800.0	542.218					0.6	6.29	**628.72**	735.41	735	1100
70	44016700.0	585.662					0.7	6.62	**661.87**	782.18	800	1150
80	57491200.0	626.099					0.8	6.92	**692.00**	825.10	835	1220
90	72762300.0	664.078					0.9	7.20	**719.71**	864.90	900	1300
100	89830000.0	700.000					1	7.45	**745.43**	902.13	955	1405
200	359320000.0	989.949					2	9.39	**939.18**	1190.37	1350	1850
300	808470000.0	1212.436					3	10.75	**1075.10**	1399.96	1650	2250
400	1437280000.0	1400.000					4	11.83	**1183.30**	1570.70	1850	2500
500	2245750000.0	1565.248					5	12.75	**1274.67**	1717.34	2100	2750
600	3233880000.0	1714.643					6	13.55	**1354.54**	1847.26	2350	2900
700	4401670000.0	1852.026					7	14.26	**1425.96**	1964.75	2550	3200
800	5749120000.0	1979.899					8	14.91	**1490.86**	2072.55	2700	3350
900	7276230000.0	2100.000					9	15.51	**1550.56**	2172.53	2800	3400
1000	8983000000.0	2213.594					10	16.06	**1605.98**	2266.04	2900	3600

APPENDIX C

GRAIN SIZE DISTRIBUTION METHODS

C.1 Wolman Pebble Count

Table C.1 contain Wolman pebble count grain size distribution data, calculation, and results for the 12 study bridges.

Table C.1 Wolman Pebble Count Grain Size Distribution Calculation

Bridge #	0709-150	1809-153	0711-150	1612-154	2108-162	1605-158	1417-156	1605-153	1405-156	1912-160	2107-156	2111-155
Median Grain Size	**5.65**	**5.79**	**5.8**	**12.79**	**13.83**	**17.92**	**20.13**	**22.39**	**30.58**	**11.9**	**18.21**	**25.17**
Sieve Sizes (mm)	Percentage passing											
1200	100.00%	100.00%	100.00%	100.00%	100.00%	100.00%	100.00%	100.00%	100.00%	100.00%	100.00%	100.00%
1185	100.00%	100.00%	100.00%	100.00%	100.00%	100.00%	100.00%	99.04%	95.38%	100.00%	100.00%	100.00%
1170	100.00%	100.00%	100.00%	100.00%	100.00%	100.00%	100.00%	99.04%	95.38%	100.00%	100.00%	100.00%
1155	100.00%	100.00%	100.00%	100.00%	100.00%	100.00%	100.00%	99.04%	95.38%	100.00%	100.00%	100.00%
1140	100.00%	100.00%	100.00%	100.00%	100.00%	100.00%	100.00%	99.04%	95.38%	100.00%	100.00%	100.00%
1125	100.00%	100.00%	100.00%	100.00%	100.00%	100.00%	100.00%	99.04%	95.38%	100.00%	100.00%	100.00%
1110	100.00%	100.00%	100.00%	100.00%	100.00%	100.00%	100.00%	99.04%	95.38%	100.00%	100.00%	100.00%
1095	100.00%	100.00%	100.00%	100.00%	100.00%	100.00%	100.00%	99.04%	95.38%	100.00%	100.00%	100.00%
1080	100.00%	100.00%	100.00%	100.00%	100.00%	100.00%	100.00%	99.04%	95.38%	100.00%	100.00%	100.00%
1065	100.00%	100.00%	100.00%	100.00%	100.00%	100.00%	100.00%	99.04%	95.38%	100.00%	100.00%	100.00%
1050	100.00%	100.00%	100.00%	100.00%	100.00%	100.00%	100.00%	99.04%	95.38%	100.00%	100.00%	100.00%
1035	100.00%	100.00%	100.00%	100.00%	100.00%	100.00%	100.00%	99.04%	95.38%	100.00%	100.00%	100.00%
1020	100.00%	100.00%	100.00%	100.00%	100.00%	100.00%	100.00%	99.04%	95.38%	100.00%	100.00%	100.00%
1005	100.00%	100.00%	100.00%	100.00%	100.00%	100.00%	100.00%	99.04%	95.38%	100.00%	100.00%	100.00%
990	100.00%	100.00%	100.00%	100.00%	100.00%	100.00%	95.65%	99.04%	95.38%	100.00%	100.00%	100.00%
975	100.00%	100.00%	100.00%	100.00%	100.00%	100.00%	95.65%	99.04%	95.38%	100.00%	100.00%	100.00%
960	100.00%	100.00%	100.00%	100.00%	100.00%	100.00%	95.65%	99.04%	95.38%	100.00%	100.00%	100.00%
945	100.00%	100.00%	100.00%	100.00%	100.00%	100.00%	95.65%	99.04%	95.38%	100.00%	100.00%	100.00%
930	100.00%	100.00%	100.00%	100.00%	100.00%	100.00%	95.65%	99.04%	95.38%	100.00%	100.00%	100.00%
915	100.00%	100.00%	100.00%	100.00%	100.00%	100.00%	95.65%	99.04%	95.38%	100.00%	100.00%	100.00%
900	100.00%	100.00%	100.00%	100.00%	100.00%	100.00%	95.65%	99.04%	95.38%	100.00%	100.00%	96.00%
885	100.00%	100.00%	100.00%	100.00%	100.00%	100.00%	95.65%	99.04%	95.38%	100.00%	100.00%	96.00%
870	100.00%	100.00%	100.00%	100.00%	100.00%	100.00%	95.65%	99.04%	95.38%	100.00%	100.00%	96.00%
855	100.00%	100.00%	100.00%	100.00%	100.00%	98.65%	95.65%	99.04%	95.38%	100.00%	100.00%	96.00%
840	100.00%	100.00%	100.00%	100.00%	100.00%	98.65%	95.65%	99.04%	95.38%	100.00%	98.01%	96.00%
825	100.00%	100.00%	100.00%	100.00%	100.00%	98.65%	95.65%	99.04%	95.38%	100.00%	98.01%	96.00%
810	100.00%	100.00%	100.00%	100.00%	100.00%	98.65%	88.41%	99.04%	95.38%	100.00%	98.01%	96.00%
795	100.00%	100.00%	100.00%	100.00%	100.00%	98.65%	88.41%	99.04%	95.38%	100.00%	98.01%	96.00%
780	100.00%	100.00%	100.00%	100.00%	100.00%	98.65%	88.41%	99.04%	95.38%	100.00%	98.01%	96.00%
765	100.00%	100.00%	100.00%	100.00%	100.00%	98.65%	88.41%	99.04%	95.38%	100.00%	98.01%	96.00%
750	100.00%	100.00%	100.00%	100.00%	100.00%	98.65%	88.41%	96.15%	95.38%	100.00%	98.01%	96.00%
735	100.00%	100.00%	100.00%	100.00%	100.00%	98.65%	88.41%	96.15%	95.38%	100.00%	98.01%	96.00%
720	100.00%	100.00%	100.00%	100.00%	100.00%	98.65%	88.41%	96.15%	95.38%	100.00%	98.01%	94.00%
705	100.00%	100.00%	100.00%	100.00%	100.00%	98.65%	88.41%	96.15%	95.38%	100.00%	98.01%	94.00%
690	100.00%	100.00%	100.00%	100.00%	100.00%	98.65%	88.41%	94.23%	95.38%	100.00%	98.01%	94.00%
675	100.00%	100.00%	100.00%	100.00%	100.00%	98.65%	88.41%	94.23%	95.38%	100.00%	98.01%	94.00%

Table C.1 (Continued) Wolman Pebble Count Grain Size Distribution Calculation

Bridge #	0709-150	1809-153	0711-150	1612-154	2108-162	1605-158	1417-156	1605-153	1405-156	1912-160	2107-156	2111-155
Sieve Sizes (mm)	Percentage passing											
660	100.00%	100.00%	100.00%	100.00%	100.00%	98.65%	88.41%	94.23%	95.38%	100.00%	98.01%	94.00%
645	100.00%	100.00%	100.00%	100.00%	100.00%	98.65%	88.41%	94.23%	95.38%	100.00%	97.01%	94.00%
630	100.00%	100.00%	100.00%	100.00%	98.64%	98.65%	88.41%	94.23%	95.38%	100.00%	97.01%	94.00%
615	100.00%	100.00%	100.00%	100.00%	98.64%	98.65%	88.41%	94.23%	95.38%	100.00%	97.01%	94.00%
600	100.00%	100.00%	100.00%	100.00%	98.64%	98.65%	88.41%	94.23%	95.38%	100.00%	97.01%	94.00%
585	100.00%	100.00%	100.00%	100.00%	98.64%	98.65%	88.41%	92.31%	95.38%	100.00%	97.01%	92.00%
570	100.00%	100.00%	100.00%	100.00%	98.64%	98.65%	88.41%	90.38%	90.77%	100.00%	97.01%	92.00%
555	100.00%	100.00%	100.00%	100.00%	98.64%	98.65%	88.41%	90.38%	90.77%	100.00%	97.01%	92.00%
540	100.00%	100.00%	100.00%	97.80%	98.64%	98.65%	86.96%	90.38%	86.15%	100.00%	97.01%	90.00%
525	100.00%	100.00%	100.00%	95.60%	97.28%	98.65%	86.96%	90.38%	86.15%	100.00%	97.01%	90.00%
510	100.00%	100.00%	100.00%	95.60%	97.28%	95.95%	85.51%	88.46%	84.62%	100.00%	96.52%	90.00%
495	100.00%	100.00%	100.00%	95.60%	97.28%	95.95%	85.51%	88.46%	84.62%	100.00%	96.52%	88.00%
480	100.00%	100.00%	100.00%	95.60%	97.28%	95.95%	85.51%	88.46%	81.54%	100.00%	96.52%	85.00%
465	100.00%	100.00%	100.00%	95.60%	97.28%	95.95%	85.51%	87.50%	81.54%	100.00%	96.52%	85.00%
450	100.00%	100.00%	100.00%	95.60%	95.24%	95.95%	85.51%	85.58%	75.38%	100.00%	95.02%	85.00%
435	100.00%	100.00%	100.00%	95.60%	95.24%	95.95%	85.51%	85.58%	75.38%	100.00%	95.02%	85.00%
420	100.00%	100.00%	100.00%	95.60%	95.24%	95.95%	85.51%	83.65%	72.31%	100.00%	95.02%	82.00%
405	100.00%	100.00%	100.00%	93.41%	95.24%	95.95%	85.51%	83.65%	72.31%	100.00%	94.53%	82.00%
390	100.00%	100.00%	100.00%	93.41%	94.56%	95.95%	84.06%	81.73%	72.31%	100.00%	94.03%	81.00%
375	100.00%	100.00%	100.00%	93.41%	94.56%	94.59%	84.06%	81.73%	72.31%	100.00%	92.04%	80.00%
360	100.00%	100.00%	100.00%	92.31%	94.56%	94.59%	84.06%	80.77%	69.23%	100.00%	91.04%	78.00%
345	100.00%	100.00%	100.00%	92.31%	92.52%	94.59%	84.06%	79.81%	69.23%	100.00%	88.06%	75.00%
330	100.00%	100.00%	100.00%	91.21%	91.16%	91.89%	82.61%	78.85%	69.23%	100.00%	85.57%	73.00%
315	100.00%	100.00%	100.00%	90.11%	89.80%	91.89%	82.61%	78.85%	69.23%	100.00%	84.58%	73.00%
300	100.00%	100.00%	100.00%	86.81%	89.12%	91.89%	82.61%	76.92%	64.62%	96.70%	83.08%	68.00%
285	100.00%	100.00%	100.00%	86.81%	89.12%	91.89%	82.61%	75.96%	64.62%	95.60%	81.59%	67.00%
270	100.00%	100.00%	100.00%	83.52%	89.12%	90.54%	81.16%	73.08%	58.46%	94.51%	78.61%	65.00%
255	100.00%	100.00%	100.00%	82.42%	88.44%	87.84%	81.16%	72.12%	50.77%	94.51%	77.11%	62.00%
240	100.00%	100.00%	100.00%	81.32%	85.71%	77.03%	79.71%	67.31%	47.69%	94.51%	72.64%	59.00%
225	100.00%	100.00%	100.00%	81.32%	83.67%	72.97%	78.26%	64.42%	44.62%	92.31%	71.64%	56.00%
210	98.65%	100.00%	100.00%	79.12%	80.27%	71.62%	78.26%	59.62%	40.00%	87.91%	67.66%	49.00%
195	98.65%	100.00%	100.00%	76.92%	78.23%	66.22%	78.26%	57.69%	40.00%	84.62%	65.17%	47.00%
180	95.95%	97.78%	100.00%	74.73%	72.11%	60.81%	73.91%	52.88%	36.92%	79.12%	60.70%	40.00%
165	95.95%	93.33%	99.04%	72.53%	70.07%	54.05%	73.91%	49.04%	32.31%	75.82%	56.72%	38.00%
150	94.59%	91.11%	98.08%	72.53%	65.99%	43.24%	66.67%	41.35%	24.62%	63.74%	53.23%	33.00%
135	94.59%	84.44%	96.15%	72.53%	61.22%	40.54%	62.32%	39.42%	18.46%	56.04%	50.75%	29.00%
120	90.54%	82.22%	93.27%	67.03%	56.46%	29.73%	57.97%	32.69%	16.92%	43.96%	41.29%	26.00%
105	89.19%	80.00%	88.46%	60.44%	52.38%	22.97%	50.72%	29.81%	15.38%	40.66%	37.81%	24.00%
90	83.78%	77.78%	80.77%	54.95%	45.58%	18.92%	46.38%	25.96%	13.85%	35.16%	28.86%	20.00%
75	78.38%	71.11%	72.12%	49.45%	36.73%	12.16%	42.03%	24.04%	7.69%	27.47%	25.37%	19.00%
60	63.51%	62.22%	50.96%	40.66%	22.45%	8.11%	31.88%	20.19%	3.08%	24.18%	14.93%	16.00%
45	41.89%	51.11%	39.42%	24.18%	14.97%	1.35%	23.19%	17.31%	3.08%	23.08%	5.97%	15.00%
30	20.27%	28.89%	21.15%	14.29%	8.84%	0.00%	8.70%	13.46%	1.54%	15.38%	1.00%	14.00%
15	8.11%	17.78%	8.65%	7.69%	4.08%	0.00%	4.35%	11.54%	0.00%	7.69%	0.00%	9.00%
0	0.00%	0.00%	0.00%	0.00%	0.00%	0.00%	0.00%	0.00%	0.00%	0.00%	0.00%	0.00%

C.2 WIPFRAG

During this research we ran actual WipFrag grain size distribution analysis as well as a more precise manual WipFrag analysis for four of the 12 study bridges. The data and analysis results for each of the four bridges presented in **Tables C.2** through **C.5**.

Table C.2 Comparison of Actual vs Manual WipFrag Analysis, Bridge # 1605-158

	Sediment Grading, 'n'			Median Grain Size, 'Xc'		
	Adjusted	Actual	Ratio, 'K1'	Adjusted	Actual	Ratio, 'K2'
Photo #	n2	n1	K1 = n2/n1	Xc2	Xc1	K2 = Xc2/Xc1
1	1.28	0.85	1.51	181.61	207.95	0.87
2	1.36	0.94	1.44	143.74	186.15	0.77
3	1.29	0.85	1.51	165.22	113.84	1.45
4	1.38	0.91	1.51	166.20	214.21	0.78
5	1.21	0.96	1.26	267.12	113.54	2.35
6	1.35	0.80	1.68	253.36	175.23	1.45
7	1.19	0.77	1.54	234.69	114.13	2.06
8	1.27	0.69	1.84	242.33	206.02	1.18
10	1.14	0.88	1.30	153.54	102.57	1.50
11	1.31	0.94	1.38	126.76	80.55	1.57
12	1.33	0.91	1.47	155.51	180.00	0.86
Average	1.28	0.86	**1.50**	190.01	154.02	**1.35**

Table C.3 Comparison of Actual vs Manual WipFrag Analysis, Bridge # 1417-156

	Sediment Grading, 'n'			Median Grain Size, 'Xc'		
	Adjusted	Actual	Ratio, 'K1'	Adjusted	Actual	Ratio, 'K2'
Photo #	n2	n1	K1 = n2/n1	Xc2	Xc1	K2 = Xc2/Xc1
1	1.35	1.13	1.20	107.35	82.65	1.30
2	1.24	1.21	1.02	82.54	67.02	1.23
3	1.01	1.05	0.96	139.32	47.45	2.94
4	0.93	0.89	1.04	325.69	55.18	5.90
Average	1.13	1.07	**1.05**	163.73	63.08	**2.84**

Table C.4 Comparison of Actual vs Manual WipFrag Analysis, Bridge # 1405-156

	Sediment Grading, 'n'			Median Grain Size, 'Xc'		
	Adjusted	Actual	Ratio, 'K1'	Adjusted	Actual	Ratio, 'K2'
Photo #	n2	n1	K1 = n2/n1	Xc2	Xc1	K2 = Xc2/Xc1
1	1.55	1.33	1.17	263.21	290.39	0.91
2	1.60	1.16	1.37	259.74	249.38	1.04
3	1.41	1.05	1.34	256.79	220.87	1.16
4	1.76	0.99	1.79	239.17	170.05	1.41
5	1.59	1.00	1.59	261.17	194.87	1.34
6	1.19	1.05	1.13	355.23	66.94	5.31
7	1.47	1.03	1.42	212.77	177.01	1.20
8	1.30	0.86	1.51	282.14	163.61	1.72
Average	1.48	1.06	**1.41**	266.28	191.64	**1.76**

Table C.5 Comparison of Actual vs Manual WipFrag Analysis, Bridge # 2107-156

	Sediment Grading, 'n'			Median Grain Size, 'Xc'		
	Adjusted	Actual	Ratio, 'K1'	Adjusted	Actual	Ratio, 'K2'
Photo #	n2	n1	K1 = n2/n1	Xc2	Xc1	K2 = Xc2/Xc1
1	1.36	1.24	1.10	262.75	262.98	1.00
2	1.44	1.24	1.16	170.34	195.84	0.87
3	1.38	1.19	1.16	191.33	160.25	1.19
4	1.37	0.91	1.50	268.76	153.93	1.75
5	1.68	1.58	1.06	102.50	97.43	1.05
6	1.46	0.96	1.53	136.91	181.00	0.76
7	1.26	1.11	1.14	126.09	46.20	2.73
8	1.24	0.97	1.28	160.14	39.39	4.07
9	1.22	1.20	1.01	124.29	30.16	4.12
10	1.09	0.95	1.15	208.94	56.29	3.71
11	1.38	0.89	1.55	260.39	98.22	2.65
12	1.42	1.12	1.27	296.65	232.72	1.27
13	1.55	1.15	1.36	288.71	303.92	0.95
14	1.62	1.25	1.30	277.91	275.64	1.01
15	1.42	1.22	1.17	66.03	65.82	1.00
16	1.30	1.13	1.15	130.39	114.57	1.14
17	1.49	1.19	1.25	101.42	101.25	1.00
18	1.36	1.14	1.20	258.20	154.69	1.67
Average	1.39	1.13	**1.24**	190.65	142.79	**1.77**

C.3 Visual Estimation

Streambed sediment categories estimation along with median grain size calculation and results for all 12 study bridges presented in **Table C.6**.

Table C. 6 Grain Size Calculation and Analysis of Visual Estimation Method for All 12 Study Bridges

		Bridge # 0709-150			Bridge # 1809-153	
Category	Category Median Size (mm)	% Estimat	Category Average		% Estimat	Category Average
Boulders	299	0%	0		5%	11.45
Cobbles	166	30%	48		25%	40
Gravel	33	60%	19.8		40%	13.2
Sand/Silt	0.5	10%	0.05		30%	0.15
Overall Median Grain Size			**67.85**			**64.8**
		Bridge # 0711-150			Bridge # 1612-154	
Category	Category Median Size (mm)	% Estimat	Category Average		% Estimat	Category Average
Boulders	299	0%	0		10%	22.9
Cobbles	166	40%	64		60%	96
Gravel	33	40%	13.2		20%	6.6
Sand/Silt	0.5	20%	0.1		10%	0.05
Overall Median Grain Size			**77.3**			**125.55**
		Bridge # 2108-162			Bridge # 1605-158	
Category	Category Median Size (mm)	% Estimat	Category Average		% Estimat	Category Average
Boulders	299	20%	45.8		50%	114.5
Cobbles	166	50%	80		10%	16
Gravel	33	20%	6.6		10%	3.3
Sand/Silt	0.5	10%	0.05		30%	0.15
Overall Median Grain Size			**132.45**			**133.95**
		Bridge # 1417-156			Bridge # 1605-153	
Category	Category Median Size (mm)	% Estimat	Category Average		% Estimat	Category Average
Boulders	299	25%	57.25		50%	114.5
Cobbles	166	50%	80		25%	40
Gravel	33	20%	6.6		10%	3.3
Sand/Silt	0.5	5%	0.025		15%	0.075
Overall Median Grain Size			**143.875**			**157.875**
		Bridge # 1405-156			Bridge # 1912-160	
Category	Category Median Size (mm)	% Estimat	Category Average		% Estimat	Category Average
Boulders	299	70%	160.3		20%	45.8
Cobbles	166	20%	32		50%	80
Gravel	33	5%	1.65		20%	6.6
Sand/Silt	0.5	5%	0.025		10%	0.05
Overall Median Grain Size			**193.975**			**132.45**
		Bridge # 2107-156			Bridge # 2111-155	
Category	Category Median Size (mm)	% Estimat	Category Average		% Estimat	Category Average
Boulders	299	40%	91.6		50%	114.5
Cobbles	166	50%	80		30%	48
Gravel	33	10%	3.3		10%	3.3
Sand/Silt	0.5	0%	0		10%	0.05
Overall Median Grain Size			**174.9**			**165.85**

APPENDIX D

FLOW VELOCITY CALCULATION

D.1 Interpolation / Extrapolation from Stage II Studies

Stage II flow discharge for 50,100, and 500 years as well as maximum limit discharge and the corresponding calculated velocity based on interpolation or extrapolation method presented in **Table D.1**. Limit velocity versus median grain size plot drawn in **Figure D.1** which shows where each bridge representative point fall in the chart corresponding to other Fundamental Sediment Transport Relationships.

Table D.1 Interpolation and Extrapolation of Discharge and Velocity Values

	Bridge #	Q50	V50	Q100	V100	Q500	V500	Q limit	V-velocity	
		cfs	ft/s	cfs	ft/s	cfs	ft/s	cfs	ft/s	cm/s
1	0709-150	600	9.91	720	9.96	1200	12.77	610	9.92	**302**
2	1809-153	430	8	545	8.2	920	8.5	1033	9	**274**
3	0711-150	1150	11.47	1405	12.26	2200	14.15	877	8.04	**245**
4	1612-154	1525	8.24	1920	9.29	2945	12.01	2148	9.9	**302**
5	2108-162	2450	4.58	2926	6.03	4264	8.61	5078	10.17	**310**
6	1605-158	1446	11.38	2059	12.75	3500	15.21	1008	9.9	**302**
7	1417-156	984	30.92	1215	31.92	2065	33.83	2785	43.1	**1314**
8	1605-153	2602	13.77	3440	14.86	5200	17.15	4873	16.8	**512**
9	1405-156	3515	10.03	4265	10.84	6285	13.77	5043	12	**366**
10	1912-160	1969	6.12	2398	7.2	3395	7.84	6524	10	**305**
11	2107-156	6783	11.76	8117	11.77	11939	11.8	10690	11.77	**359**
12	2111-155	2010	5.1	2372	5.5	3025	6	2473	5.7	**174**

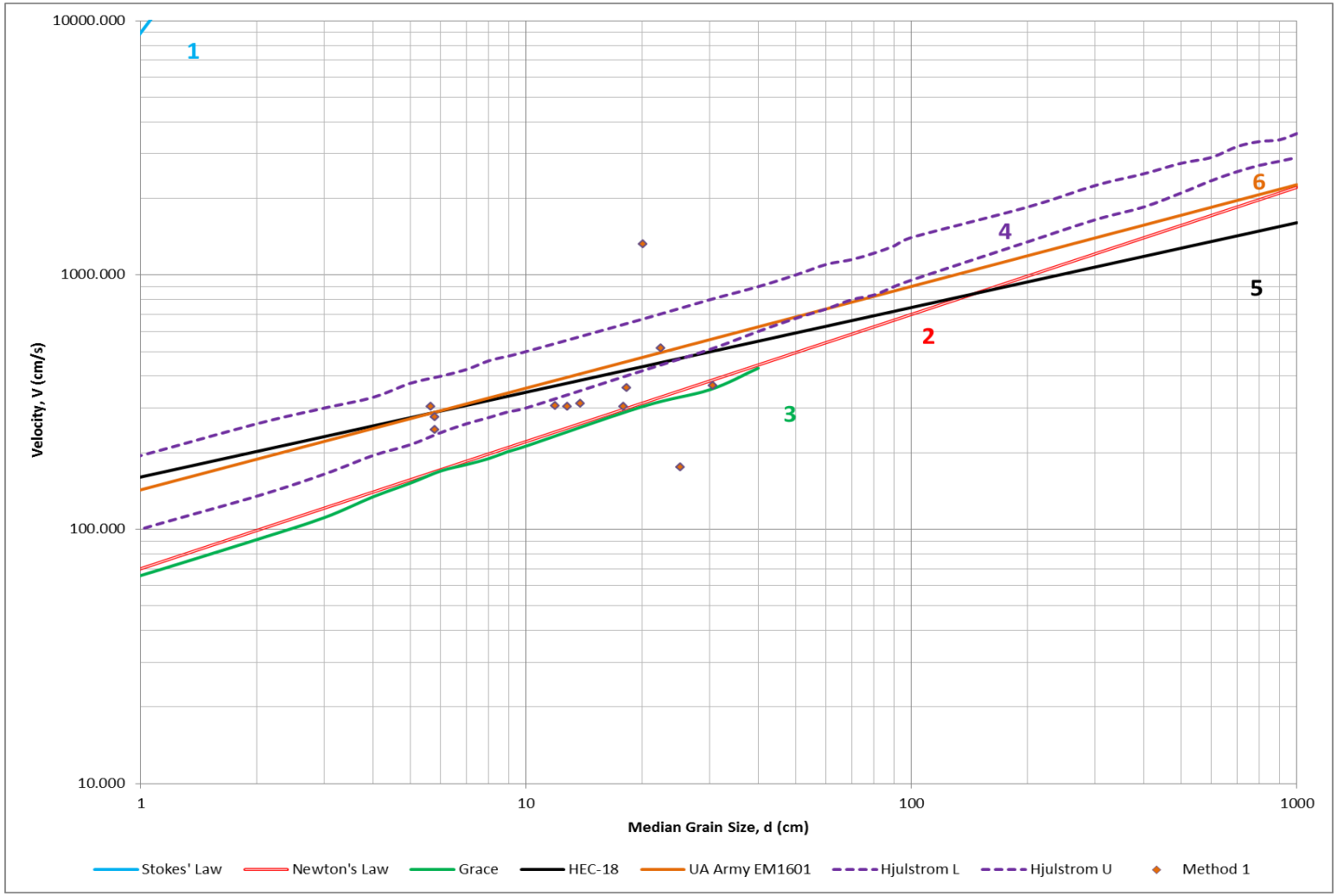

Figure D.1 Stage II interpolation/extrapolation method, velocity vs. median grain size.

D.2 Flow Area Calculation from Stage II Study

Flow discharge area for the 12 study bridges calculated from Stage II bridge cross section drawing for 100 years of storm. Then the flows limit velocity calculated by dividing limit flow discharge over calculated flow discharge area. Limit velocity results as well as median grain size for each of the 12 study bridges presented in **Table D.2** and plotted in **Figure D.2** for the purpose of comparing the limit analysis results with other Fundamental Sediment Transport Relationships.

Table D.2 Calculated Discharge Area and Velocity Based on Stage II Bridge Elevations

	Bridge #	Median Grain Size	Q limit	A sII calculated	V-velocity	
		D (cm)	cfs	sf	ft/s	cm/s
1	0709-150	5.65	610	80.00	7.63	**232**
2	1809-153	5.79	1033	38.25	27.00	**823**
3	0711-150	5.80	877	162.80	5.39	**164**
4	1612-154	12.79	2148	232.50	9.24	**282**
5	2108-162	13.83	5078	877.50	5.79	**176**
6	1605-158	17.92	1008	288.12	3.50	**107**
7	1417-156	20.13	2785	33.10	84.15	**2565**
8	1605-153	22.39	4873	380.10	12.82	**391**
9	1405-156	30.58	5043	980.40	5.14	**157**
10	1912-160	11.90	6524	280.80	23.23	**708**
11	2107-156	18.21	10690	1164.18	9.18	**280**
12	2111-155	25.17	2473	137.20	18.03	**549**

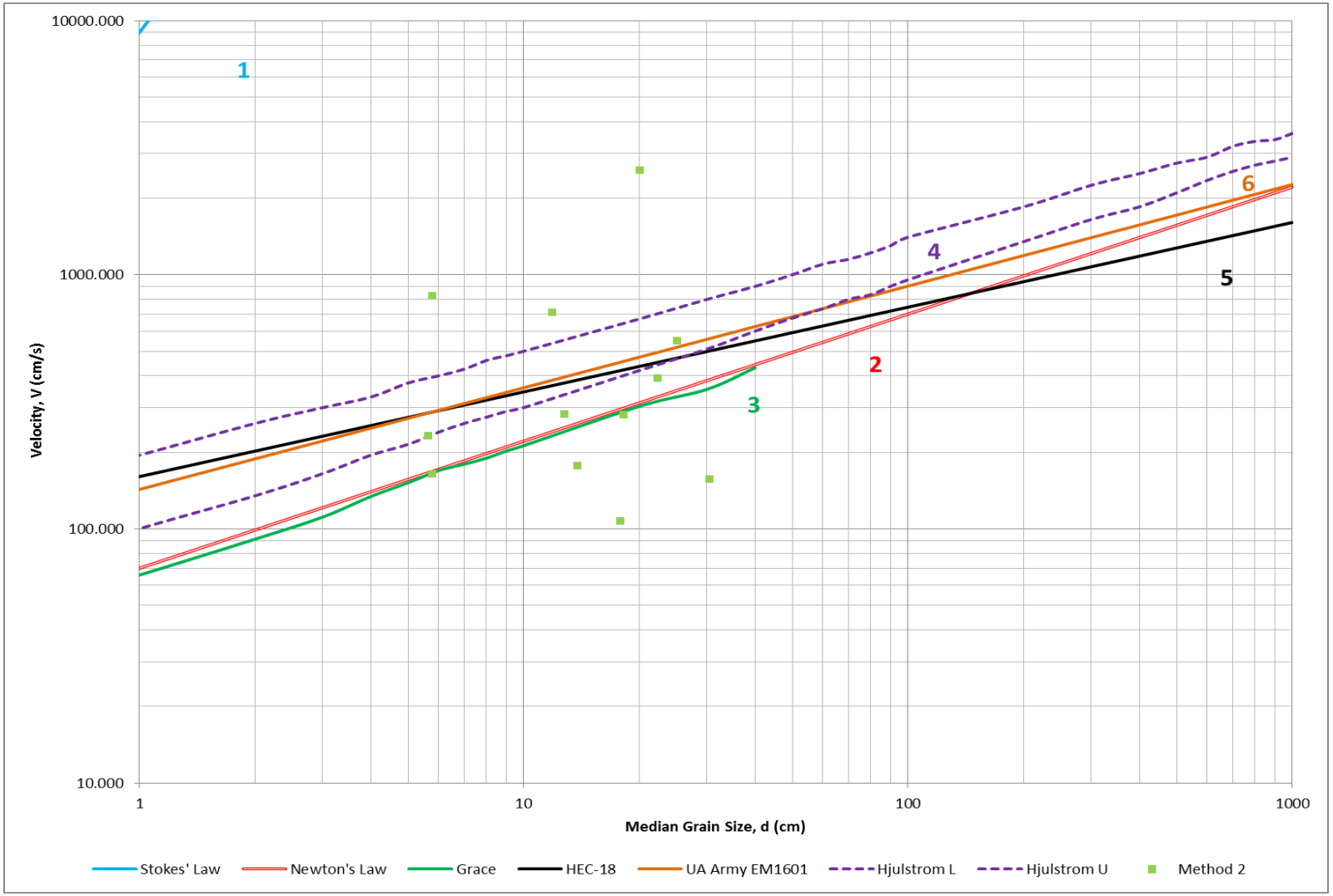

Figure D.2 Flow opening area calculation method, velocity vs. median grain size.

D.3 Manning's Equation Method

The most fundamental and comprehensive limit velocity calculation that conducted during this research study was based on manning's equation. At first all the essential parameters of the equation which are roughness coefficient and slope of the channel were calculated very carefully and precisely. Next the average heights of the flow calculated, and during the final step flow limit velocity calculated. **Table D.3** contains all the calculation results. Limit velocity versus median grain size based on the manning's equation method plotted in **Figure D.3**.

Table D.3 Manning's Equation Parameters and Values

		Qlimit	w- Openning	n-Roughness	s-Slope	h- flow hight	A-area	V- velocity	
	Bridge #	cfs	ft			ft	sf	ft/s	cm/s
1	0709-150	610	22	0.034	0.0067	3.85	85	7.20	**219**
2	1809-153	1033	8.5	0.036	0.0211	9.82	83	12.38	**377**
3	0711-150	877	24	0.034	0.0069	4.55	109	8.04	**245**
4	1612-154	2148	31	0.039	0.0070	7.42	230	9.34	**285**
5	2108-162	5078	60	0.049	0.0054	9.94	597	8.52	**260**
6	1605-158	1008	42	0.046	0.0173	2.64	111	9.08	**277**
7	1417-156	2785	20	0.0575	0.0288	10.64	213	13.09	**399**
8	1605-153	4873	30	0.054	0.0082	16.50	495	9.85	**300**
9	1405-156	5043	152	0.072	0.0149	4.81	732	6.89	**210**
10	1912-160	6524	52	0.042	0.0083	10.28	534	12.20	**372**
11	2107-156	10690	144	0.047	0.0007	8.56	1231	8.70	**265**
12	2111-155	2473	56	0.06	0.0041	8.15	457	5.42	**165**

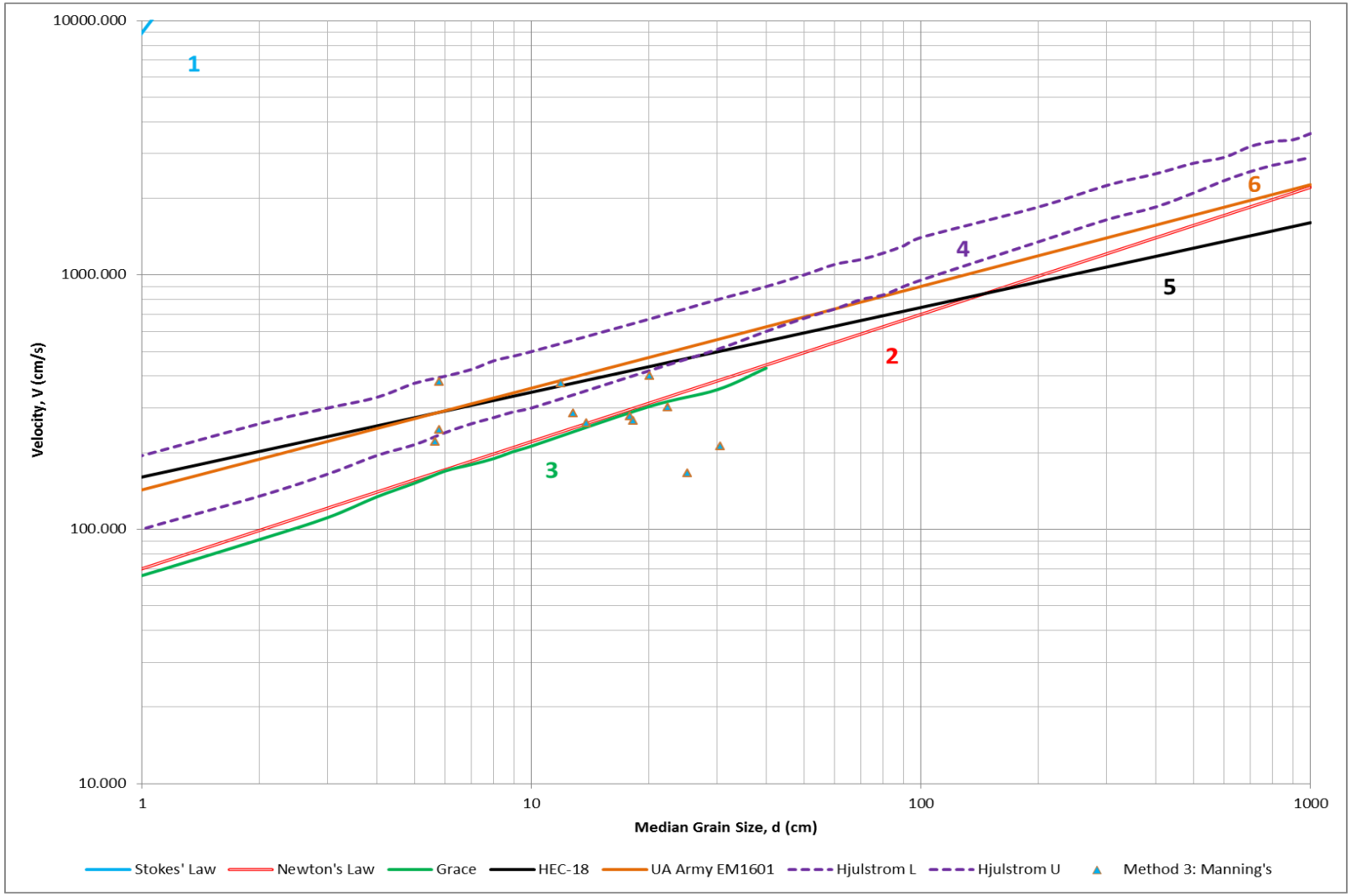

Figure D.3 Manning's equation method, velocity vs. median grain size.

APPENDIX E

12 STUDY BRIDGES GENERAL INFORMATION, ELEVATION PHOTO, AND GRAIN SIZE DISTRIBUTION PLOT

E.1 Bridge # 0709-150

NJDOT bridge number 0709-150, located on NJ route 10 over Willow Meadow Brook, Essex county, Piedmont physiographic province. This bridge was constructed in 1959, and it is a single-span, simply supported structure consisting of a reinforced concrete slab and reinforced concrete spread footing. The bridge length and width are 22 and 108 feet, respectively. An elevation of the bridge is shown in **Figure E.1**. An example of streambed sediments and analysis of streambed grain size distribution based on Wolman Pebble Count method shown in **Figures E.2** and **E.3**.

Figure E.1 Bridge # 0709-150 elevation, up-stream looking down-stream.

Figure E.2 Bridge # 0709-150 stream-bed sediments close-up and Wolman Pebble Count section installation.

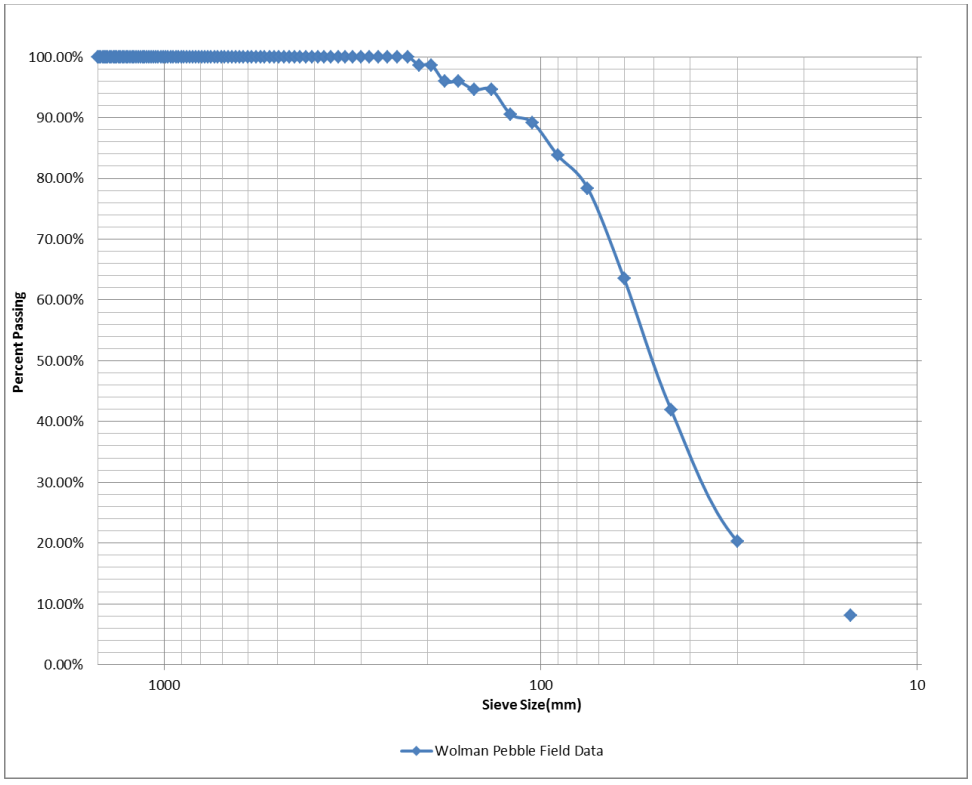

Figure E.3 Bridge # 0709-150 stream-bed grain size distribution analysis.

E.2 Bridge # 1809-153

NJDOT bridge number 1809-153, located on NJ route 202 over Branch of Mine Brook, Somerset county, Piedmont physiographic province. This bridge was constructed in 1900, and it is a single-span, simply supported structure consisting of filled concrete and stone arch and stone and mortar footing. The bridge length and width are 20 and 34 feet, respectively. An elevation of the bridge is shown in **Figure E.4**. An example of streambed sediments and analysis of streambed grain size distribution based on Wolman Pebble Count method shown in **Figures E.5** and **E.6**.

Figure E.4 Bridge # 1809-153 elevation, down-stream looking up-stream.

Figure E.5 Bridge # 1809-153 stream-bed sediments close-up.

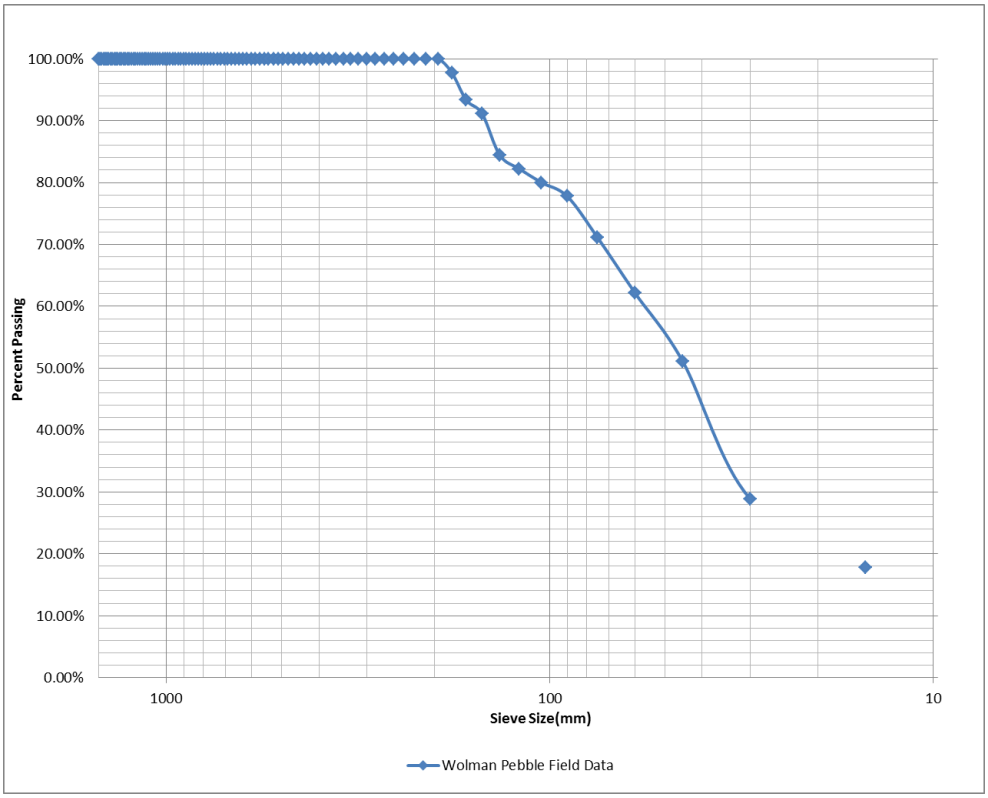

Figure E.6 Bridge # 1809-153 stream-bed grain size distribution analysis.

E.3 Bridge # 0711-150

NJDOT bridge number 0711-150, located on NJ route 10 over Canoe Brook, Essex county, Piedmont physiographic province. This bridge was constructed in 1961, and it is a single-span, simply supported structure consisting of a reinforced concrete slab and reinforced concrete spread footing. The bridge length and width are 32 and 66 feet, respectively. An elevation of the bridge is shown in **Figure E.7**. An example of streambed sediments and analysis of streambed grain size distribution based on Wolman Pebble Count method shown in **Figures E.8** and **E.9**.

Figure E.7 Bridge # 0711-150 elevation, down-stream looking up-stream.

Figure E.8 Bridge # 0711-150 stream-bed sediments close-up.

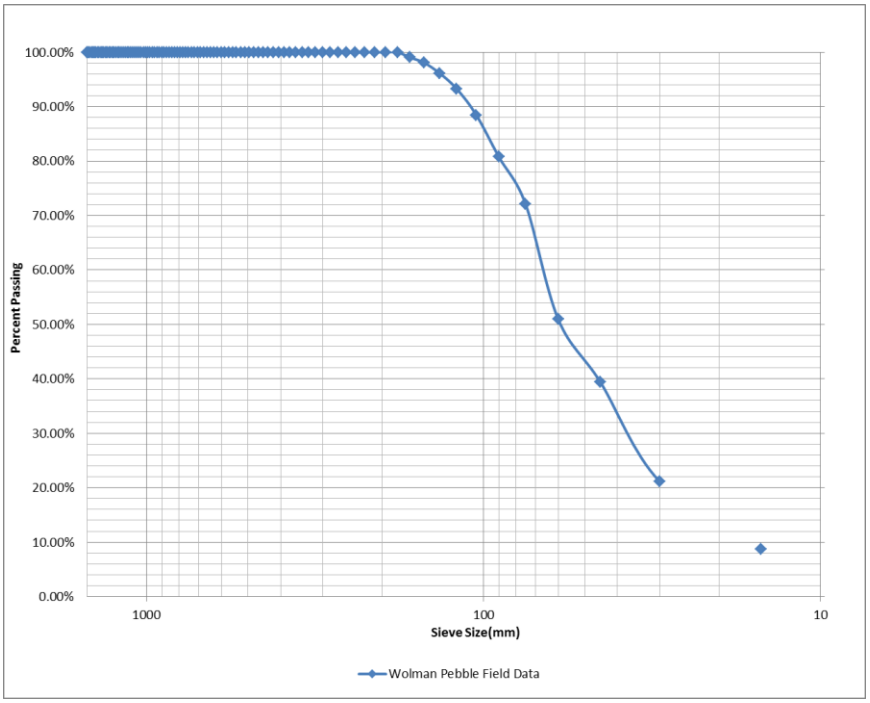

Figure E.9 Bridge # 0711-150 stream-bed grain size distribution analysis.

E.4 Bridge # 1612-154

NJDOT bridge number 1612-154, located on NJ route 208 Ramp A over Goffle Brook, Passaic county, Piedmont physiographic province. This bridge was constructed in 1958, and it is a single-span, simply supported structure consisting of a hinged rigid frame with fill and concrete hinged spread footing. The bridge length and width are 31 and 60.7 feet, respectively. An elevation of the bridge is shown in **Figure E.10**. An example of streambed sediments and analysis of streambed grain size distribution based on Wolman Pebble Count method shown in **Figures E.11** and **E.12**.

Figure E.10 Bridge # 1612-154 elevation, up-stream looking down-stream.

Figure E.11 Bridge # 1612-154 stream-bed sediments close-up.

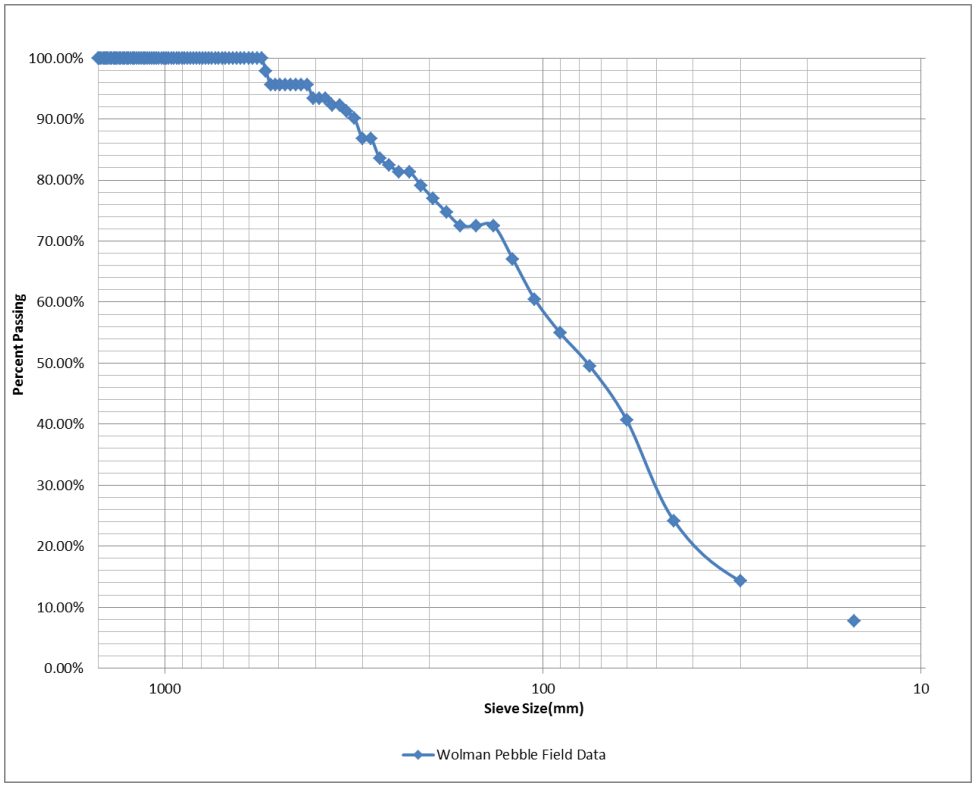

Figure E.12 Bridge # 1612-154 stream-bed grain size distribution analysis.

E.5 Bridge # 2108-162

NJDOT bridge number 2108-162, located on NJ route 46 over Musconetcong River, Warren county, Highlands physiographic province. This bridge was constructed in 1924, and it is a two-span, simply supported concrete encased riveted steel through girder with rolled steel floorbeams and reinforced concrete spread footing. The bridge length and width are 127 and 32 feet, respectively. An elevation of the bridge is shown in **Figure E.13**. An example of streambed sediments and analysis of streambed grain size distribution based on Wolman Pebble Count method shown in **Figures E.14** and **E.15**.

Figure E.13 Bridge # 2108-162 elevation, up-stream looking down-stream.

Figure E.14 Bridge # 2108-162 stream-bed sediment close-up and Wolman Pebble Count section installation.

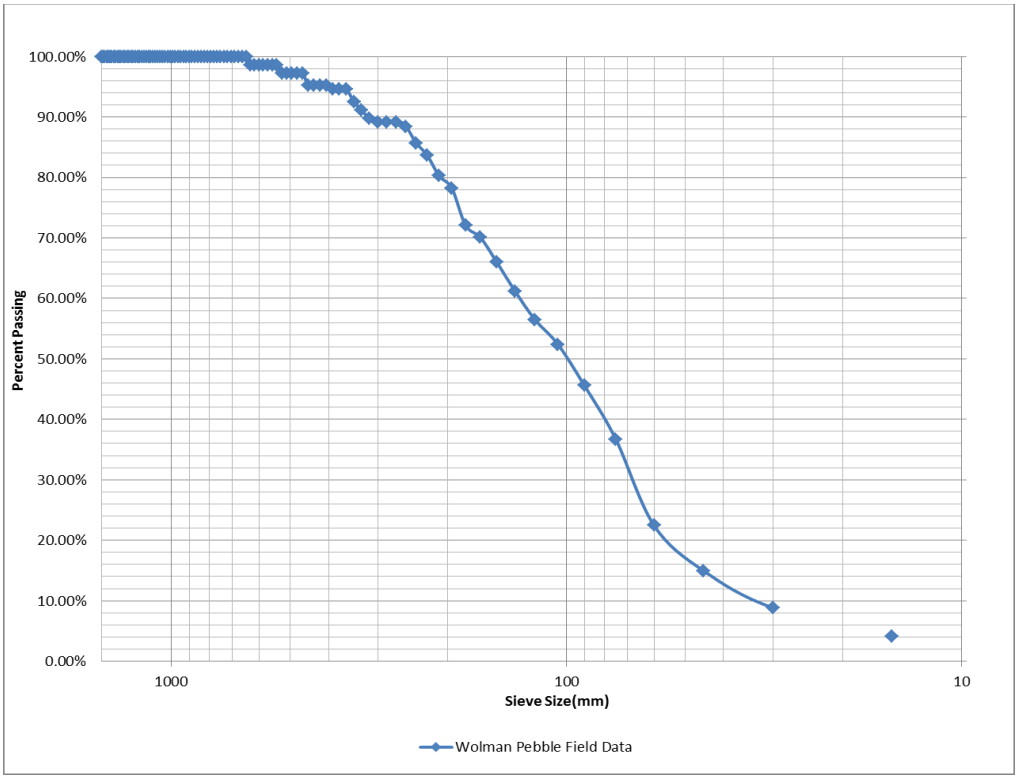

Figure E.15 Bridge # 2108-162 stream-bed grain size distribution analysis.

E.6 Bridge # 1605-158

NJDOT bridge number 1605-158, located on NJ route 23 north branch over Macopin River, Passaic county, Highlands physiographic province. This bridge was constructed in 1924 and reconstructed in 1990. It is a single-span, simply supported roll steel stringers with cover plate and reinforced concrete spread footing. The bridge length and width are 55.25 and 45.75 feet, respectively. An elevation of the bridge is shown in **Figure E.16**. An example of streambed sediments and analysis of streambed grain size distribution based on Wolman Pebble Count method shown in **Figures E.17** and **E.18**.

Figure E.16 Bridge # 1605-158 elevation, under the bridge, Wolman Pebble Count section installation and data collection.

Figure E.17 Bridge # 1605-158 stream-bed sediments close-up.

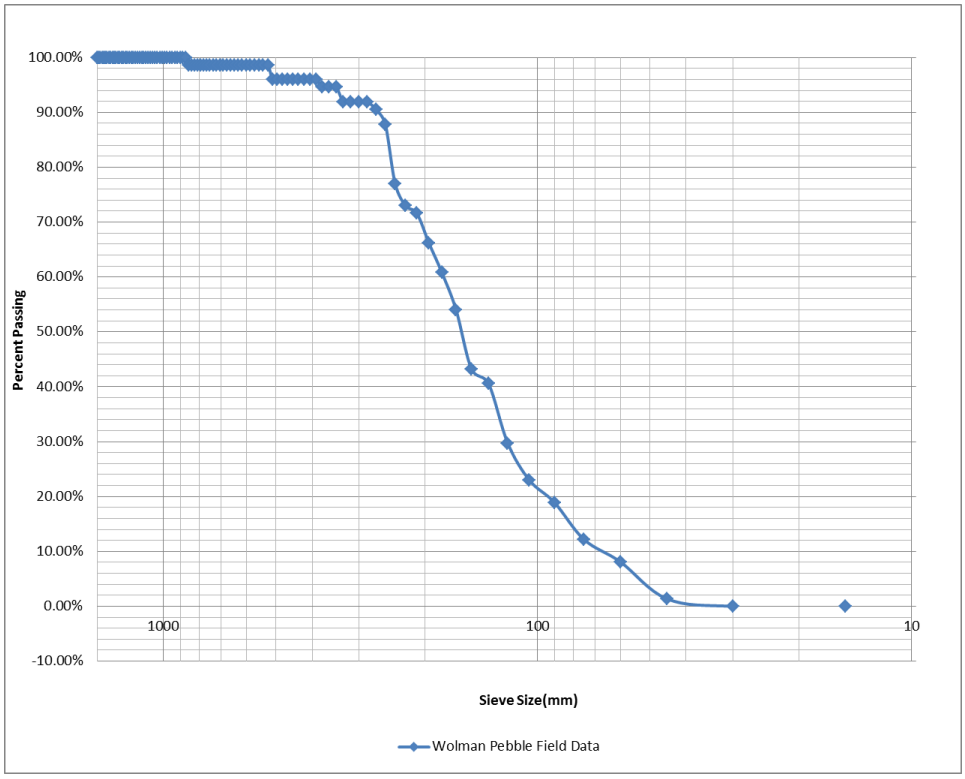

Figure E.18 Bridge # 1605-158 stream-bed grain size distribution analysis.

E.7 Bridge # 1417-156

NJDOT bridge number 1417-156, located on NJ route 206 over south branch of Raritan river, Morris county, Highlands province. This bridge was constructed in 1928, and it is a single-span, simply supported structure consisting of a reinforced concrete rigid frame with earth fill and unreinforced concrete spread footing. The bridge length and width are 28 and 54 feet, respectively. An elevation of the bridge is shown in **Figure E.19**. An example of streambed sediments and analysis of streambed grain size distribution based on Wolman Pebble Count method shown in **Figures E.20** and **E.21**.

Figure E.19 Bridge # 1417-156 elevation, up-stream looking down-stream.

Figure E.20 Bridge # 1417-156 stream-bed sediments close-up and Wolman Pebble Count section installation.

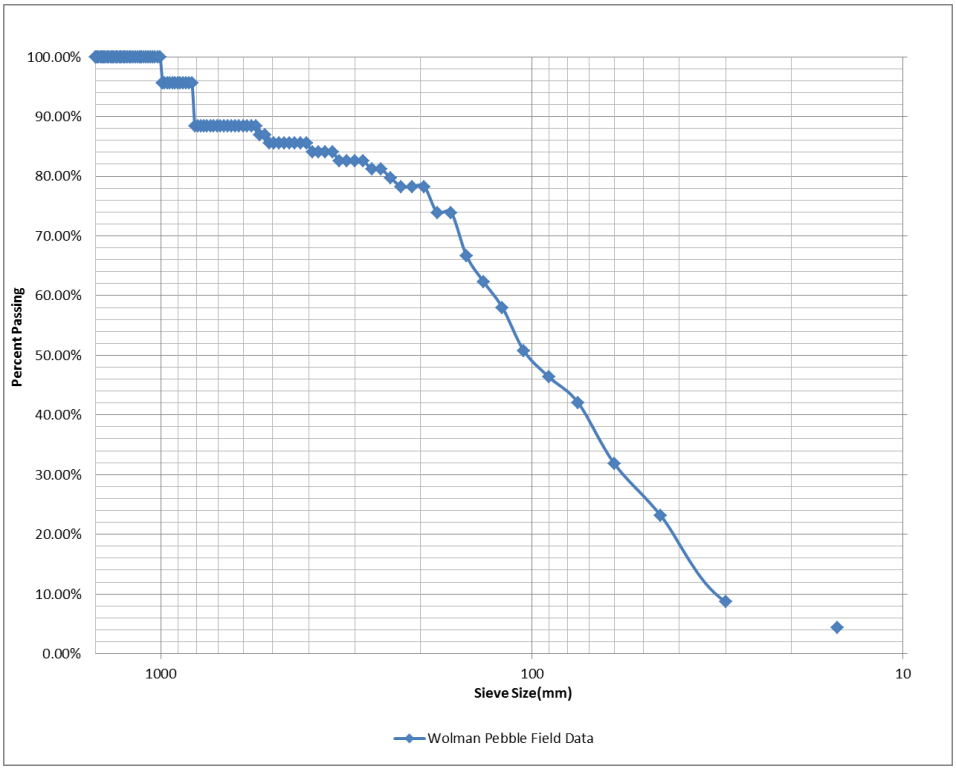

Figure E.21 Bridge # 1417-156 stream-bed grain size distribution analysis.

E.8 Bridge # 1605-153

NJDOT bridge number 1605-153, located on NJ route 23 south branch over Pequannock River, Passaic county, Highlands physiographic province. This bridge was constructed in 1952, and it is a single-span, reinforced concrete arch culvert with fill and continuous concrete spread footing. The bridge length and width are 43 and 222 feet, respectively. An elevation of the bridge is shown in **Figure E.22**. An example of streambed sediments and analysis of streambed grain size distribution based on Wolman Pebble Count method shown in **Figures E.23** and **E.24**.

Figure E.22 Bridge # 1605-153 elevation, up-stream looking down-stream.

Figure E.23 Bridge # 1605-153 stream-bed sediments close-up.

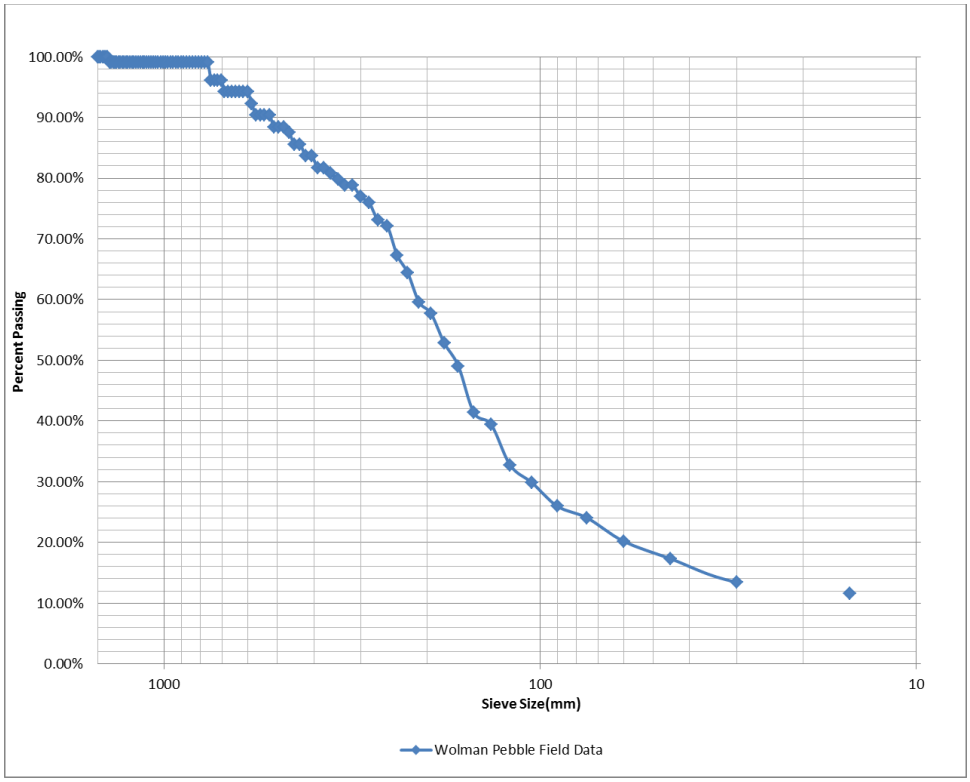

Figure E.24 Bridge # 1605-153 stream-bed grain size distribution analysis.

E.9 Bridge # 1405-156

NJDOT bridge number 1405-156, located on NJ route 23 over Pequannock River, Morris/ Passaic county, Highlands physiographic province. This bridge was constructed in 1934, and it is an eight-span, concrete encased, steel through girder- floorbeam-stringer system consisting of two simply supported end spans and three, two span continuous through girder and reinforced concrete spread footing. The bridge length and width are 513 and 59.4 feet, respectively. An elevation of the bridge is shown in **Figure E.25**. An example of streambed sediments and analysis of streambed grain size distribution based on Wolman Pebble Count method shown in **Figures E.26** and **E.27**.

Figure E.25 Bridge # 1405-156 elevation, up-stream looking down-stream.

Figure E.26 Bridge # 1405-156 stream-bed sediments close-up.

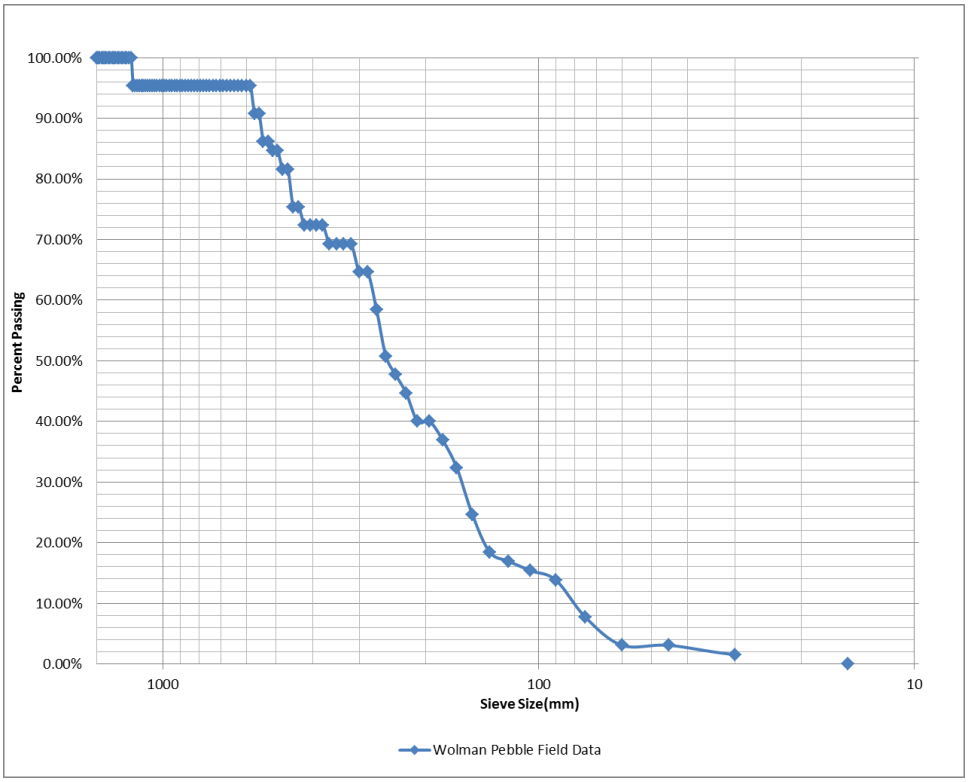

Figure E.27 Bridge # 1405-156 stream-bed grain size distribution analysis.

E.10 Bridge # 1912-160

NJDOT bridge number 1912-160, located on NJ route 206 over Big Flat Brook, Sussex county, Valley and Ridge physiographic province. This bridge was constructed in 1929, and it is a two-span, simply supported, concrete encased stringers and plain concrete spread footings. The bridge length and width are 93 and 44 feet, respectively. An elevation of the bridge is shown in **Figure E.28**. An example of streambed sediments and analysis of streambed grain size distribution based on Wolman Pebble Count method shown in **Figures E.29** and **E.30**.

Figure E.28 Bridge # 1912-160 elevation, up-stream looking down-stream, and Wolman Pebble Count section installation.

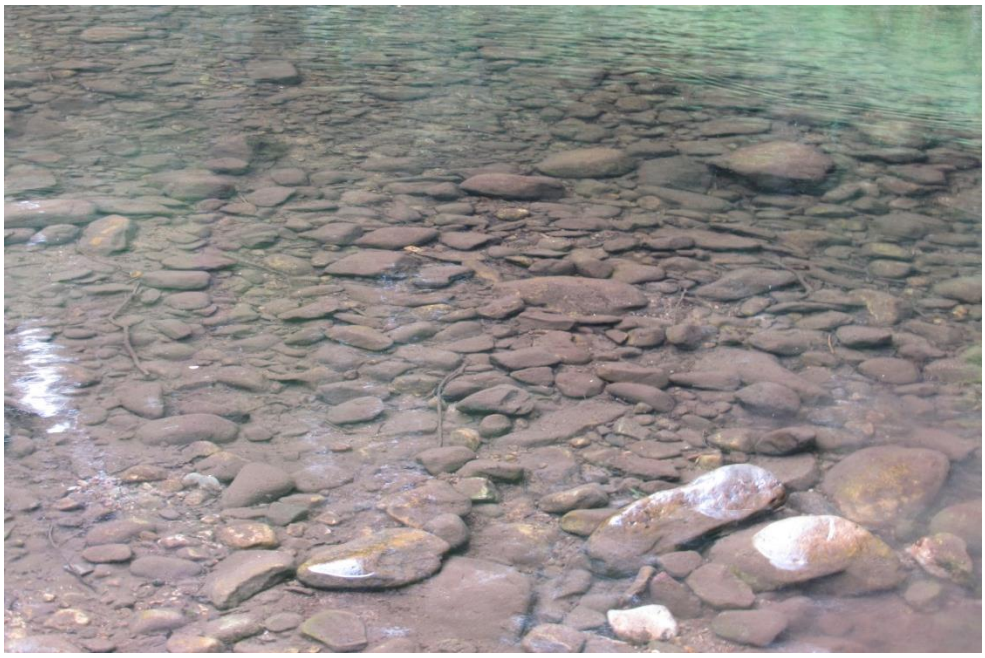

Figure E.29 Bridge # 1912-160 stream-bed sediments close-up.

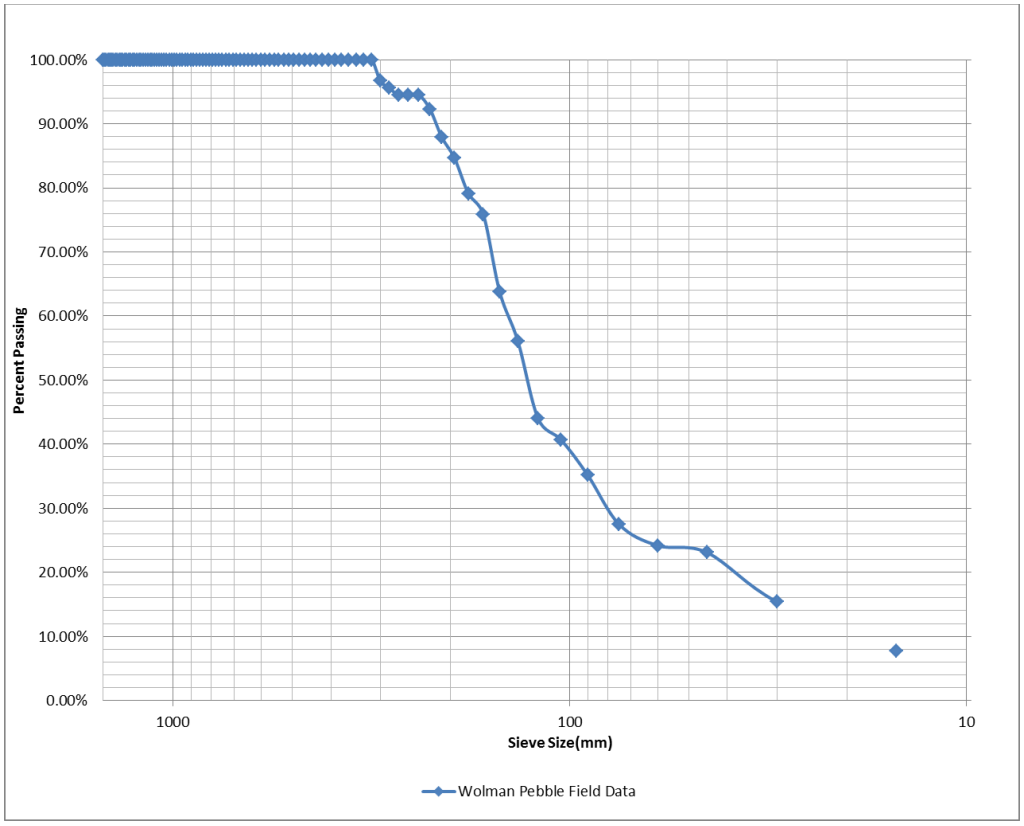

Figure E.30 Bridge # 1912-160 stream-bed grain size distribution analysis.

E.11 Bridge # 2107-156

NJDOT bridge number 2107-156, located on NJ route 46 over Paulins Kill, Warren county, Valley and Ridge physiographic province. This bridge was constructed in 1933, and it is a three-span, simply supported, non-composite rolled steel stringers and reinforced concrete spread footing. The bridge length and width are 174.3 and 91.3 feet, respectively. An elevation of the bridge is shown in **Figure E.31**. An example of streambed sediments and analysis of streambed grain size distribution based on Wolman Pebble Count method shown in **Figures E.32** and **E.33**.

Figure E.31 Bridge # 2107-156 elevation, up-stream looking down-stream.

Figure E.32 Bridge # 2107-156 stream-bed sediments close-up.

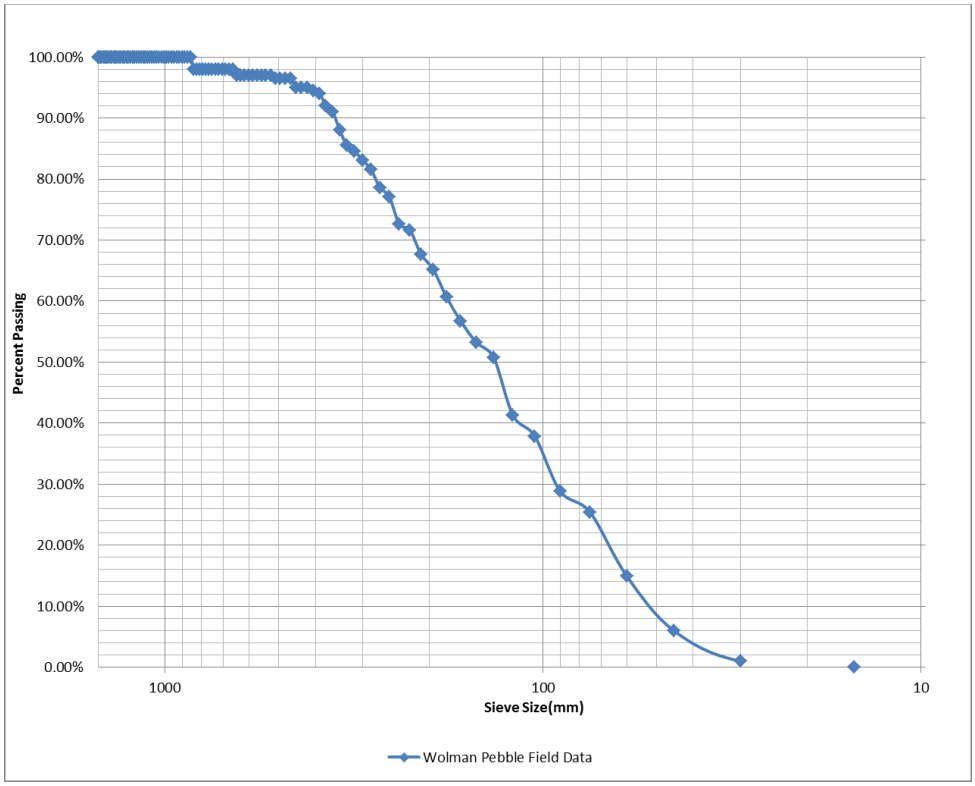

Figure E.33 Bridge # 2107-156 stream-bed grain size distribution analysis.

E.12 Bridge # 2111-155

NJDOT bridge number 2111-155, located on NJ route 31 over Pequest River, Warren county, Valley and Ridge physiographic province. This bridge was constructed in 1922, and it is a two-span, reinforced concrete spandrel filled arch and reinforced concrete spread footing. The bridge length and width are 116 and 33.3 feet, respectively. An elevation of the bridge is shown in **Figure E.34**. An analysis of streambed grain size distribution based on Wolman Pebble Count method shown in **Figure E.35.**

Figure E.34 Bridge # 2111-155 elevation, up-stream looking down-stream.

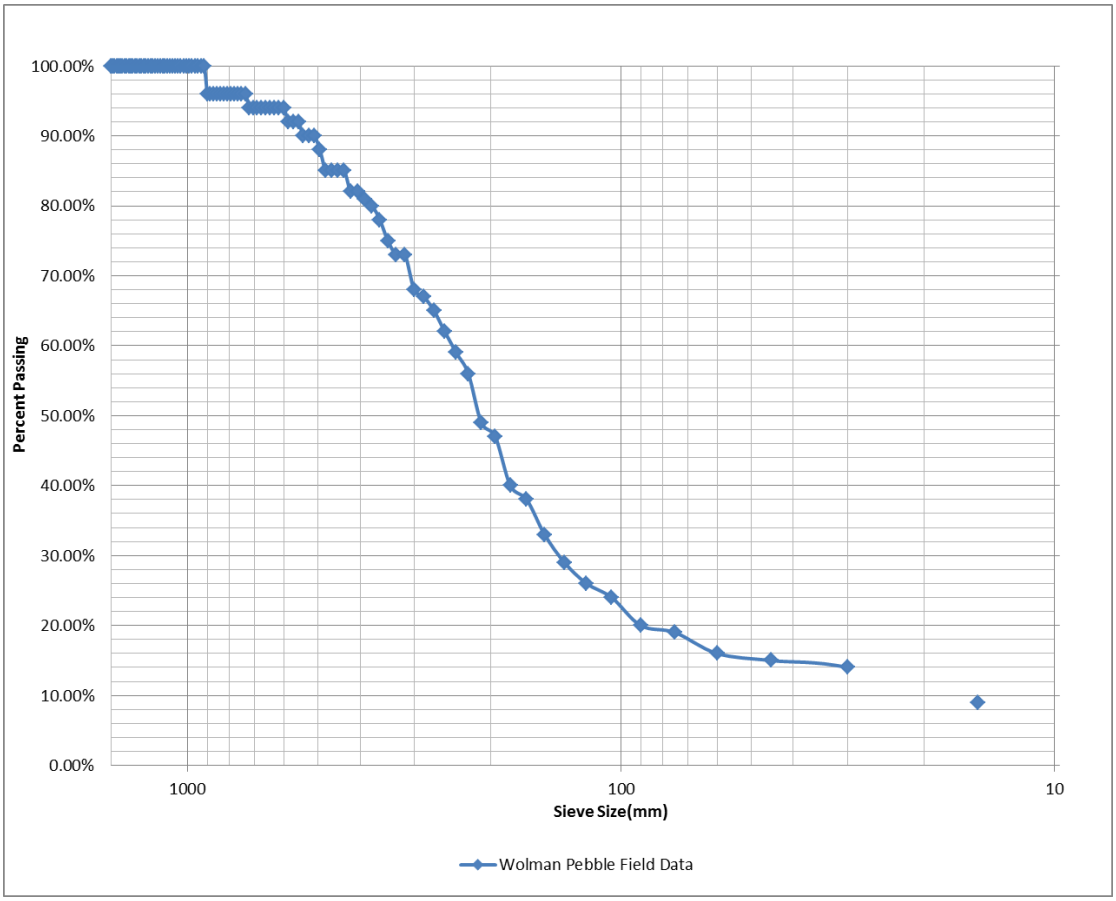

Figure E.35 Bridge # 2111-155 stream-bed grain size distribution analysis.

APPENDIX F

GENERAL SCOUR RISK ASSESSMENT ILLUSTRATION

One of the main applications of this research study is to use the limit analysis for direct assessment of scour risk. An example will now be presented illustrating how this may be accomplished using bridge # 2107-156.

Step 1. Estimate the grain size distribution of the bed: **Figure F.1** shows the bridge elevation and a sample of streambed sediments. The sediments were analyzed using the Wolman Pebble Count, and the results are presented in **Figure F.2**. The median grain size is equal to 18.2 cm.

Figure F.1 Elevation and a sample of streambed sediments, bridge # 2107-156.

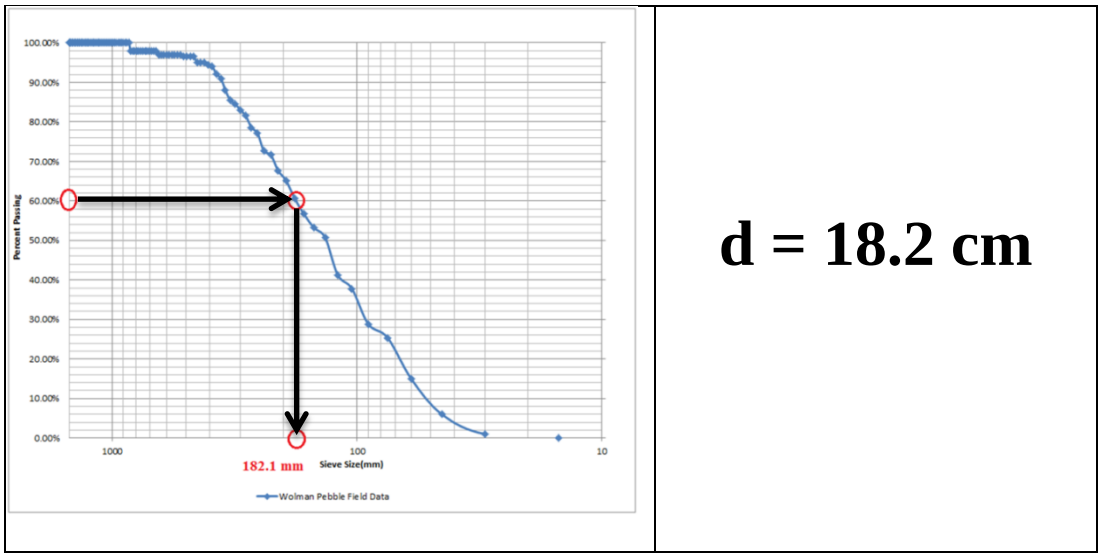

Figure F.2 Grain size distribution curve, bridge # 2107-156.

Step 2. Calculate the limit velocity using Equation (5.1) or **Figure F.3**.

$V_{Limit} = 137.8 \times d^{0.34} = 137.8 \times (18.21)^{0.34} = 372.2$ cm/s (12.2 ft. /s).

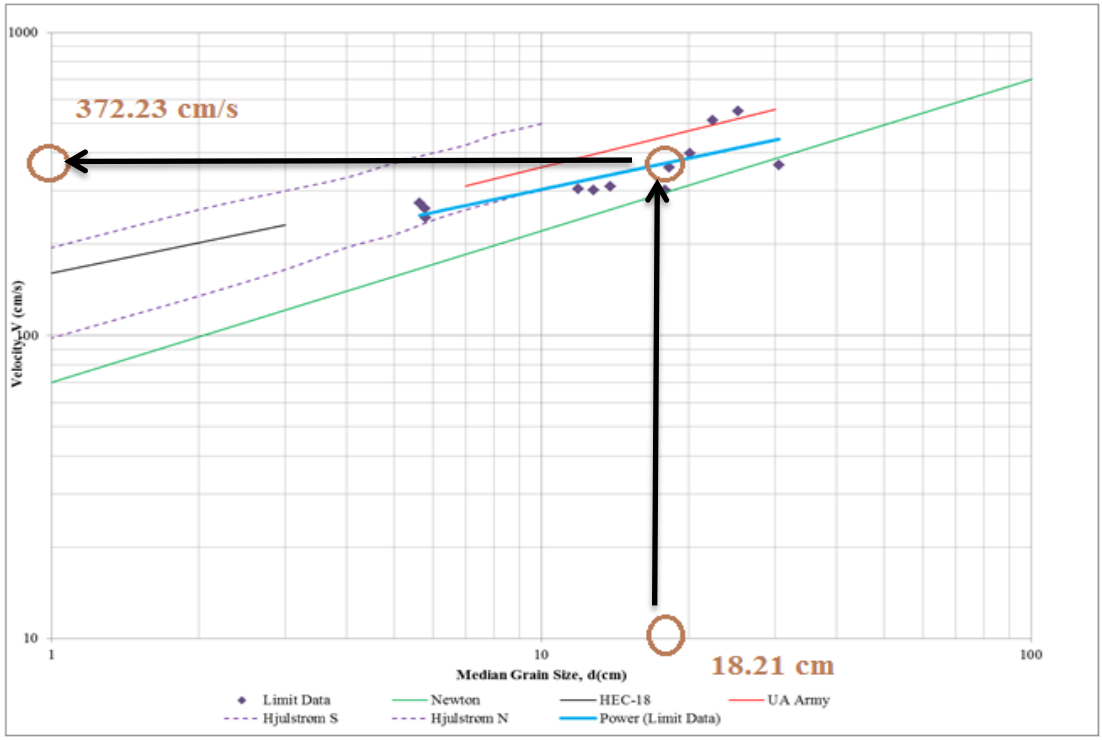

Figure F.3 Velocity vs. median grain size, bridge # 2107-156.

Step 3. Choose a scour design storm and compute the corresponding flow velocity. For existing bridges, Q_{100} is commonly used.

$$Q_{100(u)g} = \left(\frac{DA_u}{DA_g}\right)^b Q_{100(o)g} \quad \text{(F.1)}$$

where:

$Q_{100\,(u)g}$: Discharge for 100 year storm at the bridge,
$Q_{100\,(o)g}$: Discharge for 100 year storm at the USGS gage,
DA_u : Drainage area at the bridge, and
DA_g : Drainage area at the USGS gage.

$Q_{100\,(u)g}$ = [(177/126)^0.59] × 7100 = 8677 cfs

The velocity corresponding to this discharge is determined from a previous HEC-RAS analysis for the bridge:

V_{100} = V_{Design} = 309 cm/s (10.1 ft/s)

Step 4. Finally, the scour design velocity is compared with the limit velocity for the chosen median grain size. If the scour design velocity is less than limit velocity, then the bridge is likely to have a low scour risk. But if the scour design velocity exceeds the limit velocity, then the bridge may not be safe and countermeasures or monitoring should be contemplated. In this example:

V_{Design} = 309 cm/s < V_{Limit} = 372 cm/s

The bridge is considered to have a low scour risk!

REFERENCES

Adams, J., 1979, "Gravel size analysis from photographs." ASCE Journal of the Hydraulics Division 105(10): 1247–1255.

Ahrens, J.P., 2000, "A fall –velocity equation: Journal of Waterway." Port, Coastal, and Ocean Engineering, American Society of Civil Engineers, v. 126, p. 99-102.

American Association of State Highway and Transportation Officials, 1992a, "Standard Specifications for Highway Bridges," Fifteenth Edition, Washington, D.C.

Annandale, G.W., 2006, "Scour Technology," New York, McGraw-Hill.

Arneson, L.A., Zevenbergen, L.W., Lagasse, P.F., and Clopper, P.E., 2012, "Evaluating scour at bridges (5th ed.)." HEC-18, Report No. FHWA-HIF-12-003, Federal Highway Administration., U.S. Department of Transportation, Washington D.C.

Bunte, Kristen, and Abt, S.R., 2001, "Sampling surface and subsurface particle-size distributions in wadable gravel- and cobble-bed streams for analysis in sediment transport, hydraulics, and streambed monitoring." U.S. Department of Agriculture, Forest Service, Rocky Mountain Research Station, General Technical Report, RMRS GTR–74, 428 p.

Buscombe, D., 2008, "Estimation of grain-size distributions and associated parameters from digital images of sediment." Sedimentary Geology 210: 1–10, doi: 10.1016/j.sedgeo.2008.06.007.

Butler, J.B., Lane S.N., and Chandler J.H., 2001, "Automated extraction of grain–size from gravel surfaces using digital image processing," Journal of Hydraulic Research 39: 519–529.

Chang, F. and S.R. Davis, 1999, "Maryland SHA Procedure for Estimating Scour at Bridge Abutments, Part I - Live Bed Scour," ASCE Compendium, Stream Stability and Scour at Highway Bridges, Richardson and Lagasse, Reston, VA.

Chase, K.J., and Holnbeck, S.R., 2004, "Evaluation of pier-scour equations for coarse-bed streams." U.S. Geological Survey Scientific Investigations Report 2004–5111.

Cheng, N.S., 1997, "Simplified settling velocity formula for sediment particle." Journal of Hydraulic Engineering, American Society of Civil Engineers, v. 123, p. 149-152.

Collins, D., 2012, "Prediction of sediment erosion using optical granulometric methods." NJIT Undergraduate Research 2012.

Church, M.A., McLean, D.G., and Wolcott, J.F., 1987, "River bed gravels: sampling and analysis in sediment transport in gravel-bed rivers," Thorne CR, Bathurst JC, Hey RD (eds). Chichester; 43–78, John Wiley & Sons.

Dade, W.B., and Friend, P.F., 1998, "Grain-size, sediment-transport regime, and channel slope in alluvial rivers." Journal of Geology, v. 106,p. 661-675.

Dargahi, B., 1982, "Local Scour at bridge piers –A review of theory & practice," Ph.D. Dissertation, Royal Institute of Technology, Stockholm, Sweden.

Federal Highway Administration, 1988, "Scour at Bridges," Technical Advisory T5140.20, updated by Technical Advisory T5140.23, October 28, 1991, "Evaluating Scour at Bridges," U.S. Department of Transportation, Washington, D.C.

Federal Highway Administration, 2012, "Pier Scour in Clear-Water Conditions with Non-uniform Bed Materials," Federal Highway Administration, Report No. FHWA-HRT-12-022 (Guo, J., O. Suaznabar, H. Shan, Z. Xie, J. Shen, and K. Kerenyi).

Ferguson, R.I., and Church, M., 2004, "A simple universal equation for grain settling velocity." Journal of Sedimentary Research 74(6): 933-937.

Ferguson, R.I., 2005, " Estimating critical stream power for bed-load transport calculations in gravel-bed rivers." Geomorphology. 2005;70:33-41.

Fischer, Edward E., 1993, "Scour at bridge over the Weldon river," Iowa." Proc., Hydraulic Engineering, ASCE, San Francisco, CA, pp.1854-1859

Froehlich, D.C., 1988, "Analysis of on-site measurements of scour at piers," in Abt, S.R., and Gessler, Johannes, eds.

Grace, J.R., 1986, "Contacting modes and behaviour classification of gas-solid and other two-phase suspensions." Can. J. Chem. Eng., 64, 353-63.

Graham, D.J., Rice S.P., and Reid I., 2005, "A transferable method for the automated grain sizing of river gravels.' Water Resources Research 41, W07020, doi:10.1029/2004WR003868.

Guy, H.P., 1969, "Laboratory theory and methods for sediment analysis." U.S. Geological Survey Techniques of Water-Resources Investigations, book 5.

Hey, R.D., and Thorne, C.R., 1983, "Accuracy of surface samples from gravel bed material." Journal of Hydraulic Engineering, Engineering, American Society of Civil Engineers, v. 109, no. 6, p. 842-851.

Hjulstrøm, F., 1935, "Studies of the morphological activity of rivers as illustrated by the River Fyris." Bulletin of the Geological Institute, 25, 221–527. University of Uppsala.

Hjulstrøm, F., 1939, "Transportation of debris by moving water, in Trask," P.D., ed., Recent Marine Sediments. A Symposium: Tulsa, Oklahoma, American Association of Petroleum Geologists, (pp. 5-31). Tulsa, Oklahoma.

Leopold, L.B., 1970, "An improved method for size distribution of stream bed gravel." Water Resources Research 6: 1357–1366.

Linda, P. W., 2011, "Scour at bridges: stream stability and scour assessment at bridges in massachusetts," U.S. Geological Survey.

Laursen, E.M., 1980, "Predicting Scour at Bridge Piers and Abutments," General Report No. 3, Arizona Department of Transportation, Phoenix, AZ.

Maerz, N.H., Palangio, T.C., and Franklin, J.A., 1996, "WipFrag image based granulometry system." Proceedings of the FRAGBLAST 5 Workshop on Measurement of Blast Fragmentation, Montreal, Quebec, Canada, 23-24 Aug., 1996, pp. 91-99.

Maerz, N.H., and Zhou, W., 1999, "Calibration of optical digital fragmentation measuring systems." FRAGBLAST 6, Sixth International Symposium For Rock Fragmentation By Blasting, Johannesburg, South Africa, Aug. 8-12 1999, pp. 125-130.

Melville, B.W., and Dongol, D.M., 1992, "Bridge Pier Scour with Debris Accumulation." Journal of Hydraulic Engineering., ASCE, 118(9).

Melville, B.W., 1992, "Local Scour at Bridge Abutments." Journal of Hydraulic Engineering, 118(4).

Mueller, D.S., and Wagner, C.R., "Field observations and evaluations of streambed scour at bridges." U.S. Department of Transportation, Federal Highway Administration Publication FHWA-RD-01-041.

Mueller, D.S., 1996, "Local scour at bridge piers in non-uniform sediment under dynamic conditions." Ph.D. dissertation, Fort Collins, Colo., Colorado State University.

Rantz, S.E., 1982, "Measurement and computation of streamflow." U.S. Geological Survey Water-Supply Paper 2175, 2 v., 631 p.

Richardson, E.V., and Davis, S.R., 2001, "Evaluating scour at bridges," 4th ed.: U.S. Department of Transportation, Federal Highway Administration, Hydraulic Engineering Circular 18, Publication FHWA NHI 01-001, 378 p.

Sambrook, G.H., and Ferguson, R.I., 1995, "The gravel-sand transition along river channels." Journal of Sedimentary Research, v. A65, p. 423-430.

Schuring, J.R., Dresnack R., Golub E., Khan M.A., Young M.R., Dunne R., and Aboobaker N. , 2010, "Review of Bridge Scour Practice in the U.S.," ASCE Geotechnical Special Publication No. 210, Scour and Erosion, Proceedings of the Fifth International Conference on Scour and Erosion, Nov. 7-10, 2010, San Francisco, CA, pp. 1110-1119.

Sedimetrics, 2008, "Sedimetrics Digital Gravelometer documentation," available at: http://www.sedimetrics.com/documentation/ introduction.html (accessed July 1, 2008).

Sime, L.C., and Ferguson, R.I., 2003, "Gravel-bed river grain size information by automated image analysis." Journal of Sedimentary Research. 73:630-636.

Stokes, G.,1880, “Mathematical and physical papers,” Vol. 1, Cambridge University Press, Cambridge, U.K.

Sundborg, A., 1956, “The River Klarålven”: Chapter 2. “The morphological activity of flowing water erosion of the stream bed”. Geografiska Annaler,” 38, 165-221.

U.S. Army Corps of Engineers, 1995, “Constructing Quality Management,” Engineering Regulation No. 1180-1-6, Washington, D.C.

U.S. Army Corps of Engineers, 2013, “Methodology for Scour Evaluation of U.S. Army Installation Bridges”. Deborah Suazo-Davila, Walter Silva-Araya, and Jorge Rivera-Santos, January 2013.

Van Run, L.C., 1989, “Handbook on sediment Transport by Currents and Waves,” Draft, the Netherlands, Draft Hydraulics, Report H461.

Wolman, M.G., 1954, “A method of sampling coarse river-bed material,” American Geophysical Union Transactions, v. 35, no. 6, p. 951-956.

Yalin, M.S., 1972, “Mechanics of Sediment transport,”: Oxford, U.K., Pergamon, 290 p.May 2004.

Yang, C. T., 2003, “Sediment Transport: Theory and Practice.” New York, NY: McGraw-Hill College.